JANUARY 2017

Ph.D. in Engineering Physics

SERA İFLAZOĞLU

UNIVERSITY OF GAZİANTEP

GRADUATE SCHOOL OF

NATURAL & APPLIED SCIENCES

DEVELOPMENT OF NEW THERMOLUMINESCENT DOSIMETERS FOR NEUTRON MEASUREMENTS

Ph.D. THESIS

IN

ENGINEERING PHYSICS

BY

SERA İFLAZOĞLU

JANUARY 2017

Development of New Thermoluminescent Dosimeters for Neutron Measurements

Ph.D. Thesis
in
Engineering Physics
University of Gaziantep

Supervisor
Prof. Dr. A. Necmeddin YAZICI

Co-Supervisor
Assoc. Prof. Dr. V. Emir KAFADAR

By
Sera İFLAZOĞLU

January 2017

REPUBLIC OF TURKEY
GAZİANTEP UNIVERSITY
GRADUATE SCHOOL OF
NATURAL AND APPLIED SCIENCES
ENGINEERING PHYSICS

Name of the Thesis	:	Development of New Thermoluminescent Dosimeters for Neutron Measurements
Name of the Student	:	Sera İFLAZOĞLU
Exam Date	:	18.01.2017

Approval of the Graduate School of Natural and Applied Sciences.

Prof. Dr. A. Necmeddin YAZICI
Director

I certify that this thesis satisfies all the requirements as a thesis for the degree of Doctor of Philosophy.

Prof. Dr. Ramazan KOÇ
Head of Department

This is to certify that we have read this thesis and that in our opinion it is fully adequate, in scope and quality, as a thesis for the degree of Doctor of Philosophy.

Assoc. Prof. Dr. V. Emir KAFADAR
Co-Supervisor

Prof. Dr. A. Necmeddin YAZICI
Supervisor

Examining Committee Members:

Prof. Dr. Zihni ÖZTÜRK

Prof. Dr. A. Necmeddin YAZICI

Prof. Dr. Ayşen YILMAZ

Prof. Dr. Mustafa TOPAKSU

Assist. Prof. Dr. R. Güler YILDIRIM

I hereby declare that all information in this document has been obtained and presented in accordance with academic rules and ethical conduct. I also declare that, as required by these rules and conduct, I have fully cited and referenced all material and results that are not original to this work.

Sera İFLAZOĞLU

ABSTRACT

DEVELOPMENT OF NEW THERMOLUMINESCENT DOSIMETERS FOR NEUTRON MEASUREMENTS

İFLAZOĞLU, Sera

Ph.D. in Engineering Physics

Supervisor: Prof. Dr. A. Necmeddin YAZICI

Co-Supervisor: Assoc. Prof. Dr. V. Emir KAFADAR

January 2017, 15

The main purpose of the proposed study is the investigation of the possibility to be used as neutron dosimeters with the analysis of the dependence on thermoluminescent radiation dose by synthesizing the borates which is doped metal ions and were development of materials until obtaining the best thermoluminescent neutron dosimeters. Borate anion group-containing materials such as LiB_3O_5, $Li_2B_4O_7$, BaB_4O_7, CaB_4O_7 and MgB_4O_7 were produced for to be used as neutron dosimeters by solid-state synthesis method and after the synthesizing process compounds which include borate anion group were be doped with metal ions by high temperature solid state method. Afterwards, for thermoluminescence measurement of doped materials with the aim of the characterization of dosimetric materials X-ray powder diffraction (XRD), Thermal (DTA, TGA), Scanning Electron Microscope (SEM) and Fourier Transform Infrared Spectroscopy (FTIR) analyses are done. As a result of this analyses, the thermoluminescence measurements of materials are taken.

XRD patterns of the synthesized compounds have demonstrated compliance with borate peak in JCPDS card. FT-IR spectra results did not yield different band structure in compounds. Thermoluminescent measurement results show that neutron radiation-sensitive borate compound are produced. Thermal analysis of the neutron-sensitive compounds were performed. According to the results of this analysis borate compounds are thermally stable. In all borate compunds, 0.5Dy% doped CaB_4O_7 yielded highest thermoluminescence response. Doping with Dy, MgB_4O_7 compounds shows increased thermoluminescence response for neutron radiation. Using different concentrations of Dy, Ag, Cu, Eu, Mg and Gd dopants into $Li_2B_4O_7$ gave good results of neutron-radiation sensitivity. In this study, borate compounds that result after neutron irradiation were compared with TLD-600/TLD-700 neutron dosimeters. Accordingly, the compounds exhibit an ideal fit for all conditions required for a neutron dosimeter. The work carried out under this thesis has reached the objectives.

Key words: Neutron dosimetry, Thermoluminescence, Borate compounds.

ÖZET

NÖTRON ÖLÇÜMLERİ İÇİN YENİ TERMOLÜMİNESANS DOZİMETRELERİN GELİŞTİRİLMESİ

İFLAZOĞLU, Sera

Doktora Tezi, Fizik Mühendisliği Bölümü

Tez Yöneticisi: Prof. Dr. A. Necmeddin YAZICI

Yardımcı Danışman: Do¸

Ocak 2017, 15

Bu çalışmanın temel amacı farklı metal iyonları katkılı çeşitli borat bileşiklerinin sentezlenerek termolüminesans ve radyasyon dozuna bağımlılığının incelenmesiyle nötron dozimetresi olarak kullanılabilme olasılığının araştırılması ve en iyi termolüminesans nötron dozimetresinin belirlenmesidir. LiB_3O_5, $Li_2B_4O_7$, BaB_4O_7, CaB_4O_7 ve MgB_4O_7 gibi borat anyon grubu içeren bileşikler, nötron dozimetresi kullanımına yönelik katıhal sentez yöntemi ile üretilmişlerdir ve sentezleme işleminden sonra bileşiklere metal iyonları katkılaması katıhal yüksek sıcaklık yöntemi ile yapılmıştır. Daha sonra katkılı malzemelerin termolüminesans ölçümüne yardımcı olması ve hazırlanmış dozimetrik malzemelerin karakterizasyonlarının yapılabilmesi amacıyla elde edilen malzemelerin X-ışını Toz Kırınım (XRD), Termal (DTA, TGA), Taramalı Elektron Mikroskobu (SEM) ve Fourier Transform Infrared Spektroskopisi (FTIR) analizleri yapılmıştır. Bu analizlerin sonucunda malzemelerin Temolüminesans ölçümleri alınmıştır.

Sentezlenen borat bileşiklerinin XRD desenleri JCPDS kartlarındaki pikler ile uyum göstermişlerdir. Bileşiklerin FT-IR spektra sonuçlarında da farklı bant yapılarına rastlanmamıştır. Termolüminesans ölçüm sonuçlarından nötron radyasyona duyarlı borat bileşikleri elde edilmiştir. Nötrona duyarlı olan bileşiklerin termal analizleri yapılmıştır. Bu analiz sonuçlarına göre de borat bileşiklerin termal olarak kararlı oldukları görülmüştür. Borat bileşiklerinden nötrona karşı duyarlı en yüksek termolüminesans şiddetini %0.5Dy katkılı CaB_4O_7 vermiştir. MgB_4O_7 bileşiğine Dy katkılaması yapıldığı zaman nötron radyasyonuna karşı termolüminesans şiddetinin artığı görülmüştür. Farklı konstrasyonlarda Dy, Ag, Cu, Eu, Mg ve Gd katkılaması yapılan $Li_2B_4O_7$ bileşiklerde nötron radyosyonuna karşı iyi sonuçlar vermişlerdir. Bu çalışmada nötron ışınlamasından sonra sonuç veren borat bileşikleri TLD-600/TLD-700 nötron dozimetreleri ile kıyaslanmışlardır. Buna göre bileşikler ideal bir nötron dozimetresi için gerekli olan tüm şartlar için uyum göstermektedirler. Bu tez kapsamında yapılan çalışmada hedeflenen amaçlara ulaşılmıştır.

Anahtar kelimeler: Nötron dozimetresi, Termolüminesans, Borat bileşikleri

I dedicate this work to my family...

ACKNOWLEDGEMENTS

I wish to express my deepest gratitude and feeling indebted to my supervisor Prof. Dr. Ahmet Necmeddin Yazıcı and my co-supervisor Assoc. Prof. Dr. Vural Emir Kafadar for their guidance, advice, encouragement, patience and contribution at every stage of this tehesis. I would also like to extend my sincerest thanks to Prof. Dr. Ayşen Yılmaz from Chemistry Department at Middle East Technical University for her great helps, stimulating suggestions and encouragement helped me in all the time of this research. I want to thank her for all her helps, support, interest and valuable hints.

I would like to thank my Ph. D. Thesis committee members Prof. Dr. Zihni Öztürk and Prof. Dr. Mustafa Topaksu for their valuable comments about my reports. I would also like to submit my thanks to Asst. Prof. Dr. Hümbet Ahmedov for help and supporting me in my research studies. I am also grateful to my friends Dr. Ömer Lütfi Ünsal, Uygar Şaşmaz, Meral Doğruer, Emrah Merttürk, Kübra Kandemir, Leyla Yazman, Gizem Ercan, Dilara Çeliktürk and Cansu Kırık for their support and friendly help.

I want to also thank Res. Asst. Muzaffer Gencay Çelik, Res. Asst. Özde Ceren Hızal, Ali Farid, Tuba Avcı , Metehan Severoğlu and Zeynep Seda Eren for their help and peaceful working environment in the laboratory.

I wish to express my thanks form my family for their encouragement and continuous support. I want to thank TÜBİTAK and BAP for financial support.

TABLE OF CONTENTS

Page

LIST OF TABLES

Page

LIST OF FIGURES

Page

LIST OF SYMBOLS

A.u. Arbitrary Unit

Zeff: Effective Atomic Number

XRD: X-ray Powder Diffraction

DTA: Differential Thermal Analysis

TGA: Thermogravimetre Analysis

FTIR: Fourier Transformation Infrared

^{252}Cf: Californium-252 isotope

Gy: Gray (Joule per kilogram)

ICPR: International Commission on Radiation Protection

JCPDS: Joint Committee on Powder Diffraction Standards

SEM: Scanning Electron Microscopy

TL: Thermoluminescence

TLD: Thermoluminescence Dosimeter

OSL: Optical Stimulated Luminescence

VHR: Variable Heating Rate

CGCD: Computerized Glow Curve Deconvolution

n: Neutron

p: Proton

γ: Gamma Radiation

β: Beta Radiation

x: X-ray Radiation

α: Alpha Radiation

E: Energy

KE: Kinetic energy

Q: Binding energy

H: Hydrogen

e^-: Electron

m_n: Mass of neutron

m_p: Mass of proton

m_e: Mass of electron

MeV: Mega electrovolt

kEV: Kilo electrovolt

λ: Wavelength

Å: Angstrom

θ: Theta Angle

MA: Molecular weight

RT: Room Temperature

h: hour

min: minute

β: Heating rate

CHAPTER 1

INTRODUCTION

The most important effect of radiation is to bring harmful biological effects on living things. The biological effect is dependent on the energy of the absorbed radiation and the amount of absorbed dose. The main focus of protection from radioactive harmful biological effects on living things is to draw as low as possible the level of radiation that personnel may be exposed to determine the presence and extent of ionizing radiation and radioactive contamination.

Personnel working in a place exposed to radiation emitted from natural and artificial radiation sources must have tracking devices that detect the total "whole body radiation" value. Personal radiation doses to which personnel are exposed must be measured continuously so that radiation doses that a person may receive can be kept below the maximum permissible level. One of the indirect readers that measures the dose they receive during radiation work in the field is the thermoluminescence dosimeters, which require an additional device to read the doses and measure the total dose of radiation taken over a certain period of time.

The measurement of ionizing radiation is based on the ionization event occurring in the dosimetry environment during irradiation. In solid state (TL) dosimeters, this is the accumulation of a potential energy in crystal structure defects [1-3]. This energy stored in the crystal is released back to the outside with the heating of the crystal and the irradiation curve of the crystal-specific and applied dose amount is obtained after recording the radiation of the radiating end resultant with a reader.

Once solid-state dosimetry techniques and the characteristics of the detectors are understood, it has become clear that this technique can be conveniently used in personnel dosimetry services and can be generalized. With thermoluminescence dosimeters, according to the crystal used; Ionizing and non-ionizing

radiation doses such as x, β, γ, α and neutron are measured. The thermoluminescence event was first observed in 1663 in the diamond [4, 5]. The application of the thermoluminescence phenomenon to the dosimeter was possible in the late 1950s [5, 6]. In developed countries, the thermoluminescence dosimeters are widely used in the main areas of health, industry, research, military and environment, where the radiation doses of the workers working with ionizing radiation are measured and evaluated at international standards.

Such dosimeters are widely used in the dosimetry of personnel dosimetry, in the determination of age of archaeological works, in radiotherapy and in food irradiation because of their linear relationship between dose and thermoluminescence signals, their stability in room temperature after irradiation for months, tissue equivalence properties [7-9]. For this purpose, studies on the development of new thermoluminescence dosimeters in developed countries continue intensively.

There are many research groups working on dating and dosimetry studies using the TL and OSL techniques at research centers such as Oxford University in the UK, Oklohoma State University in the United States, Tel-Aviv University in Israel, and Radiation Research Department in the Riso National Laboratory in Denmark. Although, these renowned research institutions of the world, unfortunately, there are only a limited number of studies in this subject which will provide important contributions to many branches of science.

In our country, dose evaluation using thermoluminescence dosimeters is carried out only at the Ankara Nuclear Research and Education Center (ANAEM) affiliated to the Atom Energy Agency. The Atom Energy Agency purchases hundreds of thousands of thermoluminescence dosimeters from abroad every year for this purpose and this reflects negatively on the country's economy. More intensive work has been initiated in the last five years especially for the dissemination of boron products in our country and the production of new boron products, introduction of these products and their potential use areas in the industrial sector and for this purpose wide range of investigation/development studies [10-13].

The aim of this research is to synthesize borate compounds with metal ions by solid state method. By studying the thermoluminescence and neutron dosimetry properties of the materials developed by synthesis, it is possible to obtain neutron sensitive compounds which can give the best results in terms of usage purposes. It is to investigate in detail the usefulness of these compounds in major fields such as health, industry, research, military and environment.

In this thesis, the thermoluminescence (TL) dosimeters which are compatible with the measurement and evaluation of the neutron radiation doses have been developed. In this thesis, the development of thermoluminescence neutron dosimeter from borate compounds is the first study in our country.

Neutron dosimetric materials have been developed at the standards set by the International Atomic Energy Agency. In this thesis, while boron-based compounds were developed for thermoluminescence neutron dosimetry, the main features that the International Atomic Energy Agency (IAEA) identified and recommended were considered:

(1) The peak temperature (T_m) of the glow curve of the thermoluminescence dosimetry should be between 180 and 250 °C, and possibly a single peak

(2) The dose-response curve of dosimetry should be linear over a wide dose interval

(3) Almost no influence from environmental factors

(4) The wavelength of the emitted light from the dosimeter must be within the visible region boundaries

(5) Do not change the sensitivity of dosimetry on reuse

(6) The sensitivity of the dosimetry should not be too dependent on the energy of the applied radiation and the type

(7) The radiation absorption factor of the dosimetry is the same as the radiation absorption factor of the human body ($Z_{eff} = 7.42$)

(8) The dosimeter should be cheap and easily prepared in almost any laboratory environment

(9) There should not be toxic materials in the dosimetry that could harm the human

The introduction of this thesis explains the importance of thermoluminescence dosimetry studies as a result of natural and artificial radiations which we are constantly exposed to in our daily life. The recent technological developments and the presence of nuclear energy have revealed the need for this work. In the literature review of this thesis firstly the information about the studies done up

to date from the date when the thermoluminescence event first observed in 1663 was given.

Thermoluminescence dosimeters have become a necessity because of the increased natural and artificial radiation in the environment. Recently, studies on thermoluminescence have increased significantly. General information about the general properties of borates has been given. Borates have a unique crystal and electronic structure. The basic building blocks and compounds of the borate crystals are described. Due to the excellent construction properties of borates, recent work has gained a great deal of speed. It has a great advantage because approximately 75% of the boron reserves in the world are in our country. Later studies on the thermoluminescence properties of the neutron dosimeter have been reported. In this study, the studies on the dosimetry of $Li_2B_4O_7$, LiB_3O_5, MgB_4O_7, CaB_4O_7 and BaB_4O_7 borate compounds synthesized and characterized are given. Nevertheless, it has been found that the most suitable metal ion-doped borate compound for the neutron dosimetric purposes is a 0.5% Dy-doped calcium tetraborate compound. It was determined that the 0.5% Dy-added CaB_4O_7 compound gave better neutron dosimetry results (dose response).

CHAPTER 2

LITERATURE SURVEY

2.1 Historical Overview of Thermoluminescence

The first TL observations were performed on natural minerals, as diamonds or fluorspar, and were first defined for diamonds by Robert Boyle in 1663 [14]. A much more spectacular TL impact of a green fluorspar known as false emerald (a type of fluorspar) was used for scientific demonstration, and then the powdered mineral was pulverous as letters or figures on a metal plate and heated. In the 18^{th} century, a TL of minerals such as rock crystal, amethyst, topaz and of calcite, had ben defined. By the end of the 18^{th} century, an association of thermoluminescence and phosphorescence as well as triboluminescence was obvious. In the early 19^{th} century, the electric spark was monitored to excite TL by exposure to its light. Calcareous biominerals, as mother of pearl, scallop shells and egg shells, gave spark-irradiated an orange-red TL. A colouration of fluorspar by spark irradiation was observed to disappear after heating [14].

In 1888, Wiedemann was bringed the premise luminescence for the observing of more light emission over the thermal background. Wiedemann and Schmidt (1895) was the initial to detect thermoluminescence (TL) of matter regularly [15]. Cathode rays, X-rays and the perception of native radioactivity opened the way to excite TL experimentally in native and artificial minerals. The act of luminescence activators, particularly manganese, iron and rare earth elements, has since then been a topic of works supported by the conformity of synthetic irradiation sources and tried analytic methods. The first glow curves measured light intensity temperature vs. were registered by Przibram and his coworkers [16] (1922) at the Radium-Institut in Vienna. Different minerals, as alkali halides, calcium carbonates, silicates, and of track the broad variety of fluorites, were generally exposed to radium sources or X-rays, and the resultant luminescence investigated visually, registered spectrographically or measured by photoelectric detectors.

The first theoretical model of TL was referred by Randall and Wilkins (1945) for first order kinetics [17] and after expanded by Garlick and Gibson (1948) for second order kinetics [18]. At this time, study concentrated on geological materials, track impurities, and improvement of dosimeter matter doped with such metal traces. First tries to apply TL on biogenic calcium carbonates were performed by Johnson (1960) displayed that calcitic mollusc shells are convenient, while aragonitic shells do not emit TL [19]. In the next years, TL was adaptation as a technique of geological, paleontological and archaeological dating of rocks, soils, sediments, weathering deposits, fossil bones, shells, pottery and other ceramic materials [20]. Thermoluminescence as a technique for the perception of food irradiation has been improved later 1985 for irradiated spices, herbs, fruits, vegetables, and mushrooms, using the TL of mineral particles [20].

The initial application of this phenomenon for dosimetric goals was from Daniel and his friends [21]. Since then much search has been performed for a better understanding and development of the material characteristics as well as to improve new Thermoluminescence materials. In these days, the TLD is a well-established dosimetric method with applications in areas such as personnel, environmental and clinical dosimetry [22].

The Thermoluminescence is a common phenomenon. Around three quarters of 3,000 native minerals display Thermoluminescence affect; some minerals as fluorite (CaF_2) from obvious regions in Iceland, Brazil, Turkey and India are between the most accurate phosphors common [23, 24]. The thermoluminescence affect is not qualified to inorganic crystals and glasses. But; the thermoluminescence from organic compounds such as different polymers [25, 26]; and others containing teflon [27], polyethylene, and polypropylene [28] generally consists of below room temperatures. They aren't interesting for practice dosimetry.

Early researches of synthetically activated TL phosphors such as $CaSO_4$:Mn date back to the turn of the century [29]. This sample was used in 1935, and again since 1949 in rocket experiments for UV dosimetry [30, 31], and 1954 was used in the firstly medical dosimetry resarch with thermoluminescence dosimetry [32]. The affect of X-ray on CaF_2 was initially studied by Wick and Slattery in 1928 [33]. Mangenese-activated CaF_2 was promoted in mid-1950's as a susceptibility and uniformity sample which has one large glow peak [34-36].

LiF dates back to the late 1940's and firstly 1950's, when Daniels and his students [21] at university of Wisconsin researched the thermoluminescence of alkali halides [37]. They used suppressed pellets of LiF powder for dosimetry

experiments. LiF that is activated with Mg and Ti, called "TLD-100", governed the low atom numbers detector market for following years and is style the most used thermoluminescence phosphor [38, 39]. Manganese-doped lithium borate and beryllium oxide [40, 41] have been the most successful low effective atomic number materials so far.

Significant attempt have been connected during the past 50 years to the development of susceptibility and uniformity of high effective atomic numbers materials [42, 43]. Natural fluorites [44, 45] turned out to be not too successful, and thermoluminescence glasses [46, 47] could never severely contend with crystalline phosphors. High susceptive phosphors such as $CaSO_4$:Mn, CaF_2:Dy end up to be not uniformity enough for long-term measurements, however other, equivalently constant and more susceptive samples ($CaSO_4$:Dy, $CaSO_4$:Tm) became existing [21]. This area is yet advancing quickly with new detector materials or modified old ones.

A large volume of knowledge has been published on the thermoluminescence in common an private applications, involved dosimetry [22, 48, 49]. Total number of publications on the Thermoluminescence dosimetry is approaching 3000 and is increasing at rate of 200 papers per a year.

2.2 General Properties of Borates

Borates structures are naturally occurring minerals made up of boron which is the fifth element in the periodic table. People require borates, too, as an significant section of a healthy diet and an necessary content in many products essential for an reasonable standard of living. The element boron does not occur by itself in nature. Fairly, with oxygen and other elements boron combines to mode inorganic salts (boric acid) called borates. Though the millions of tons of industrial borates mined, treated and dispensed generally all over the world every year, far major of quantities boron are transferred nearby the planet by path forces of nature [50].

Figure 2.1: The shape of borates [50].

Borats are explained as "esters or salts of boric acid; a compound containing the root B_2O_3" [51]. Borates are explained by industry as any acompound that includes or requisite boric oxide. A great number of minerals to contain boric oxide, however the three are important from a world generally commercial point of view are: colemanite, borax, ulexite and these are manufactured in a restricted number of states, rule by the Turkey and United States, which cooperatively provide around 90% of the world's borate essential [52].

Borate naturel substances (minerals) having work in an extensive diversity of utilize for many nation, dating from at least the 8 century when they were utilized more desirably as a flow for trying and pertaining Ag and Au. Their valuable characterize and junction scantiness in a short period of time caused international trade in borates [53].

Boron is every time combined with oxygen to form borates. Borates are one of the most interesting groups due to the rich variety of their crystal chemistry. New borate compounds which are not accessable with any other compounds are explored [54]. Therefore borates have considerable significance for production of high technology materials.

Generally, borate crystals can be recognized as following:

(1) simple trigonal (BO_3^{3-}) and tetrahedral groups (BO_4^{5-}) which form the basis for the structure of $LiBO_2$ crystals [55]. (Figure 2.2 a and b);

(2) bitrigonal and ditetrahedral groups ($B_2O_5^{4-}$) and ($B_2O_7^{8-}$) (Figure 2.2. c and d);

(3) circular six-membered groups with a mixed coordination ($B_3O_6^{3-}$), ($B_3O_7^{5-}$), which form the basis for the structure of LiB_3O_5 crystals (Knig 1978), ($B_3O_8^{7-}$), and ($B_3O_9^{9-}$) (Figure 2.2 e–h);

(4) coupled double six-membered rings ($B_5O_{10}^{5-}$) and ($B_4O_9^{6-}$) which are the base unit of $Li_2B_4O_7$ crystals [56]. (Figure 2.2 i and j).

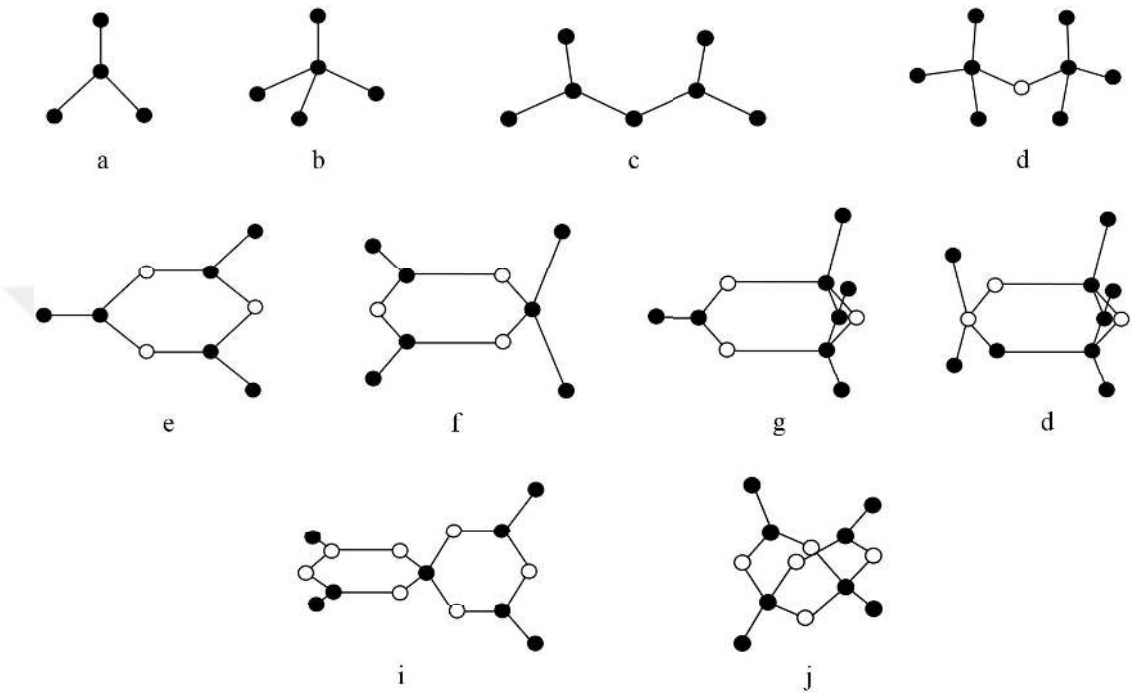

Figure 2.2: Basic structural units of borate crystals, closed and open circles are boron and oxygen atoms, respectively [57, 58].

Borates have unique crystal and electronic structures, so they have establish widespread application in regions like materials processing, medicine, etc.

Early investigation about laser was performed in 1960 [59]. Later the creation of laser, interactions between lasers and materials have been widely research by many researchers. Laser light must be powerful and it has to possess exact frequency. In order to ensure these features, laser beam need to be passed through appropriate nonlinear optical crystals for instance, ArF, XeCl and KrF since there is no suitable source occurs for the route manufacture of laser beam. However, these crystals have some disadvantages such as corrosive gases, requirement of high voltage gaseous discharges and necessity of regular maintenance. Therefore new compounds including borates were desired to be synthesized [60-62].

Investigation in the area of non-linear optical devices leads to a growing concern in new borate compounds. Lots of borates have excellent non linear optical properties such as: high polarizability and perfect transparency in ultra-violett area of planar $(BO_3)^{3-}$. Boron has just 3 electrons (1s2 2s2 2p1) to study with, thus the ion is not polarizable. It doesn't want to donate electrons and also accept them easily. Therefore, boron and oxygen make together chemical bond that is formed by sharing electrons. Due to the strong covalent B-O bond and diverse structures, generally, borates have high nonlinear optical properties [63].

Because of the nonlinear optic properties of borate, rare earth borates, alkali earth borates and rare earth alkali earth borates have been synthesized and investigated to use as the hosts of nonlinear materials and laser materials [64-66]. The initial nonlinear optic borate described was $KB_5O_8.\ 4H_2O$ in 1975 [67], and then very much of investigation concern has been based on nonlinear optic properties of inorganic borates. β-BaB_2O_4 (BBO) [68] lithium Borate [57] cesium triborate [69], $KBe_2BO_3F_2$ [70], cesium lithium borate [71], $Sr_2B_2Be_2O_7$ (SBBO) [72], $Ca_4LnO\ (BO_3)_3$ (CLnOB) [73], $K_2Al_2B_2O_7$ (KAB) [74] and BiB_3O_6 (BiBO) [75] are some of the examples.

Some activators (generally rare-earth oxides and transition metals) are added as activators into the borate compounds in order to obtain luminescent materials. These materials find widespread use in industrial application area. For instance, Eu is doped into SrB_4O_7 for ultraviolet emitting medical lamps, tiberium and cerium are doped together into $GdMgB_5O_{10}$ for the green emitted consituent in maximum-efficiency fluorescent lights and europium is doped into (Y,Gd) BO_3 for the red emitted consituent in plasma demonstrate panels for maximum description television.

Boric acid was firstly analysed by Wilhelm Homberg (1652–1715) from borax, by the mobility of mineral acids and was utilized particularly the name sedative salt of Homberg. Nonetheless, borates have been exploiting since early time in Greeks for preserving foods, cleanings and other activities.

Crystalline boric acid make up of plates of $B(OH)_3$ molecules keep along with by hydrogen bonds. The B-O bond length is 136 pm and the O-H is 97 pm with a hydrogen bond of 272 pm. The range between two neighbor plates is 318 pm.

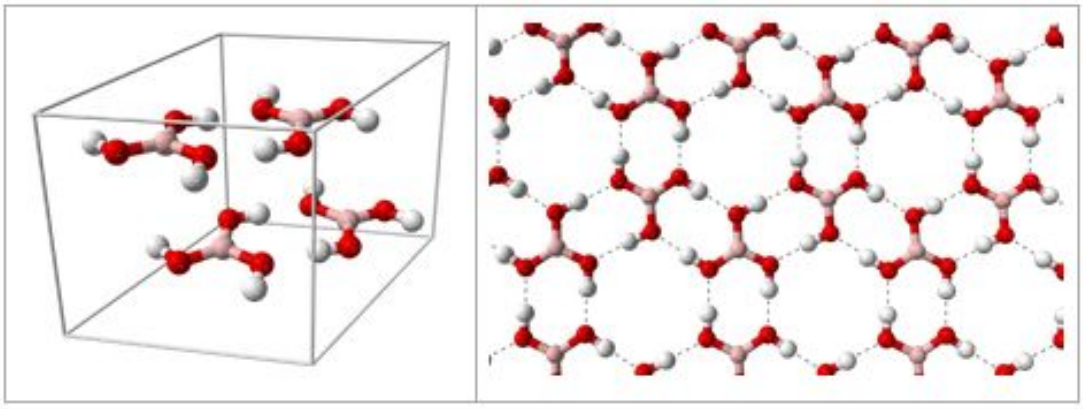

Figure 2.3: The unit cell of boric acid and hydrogen bonding lets boric acid molecules to form parallel layers in the solid state [76].

2.3 Literature Survey on the Thermoluminescence Properties of Neutron Dosimeters

In 2007, Triolo *et al.* studied the thermoluminescent glow curves of TLD-600, TLD-700 and MCP for mixed area of n and γ. The flux rates of thermal neutrons used to explain the confidently of the thermoluminescent dosimeters in this radiation area and to get knowledge on the dose absorbed rates. The glow curves found have been CGCD (computerized glow curve deconvoluted) program using general order kinetics and the determined variations for the difference linear energy transfer components have been inspected [77].

Yukihara *et al.* explained the probability of using neutron converters consolidated into Al_2O_3:C dosimeters to generate new neutron accurate optically stimulated luminescence dosimeters proper for personal monitoring. A comparison between different neutron converters show that lithium based compounds result in the best neutron susceptibility, likely due to the comparatively big range of the 2.75∼MeV triton manufactured by the $^6Li(n,\alpha)^3H$ neutron capture reaction. With these results, neutron susceptible optically stimulated luminescence material for dosimetry systems was manufactured and characterized except for the smaller gamma and enhanced neutron susceptibility. The gamma susceptibility of the new material is ∼35% because Al_2O_3:C composition is decreased in the material. The neutron susceptibility performed in this new material is ∼60% of the neutron susceptibility of TLD-600 (^{6}LiF:Mg,Ti) [78].

Horowitzt *et al.* reports in commonly accepted thermoluminescence response of fast neutrons to gamma betwen 0.05 to 0.3. A new thermoluminescence dosimeter sample of LiF:Cu,Mg,P, with a γ irradiation thermoluminescence susceptibility $\sim$20 times larger than TLD-100 (LiF:Mg,Ti) is reported. The thermoluminescence response of LiF:Cu,Mg,P to californium-252 (^{252}Cf) (a fast neutron source with an average energy of E = 2.5 MeV) is measured. Supposition of the thermoluminescence signal was performed using CGCD program [79].

Mittani *et al.* reports the OSL (optically stimulated luminescence) features of neutron dosimeters which is a mixture of C doped Al_2O_3 and neutron converters. The neutron converters researched were maximum density polyethylene, lithium fluoride, LiF 95% enriched with ^{6}Li, Li_2CO_3 95% enriched with ^{6}Li, $H_3{}^{10}BO_3$ enriched with 99% of ^{10}B and Gd_2O_3. The ratio of C doped Al_2O_3 and neutron converter in the mixture was optimised to minimize the whole optically stimulated luminescence signal and neutron susceptibility. The neutron susceptibility and dose return were reported for the optically stimulated luminescence dosimeters using a bare californium-252 neutron source and similar to the return of Harshaw neutron dosimeters ^{6}LiF:Mg,Ti and ^{7}LiF:Mg,Ti. The study indicates the probability of improving an optically stimulated luminescence dosimeter consist of C doped Al_2O_3 sample and neutron converter with a neutron susceptibility and neutron gamma separation similar to the ^{6}LiF:Mg,Ti and ^{7}LiF:Mg,Ti combination [80].

2.4 Literature Survey on the Thermoluminescence Properties of $Li_2B_4O_7$

In 2014, Dhanuskodi, Mohandoss and Vinitha studied the cobalt doped lithium tetraborate. $Li_2B_4O_7$ doped with Co ions of different concentrations were synthesized by chemical reaction and determined by XRD. SEM measurement reveals the spherical morphology of the nanoparticles and the medium particle magnitude is supposited to be 50–110 nm. Ultraviole–visible radiation response demonstrate the incorporate of $Co^{2+}$and the Li–hole pair creation. The materials are completely transparent in the visible area and having absorption peak 220 nm in ultraviolet area. For the Z-scan method, the nonlinear optical parameters such as nonlinear absorption, nonlinear optical susceptibility and non-linear refractive index are estimated as, 10^{-2}cm/W, 10^{-5} esu and 10^{-8}cm^2/W respectively [81].

Kimberlee *et al.* indicates on a determination into the OSL features of a few common thermoluminescent samples, namely, $CaSO_4$:Tm, CaF_2:Mn, LiF:Mg,Ti, and $Li_2B_4O_7$:Cu. These materials were irradiated to air doses of 15 mGy, 150 mGy and 1.5 Gy and researched using a trading existing optically stimulated luminescence reader system to designate their luminescence return to sustained infrared and blue light stimulation, centered at 830 nm and 470 nm wavelengths, respectively. Mn doped CaF_2 did not demonstrate an optically stimulated luminescence return with either blue light or infrared light excitation. Mg,Ti co-doped LiF and Cu doped $Li_2B_4O_7$ indicated comparatively low optically stimulated luminescence signals just under blue light stimulation. Tm doped $CaSO_4$ showed optically stimulated luminescence under both blue light and infrared light stimulation at susceptibility crudely one order of size less than the OSL return of C doped α-Al_2O_3 under the same situation [82].

Tou *et al.* presents the thermoluminescence return of strontium tetraborate glass related to electron rays at different Dy_2O_3concentrations ranging from 0.00 to 1.00 mol%. Overall glass materials indicated only extensive peak with maximum peak temperature located at 170–215 °C. The minumum thermoluminescence response was determined at Dy_2O_3 concentration 0.75 mol%. This glass demonstrated good linearity and higher susceptibility for 7 MeV compared to 6 MeV electrons. The determined of kinetic parameters indicated that the glasses show second order kinetic [83].

O. Annalakshmi and his colleague have studied the $Li_2B_4O_7$:Mn produced by solid state reaction shows a dosimetric peak at 280 °C. The sensitivity of Mn doped $Li_2B_4O_7$ is found to be 0.9 times that of TLD-100. The infrared spectrum of this phosphor demonstrate the existence of bond vibrations relative to BO_3 triangles and BO_4 tetrahedral. The mechanism for TL in this phosphor was focused on the thermoluminescence emission spectra and thermoluminescence glow curves measurements on non-ray and gamma-ray phosphors [84].

C. Furetta *et al.* researched the thermoluminescence properties of $Li_2B_4O_7$ polycrystaline powder undoped and doped with Cu or Eu impurities in 1996. In the case of $Li_2B_4O_7$:Eu, a high temperature thermoluminescence peak induced by the impurity is showed at any dopant concentration. Comparative analysis of undoped $Li_2B_4O_7$ reveals the contributions of impurities to the glow curves [85].

X. Zhengye and his colleagues have worked on $Li_2B_4O_7$:Cu,Ag,Mg phosphors by the sintering method. The roles of Mg and Ag dopants in the phosphors have been reported using the technique of thermoluminescence glow curves and 3D thermoluminescence spectra. The results showed that suitable concentrations of Ag and Mg can increment the thermoluminescence of $Li_2B_4O_7$:Cu. It was also demonstrated that the intensity of thermoluminescence peak at 130 °C is diminished with the rising Ag concentration, and diminished with the rising Mg concentration [86].

$Li_2B_4O_7$:Cu TLDs phosphor radiation dosimetry characteristics was also researched by A.R. Lakshmanan et al [87]. The large peak in that phosphor take placed at 230 °C and its thermoluminescence susceptibility to gamma ray is two three times larger than that of TLD-100.

In 2005, Manam and Sharma reported the Cu-doped $Li_2B_4O_7$ phosphor. They have determined the trapping parameters such as activation energy, frequency factor and order of kinetics. This work was one of the most significant studies in the area of TSL. A polycrystalline material of $Li_2B_4O_7$: Cu was synthesized using the melting technique. Sample was tested using of FT-IR spectroscopy. Termoluminesce measurements of the $Li_2B_4O_7$:Cu material indicates 3 glow peaks at temperatures of 175 °C, 290 °C and 350 °C, repectively and the intensity of the glow peak at 175 °C is the heighest one. The trapping parameters related to this featured glow peak of Cu doped $Li_2B_4O_7$ are investigated here in, using the Chen's peak shape and isothermal luminescence decay techniques. Their results indicate that very well understanding between the trapping parameters determined by the two techniques [88].

Kelemen *et al.* investigated the RL and TL data for Mn doped single crystal and glassy materials of lithium tetraborate, and single crystal create of the lithium tetraborate. The measured light output of Mn doped lithium tetraborate and Ag doped lithium tetraborate single crystal and glassy samples during the irradiation procedure and the subsequent TL process revealed that glassy structure showed much lower trapping efficiency than the corresponding single crystal [89].

Driscoll *et al.* compared the thermoluminescence features of manganese doped lithium borate sample with copper doped lithium borate and copper and silver doped lithium borate on their dose response conducts and levels of fading and the results are in good agreement with that of Wall. Driscoll et al. also compared the usable dose ranges and photon energy responses for TLD-800 chips and two different Mn doped LTB obtained from two producers. Results of this comparison reveal the two different Mn doped LTB has similar properties [90].

2.5 Literature Survey on the Thermoluminescence Properties of LiB_3O_5

Lithium triborate is considered as a technologically important material for diverse applications, such as nonlinear optical materials [54] laser harmonic generation, acoustic wave [91, 92] and recently neutron detectors. Furthermore, lithium triborate is suggested as efficient thermoluminescent material [93, 94].

Ogorodnikova and his colleague have reported the recombination processes and lattice defects in crystals of alkali metal borate lithium triborate by the implement of the thermoluminescence and ESR methods [95].

N. Senguttuvana and his collogues studied crystal growth of lithuim triborate doped with Ni, In, Ce, Ti and Cu and some works on their luminescent features. Crystals were grown by the Bridgman technic. The Ce-doped compound indicated powerful emission at 375 nm for 2 stimulation peaks at 270 and 320 nm [96].

Chen provided the probable submitting of lithium triborate crystals in nonlinear optics in 1989 [57]; lithium triborate is one of the alkali borate crystals with benzene ring same $B_2O_7^{5-}$ groups. Alkali borate crystals have an excellent nonlinear optical property because of their anionic teams [93]. Then, this compound has been used in nonlinear optical applications [98-101]. Besides, it is known that "B" and "Li" both have major neutron seizing capability which makes lithium a encouraging scintillator for neutron detection [102]. Since lithium borate crystals have great number of boron atoms per unit cell, they are very attractive for neutron detectors. This situation was investigated and showed primary for glass and ceramic samples by Van Eijk (1997) [103].

Initial studies on LiB_3O_5, which is a nonlinear optical (NLP) crystal, was performed by Mazzetti and Carli in 1926 [104] and followed by Rollet and Bouaziz [105].

Mathews et al. investigated the high temperature behavior of the Li_2O-B_2O_3 system and found that LiB_3O_5 gave three overlapping, distinct and small endotherms at 845, 880 and 907 °C. The endotherms at 845 °C and 880 °C were ascribed to the unsuitable melting of lithium heptaborate, and last endothermic peak was attributed to unsuitable melting of LiB_3O_5. In the same investigation, the unit cell parameters of LiB_3O_5, a: 8.444 (2), b: 7.380 (3), c: 5.142 (2), its density (2.43g/cc) and its solubility (1.84 g/ml) were determined [106].

Wei *et al.* (1990) investigated the lithium triborate structure depending on temperature. They reported that LiB_3O_5 decomposed above 500 °C forming $Li_2B_4O_7$. Lithium triborate powder materials were heated at 520 °C for 130 hours and 580 °C for 95 hours. After heat treatment, the peaks belonging to $Li_2B_4O_7$ were observed in the X-ray diffraction patterns of LiB_3O_5 [107].

Konig and Hoppe (1978) synthesized the first small lithium triborate crystal which was produced by solid state method of B_2O_3 glass covered with LiF powder at 750 °C for 10 hours. They determined the cell parameters and crystal system of the lithium triborate. Lithium triborate crystal was in the orthorhombic system with the space group Pna21-C2v and the unit cell parameters were determine as a= 8.466(2), b=7.380(2) and c=5.147(2). In this study, it was also observed that lithium triborate (LiB_3O_5) decomposed to lithium tetraborate ($Li_2B_4O_7$), and lithium octaborate ($Li_2B_8O_{13}$) at 595 °C [108].

The crystal structure of LiB_3O_5, depended upon thermal treatment, was investigated by Shepelev *et al* 2005. LiB_3O_5 was heated at different temperatures and crystal structure of lithium triborate was evaluated by X-Ray diffraction. They found that the intensities of certain reflections of LiB_3O_5 alteration importantly on heating. When temperature was increased above 650±20 °C, the first slight traces of $Li_3B_7O_{12}$ were observed. These investigations showed that LiB_3O_5 was a metastable compound below 600 °C. It started to decompose to $Li_2B_4O_7$ or $Li_3B_7O_{12}$ [109].

In 2008, Surovtsev *et al.* studied to establish the temperature dependent properties of structuring of lithium triborate melts. Single crystals of lithium triborate were grown by using Li_2CO_3 and B_2O_3 as well as MoO_3 as a flux by TSSG method. Surovtsev *et al.* reported that crystalline substance consisted mainly of lithium triborate and lithium tetraborate was presented with a minor concentration [110].

Eugene *et al.* (2006) [111] claimed that using stoichiometric melts of the system Li_2O-B_2O_3 for growth of major quality lithium triborate single crystals is unable. The main problem of growth of high-quality lithium triborate single crystal is reproducibility due to the low heat conductivity and high anisotropy of crystal thermal stretching, incongruently melting properties, trouble in crystallization which assumed to be relevant to the polymerization of BO_4 tetrahedra and BO_3 triangles in the melt [54, 112].

2.6 Literature Survey on the Thermoluminescence Properties of MgB_4O_7

Thermoluminescent dosimetric features of MgB_4O_7:Dy,Na were reported by Furetta [113]. The following TL dosimetric features of this sample were investigated in that work; the shape of glow curve, thermoluminescence susceptibility, annealing procedure, photon dose response, and optimum detectable dose, certain of thermoluminescence measurements, reproducibility, and energy response and fading characteristics.

A thermoluminescent material based on MgB_4O_7:Dy was also advanced at the Boris Kidric Institute of Nuclear Sciences and characterized by L.L Campos and O.O. Ferando Filho [114] .

In 2014, Kawashima and his colleague have studied the polycrystalline materials of MgB_4O_7 doped with Tb for different concentrations using the solvent evaporation procedure [115]. The material doped with 1 mol% of Tb reported the largest luminescence intensity. The glow curve of the materials indicated an intense and good described thermoluminescence peak having the highest on 220 °C and a low shoulder peak at ∼330 °C. Thermoluminescence spectra and fluorescence of 1 mol% doped material reported a powerful Tb^{3+} emission lines at 489, 545, 588 and 622 nm. The thermoluminescence dose response was calculated over the gamma ray interval between 1 and 10 Gy. The connection between peak intensity and dose was linear and the optimum perceivable dose acquired by addition take statement of 3 times the normal deviation of the dose reading was 50 Gy.

Sensitivity and fading characteristics of thermoluminescence magnesium borate was reported by C.M.H. Driscoll *et al* [116]. The new tissue equivalent magnesium borate has been studied and compared with those established materials.

Sahare *et al.* in 2015 presented the optimized dosimetric features of small atomic number Mn,Tb doped magnesium tetraborate using a thermoluminescence. The phosphor sample was produced using a traditional maximum temperature solid state method. The sample and stage naivety of synthesized sample were validated by sample XRD analysis. The sample in the micro crystalline structure was constituted to be in orthorhombic compose. The relative dosimetric features of the phosphor sample have been prevalently examined for its practices in medical and personal dosimetry. It has been constitute that the

Mn,Tb co-doped MgB_4O_7 sample, against γ radiations, indicates beter thermoluminescence susceptibility and has an point via the Mn and Tb doped materials as it is a great deal susceptible than the formers. It has an easy glow curve structure two good decomposed thermoluminescence peaks centered at approximately 475 and 650 K. At the end of the storage in the dark for 1 month, the maximum intensity of was reduced nearly $\sim$10%. It was also expressed that the thermoluminescence sensitivity of the sample is 3.5 times than that of TLD-100, effective atomic number is $\approx$8.23 and has a linear dose response up to broad interval form 0.1 Gy to $\sim$5.0 kGy of γ radiation [117].

Furetta was presented certain thermoluminescence features of Dy and Na doped magnesium borate, namely the TL response of absorbed dose and the fading manner [118]. Dy and Na doped magnesium borate indicates a better linear interval of the thermoluminescence response as a function of the absorbed dose also a small threshold dose.

J.H. Souza *et al* [119] done two sets of empirical works pursued by computer analysis of more than 200 glow curves show that a joining of at least eleven peaks of first order kinetics is essential to define the glow behavior of dysprosium doped magnesium tetra borate. It was found that for a heating rate of 1 °C/s the high intensity of singular peaks are available the pursuing temperatures: 101, 110, 126,142, 155, 160, 173,192, 224, 231 and 304 °C.

Annalakshmi *et al.* (2013) determined rare earth elements with doped magnesium tetraborate produced by high temperature solid state reaction method. Among the distinct such as Gd, Na, Ag and Li dopants worked in this MgB_4O_7 sample. The thermoluminescence susceptibility, dose response glow curve, and after irradiation storage consistency were worked for the probably use of this sample in radiation dosimetry applications. The thermoluminescence parameters, like the b, E and s were found for the MgB_4O_7:Gd phosphor. The phosphor was determined to be reusable post a few cycles of irradiation and annealing. The after ionizing radiation storage consistency works indicated that this close tissue-equivalent phosphor, which has a gamma susceptibility five times that of TLD-100, is convenient for medical dosimetry applications [120].

Environmental radiation monitoring around coal fired power plants to find the instability in measured background exposures were reported by F. Adrovic [121]. Measurements have been done using a multi-element, maximum accurate dosimeter system comprised of three solid, appropriately filtered, sintered Dy doped $CaSO_4$ thermoluminescent detectors, and single small atomic number Dy,Na doped MgB_4O_7 thermoluminiscencent detector manufactured at the Vinca Institute .

Pradhan has investigted the general characteristics of MgB_4O_7:Dy, $Li_2B_4O_7$:Cu,Ag and $Li_2B_4O_7$:Cu as promising TL dosimeters due to their tissue equivalent effective atomic number [122].

T. Karali and his team mates reported X radiation stimulated thermoluminescence spectra of either single rare earth ions Dy or Tm, or co-doped with Dy/Tm, Tm/Mn or Dy/Tb with doped magnesium borate [119]. Domestic emission from the host sample was determined in the ultraviolet/blue area at roughly 375 nm, with a tail lengthily to 200 nm. The basic dosimetric peak is detected at roughly 180 °C however light diversity are determined between the glow peak maximum from the different rare earth ions and there were alterations pursuing thermal treatments [123].

2.7 Literature Survey on the Thermoluminescence Properties of CaB_4O_7

The TL characteristics of glass containing divalent copper were studied by Fukuda *et al* [124]. The TL of X-ray irradiated copper doped borate compunds (0.01 to 1.0 mol %) is studied. The thermally stimulated luminescence for X-ray irradiated glass indicated maxima in temperature area 90-100 °C.

Haghiri *et al.* (2014) reported the dosimeteric features of rare earth Cu and Mn doped CaB_4O_7 nanocrystals sample produced by co-precipitation method. The compound and the morphology of the manufactured nanophosphor were determined by XRD and TEM. Thermoluminescence glow curve of this nanophosphor sample demonstrated two well separated peaks embed at nearly 124 °C and 256 °C. The nanocrystals sample gives good linearity response in the interval of 0.05–3000 Gy [125].

The affected of lithium co-dopant on the TL of certain thermoluminescence phosphors has been reported by Mirjana Prokic [126]. Results indicate that lithium codopant when existing in Tm doped $CaSO_4$, MgB_4O_7, CaB_4O_7, Dy doped $CaSO_4$, MgB_4O_7, CaB_4O_7, Mn doped CaF_2, MgB_4O_7 and MgB_4O_7:Tb TL phosphors causes largest luminescence efficiency either because of very well combination of activator ions or because of development in energy transfer progression.

In 2013, Padlyak and Drzewiecki studied the terbium and dysprosium with doped CaB_4O_7 and $LiCaBO_3$ glasses spectroscopy. A series of borate glasses of maximum optical quality with Tb doped CaB_4O_7, $LiCaBO_3$ and Dy doped CaB_4O, $LiCaBO_3$ compounds including 0.5 and 1.0 mol% Tb_2O_3 and Dy_2O_3 impurity compositions were acquired from associated sample compositions using normal glass improve technology. By EPR and optical spectroscopy it was indicate that the Tb and Dy impurities are combination as Tb^{3+} and Dy^{3+} ions in the Ca and Li(Ca) sites of CaB_4O_7 and $LiCaBO_3$ glasses network, respectively. The luminescence stimulation and emission spectra also luminescence kinetics of the Tb^{3+} and Dy^{3+} centres in the CaB_4O_7 and $LiCaBO_3$ glasses have been researched and determined in comporable with acquired initial conclusion for Tb^{3+} and Dy^{3+} centres in the $Li_2B_4O_7$ glasses. Luminescence kinetics indicate only exponential decay for Dy^{3+} and Tb^{3+} centres in the $LiCaBO_3$ and CaB_4O_7glass network. The obtained results show that the CaB_4O_7 and $LiCaBO_3$ glasses are encouraging luminescent samples, operating in green and yellow blue spectral fields, when activated with Tb^{3+} and Dy^{3+} ions, respectively [127].

The TL in sintered CaB_4O_7 doped with activators Eu, Dy, Pb and Cu was investigated bu Y.Fukuda and his friends [128].

Glass sample with CaB_4O_7 and $CaBO_4$, such as the $x CaB_4O_7$ - (100-x) CaB_2O_4 system ($0 \leq x \geq 100$ wt%) were acquired by the conventional melting and quenching technique by S.S. Rojas [129]. The dysprosium doped and lithuim co-doped 80% of CaB_4O_7– 20% of CaB_2O_4 glass materials were worked by the thermoluminescence method. The additional of dysprosium enhanced the signal susceptibility in concerning three times according to the undoped glass material. The additional of lithuim as a co-dopant in this sample induced an interchange to a smaller temperature of approximately 20 °C in the basic glow peak.

2.8 Literature Survey on the Thermoluminescence Properties of BaB_4O_7

Manam and S. K. Sharma firstly reported TL studies of BaB_4O_7 compound [130]. The polycrystalline material of BaB_4O_7 was prepared by a melting technique. The creation of the BaB_4O_7 composition was verified by an XRD work. The composition has orthorhombic structure at room temperature. The thermally stimulated luminescence glow curves of BaB_4O_7 compound when heated at a constant heating rate of 4 °C/s indicate two thermoluminescence glow peaks at 110 and 150 ^{o}C followed by a shoulder around 210 °C.

In 2004, Juan Li and his friends presented thermoluminescence features of dysprosium doped BaB_4O_7:Dy phosphor. The powder sample of Dy doped BaB_4O_7 phospor were synthesised by solid-state method in air with major temperature [131]. The thermoluminescence glow curves and three dimentional thermoluminescence emission spectrum was studied in 20-130 kGy dose range The emission bands about at 480, 575, 660 and 750 nm were noticed in the three dimensional emission spectrum. The experiment conclusion indicates that Dy doped BaB_4O_7 potential use as the materials of gamma radiation thermoluminescence dosimeter for cilinical dosimetry.

Mishra and his friends have studied the relation between mechanoluminescence and thermoluminescence of γ radiation BaB_4O_7:Dy phosphor compound. BaB_4O_7 and BaB_4O_7:Dy phosphor have been prepared by solid state reaction method and its TL and mechanoluminescence has been researched. A one peak at 162 °C along with to shoulders approximately 242 °C and 294 °C was noticed in thermoluminescence glow curve of BaB_4O_7 phosphor. Thermoluminescence intensity increased with added to dopant concentration and extensive band was noticed fort he material having 0.5 mol% of dopant concentrations. For larger concentrations of dopant, the concentration quenching was occurred [132].

Sangeeta and S.C. Sabharwal reported the kinetics of TSL emission from BaB_2O_4, CaB_2O_4 and SrB_2O_4 has been researched employing both isothermal decay analysis and peak shape techniques in 2004 [133]. The emission spectra of CaB_2O_4 and SrB_2O_4 were constituted to comprise two extensive emissions: single in the ultraviolet and the other in the blue green areas [133].

CHAPTER 3

THEORY

3.1 Neutrons

The invention of neutrons in 1932 lead the wide usage of nuclear energy in present day. The radiation manufactured in nuclear reactors is completely because of neutron interactions with the samples in the reactor core. A neutron has concerning the like atomic mass same as a proton, however dissimilar a proton, it has no electrical charge. A proton with its plus charge is forcefully repelled form a nucleus, however a neutron is not due to not having a charge.

Figure 3.1: A Proton is repelled; however a neutron is not [134].

Neutrons have no charge, are not pushing back if they closing nuclei, and could essentially go into nuclei. It is for this cause that they are of large significant in nuclear physics when you same, they are the blade with which the scientists can nudge about in the nucleus. Because of neutrons are electrically neutral, they reason no ionisation immediately, and thus they could travel large distant whereby substance, more same gamma rays.

The most important feature for producing neutrons is that they have to be ejected out of the nucleus. They arise from the nucleus with a large velocity, having energies of up to a few MeV. Majority of these neutrons are decelerated by collisions with nuclei. Later maybe a hundred of as collisions, the velocity of the neutrons is lower to as an rate that they have concerning the like kinetic energy as

the particles of their around. The kinetic energy of these particles is fundamental the temperature of the sample they constitute. For this reason, the neutrons that are slowed down to the similar energy level of the surrounding particles are called thermal neutrons. They are usefull for triggering fission reaction. Thermal neutrons continue to drift until they are captured by a particular nucleus [134].

The route in which neutrons interact with substance depends to a major range on their energies. For this cause, neutrons are frequently definited by energy as the under mentioned:

- Fast Neutrons - above 8 keV
- Slow Neutrons - below 8 keV
- Thermal Neutrons - about 0.025 eV

Although the thermal neutrons have as little energy as possible, thermal neutrons should not have a residual effect. They still exits and travel at speeds of 2.2 km/s [135-138].

3.2 Neutron Sources

3.2.1 Fission

Along with the techniques of decay argued precedently, there is still else methods in which weighty nuclei like uranium can reach a stable level. This is by separating into two sections. The separating of a nucleus is named fission, and the two sections of the initial nucleus are named fission fractions. These fission fractions are not a thing other than two lesser nuclei. Spontaneous fission of uranium occurs comparatively rarely. It happens almost seven times a second in one kilogram of uranium.

Figure 3.2: Fission [134].

Nevertheless, in the later years of 1930's it was find out that Uranium-235 can be caused to fission by thermal neutrons. A neutron can go into the Uranium-235 nucleus to create a stimulated composition nucleus, Uranium-236*. The asterisk * demonstrates the stimulation level. Nuclear fissions, and also the fission fractions, it besides creates 1/3 additive neutrons, and a large amount of energy in the generate of warmth and gamma ray

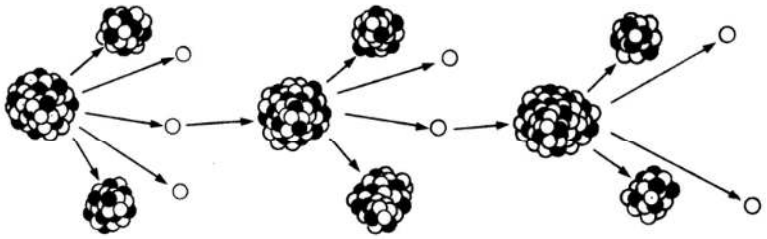

Figure 3.3: A chain reaction [134].

The production of additional neutrons in every fission carriers a significance. If these additional neutrons can be formed to reaction with other U-235 nuclei to create still very fissions, thus that every fission conclusions in extra fissions, a "self-sufficient" or chain reaction happens. This does occur when the suitable circumstances are satisfied. The fission neutrons occupy a broad energy range, however have an average energy of 2 MeV. Fission neutrons lost energy by means of collisions with the fuel, compression tubes, construction sample and moderator.

3.2.2 Photoneutrons

Gamma photons with energies higher than 2.21 MeV can to interaction with the deuterium nuclei in weighty water to create so-named photoneutrons.

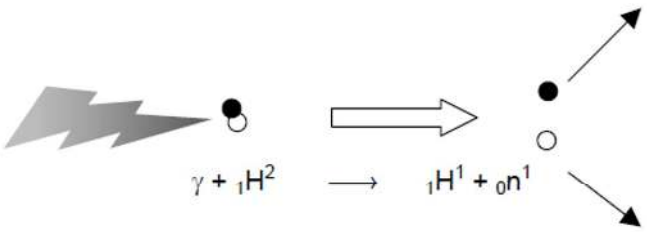

Figure 3.4: Photoneutron generation with deuterium [134].

In CANDU reactors, this interaction happens anywhere deuterium (D_2O in the reactor) is being exterminated by great energy gamma radiation. When the reactor is closedown, the photoneutron creation reduces [134].

3.2.3 Neutron Sources Used for Calibration

Whole nuclear positions have a neutron source for calibrating neutron equipment. Assuming that an alpha emitter, as americium-241, is mixture with beryllium, the alpha fragments emitted by Am-241 can induce following interaction:

$$^{4}_{2}\mathrm{He} + ^{9}_{4}\mathrm{Be} \rightarrow ^{12}_{6}\mathrm{C} + ^{1}_{0}\mathrm{n}$$

We have two sources in such a way; one for calibrating the reactor activates equipment and one for analyzing the neutron inquiry meters.

3.3 Neutron Reactions

The reactions of neutrons with nuclei are named neutron reactions. The most commonly known neutron interactions are [135-138]: Fission, scattering and activation.

3.3.1 Fission

It is the breakdown of the nucleus by interaction of the nucleus with thermal energetic neutrons (E $\approx$ 0.025 eV). After the fission, two product cores are energized in large quantities as well as other by-products [139, 140].

3.3.2 Neutron Scattering Reactions

(a) Elastic Scattering

The energy is that the neutrons, which are in the MeV range, have lost their energy and brought it to the fountain. This is scattering (n, n) type reactions, in which the total kinetic energy of the two colliding particles is preserved. The neutron multiplies the atom's core and transfers some of its kinetic energy to the nucleus. The smaller the mass of the nucleus, the greater the kinetic energy to be received by the nucleus. It then deviates from the direction of arrival and moves away from the nucleus. In this case there is no change in the structure of the nucleus. In such collisions, slow neutrons can transfer a small fraction of their energy to the core due to their small kinetic energy [139].

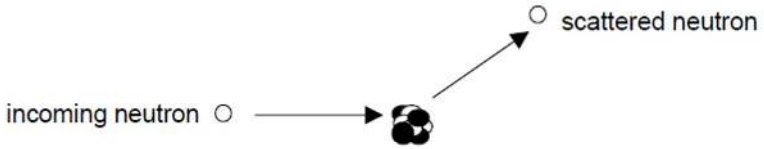

Figure 3.5: Elastic scattering [134].

(b) Inelastic Scattering

This scattering occurs when (n, n), (n, 2n) type reactions occur. Neutron with sufficient energy (E=1 MeV veya E>1 MeV) stimulates the nucleus. In this case, the neutron enters the core. This changes the physical structure of the nucleus. This takes a very short time, giving some of the neutron kinetic energy to the core. The core leaves the core in a direction different from the direction of arrival and with a smaller energy than the energy initially possessed. Below this energy value, it is only scattering. In such reactions the nucleus is left in an stimulated state. Then the excited nucleus is degraded by emitting radiation like a gamma ray [139].

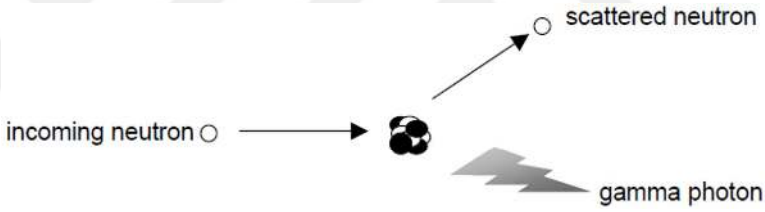

Figure 3.6: Inelastic scattering [134].

3.3.3 Neutron Activation Reactions

When an energetic neutron is incident on a nucleus and captured by it, the necleus becomes unstable. This newly formed unstable nucleus immediately ejects a proton or an alpha particle to form a different element, or radiate a gamma photon to lose its excess energy. The reaction which the unstable nucleus undergo is determined by the excess enery of the incident neutron. These reactions can be explained with the following examples;

(a) Neutron-Proton Reaction (n,p)

Oxygen-16 is a nice instance. It seizes a greater-energy neutron and emits a proton to create nitrogen-16. This is called an (n,p) interaction, since a neutron going in and a proton be released.

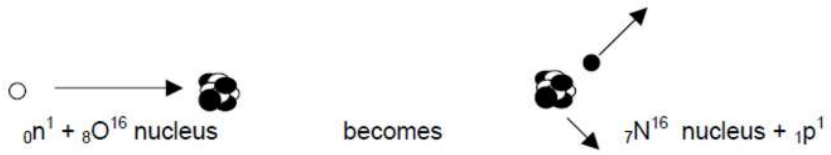

Figure 3.7: (n,p) Interaction of Oxygen-16 [134].

The product, nitrogen-16, is radioactive. It is a beta-gamma emitter with a half-life of 7.2 s. What is much more significant is that it besides emits much great-energy gamma photons in the area of 6 to 7 MeV. At potential, these gamma photons spread by the N-16 that was generated by (n,p) interactions with oxygen atoms in slight or weight water are significant in radiation conservation.

(b) Neutron-Alpha Reaction (n,α)

An instance is the slow neutron seize by boron-10 (^{10}B) in this interaction:

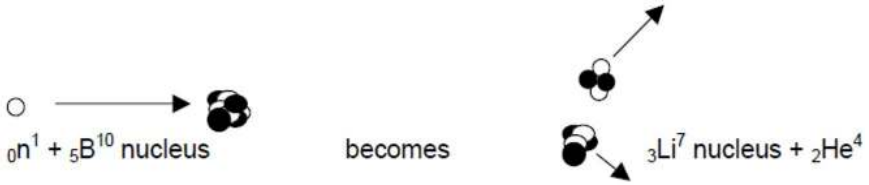

Figure 3.8: (n,α) Interaction of Boron-10 [134].

Both the alpha particle and the lithium nucleus have kinetic energy, and both induce ionisation in the general method. This is a significant interaction for equipments accustomed to receive slow neutrons and thermal neutrons.

(c) Neutron-Gamma Reaction (n,γ)

This is one of the high usual neutron interactions. The recent nucleus created emits just a gamma photon. This means that the product nucleus is an isotope of the similar element as the initial nucleus (its atomic weight will have raised by one). Much more elements will subjected like interactions, however the interaction is most probably to happen with thermal neutrons than with fast neutrons. This interaction is usual named radiative seize since a gamma photon is radiated when the neutron is seized. There are many examples; we will use only four.

1. The most easy neutron-gamma interaction (n,γ) happens with hydrogen-1 to form deuterium (hydrogen-2) in ${}_0^1n + {}_1^1H \rightarrow {}_1^2H + \gamma$:

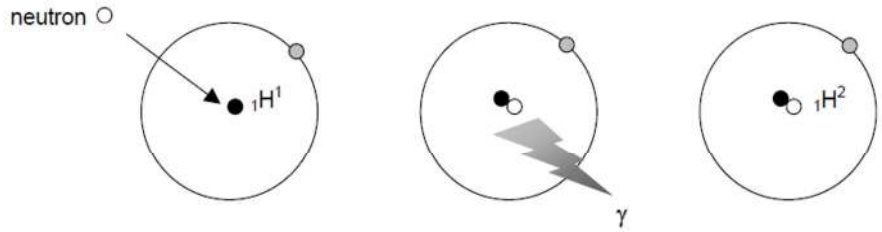

Figure 3.9: (n,γ) Interaction in H-1 to form H-2 [134].

The deuterium produced is a steady nuclide. But, many yields of (n,γ) interactions are radioactive and are beta-gamma emitter.

2. Deuterium itself can undergo an (n,γ) interaction as in ${}_0^1n + {}_1^2H \rightarrow {}_1^3H + \gamma$:

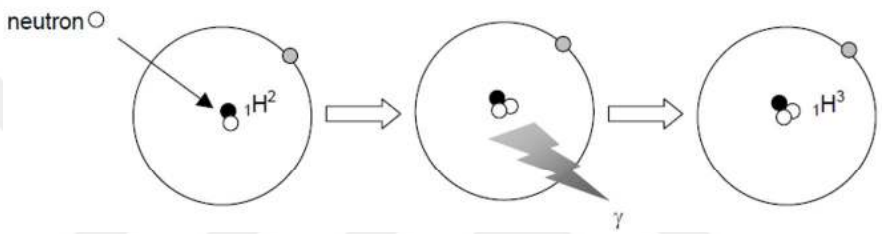

Figure 3.10: (n,γ) interaction in H-2 to generate H-3 [134].

The product is the hydrogen isotope with a mass number of three. This appears a suitable level to examination the three hydrogen isotopes shortly:

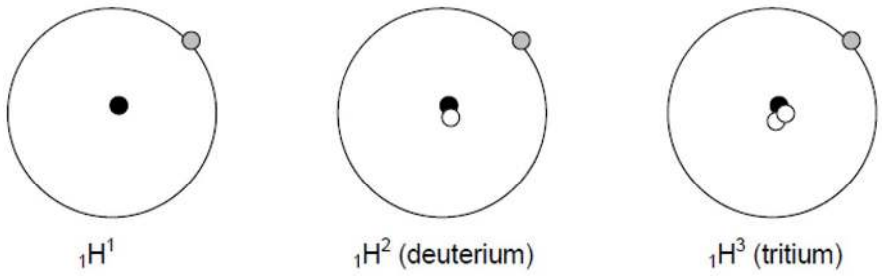

Figure 3.11: The three isotopes of Hydrogen [134].

Whole three atoms are isotopes of hydrogen and consequently their nuclei every include one proton. Moreover, the deuterium nucleus includes one neutron, and the tritium nucleus includes two neutrons. As a result chemically whole three isotopes are same, however hydrogen and deuterium are steady; tritium is radioactive. Tritium has a half-life of 12.3 years. It emits beta particles of lesser energy (high energy= 18 keV):

$_1H^3$—— $_2He^3$+ β^- (no gamma is emitted)

Tritium is produced in heavy water reactors where deuterium is against to slow neutrons. It is the most significant radionuclide in CANDU reactors.

3. An significant (n,γ) interaction is that sustained by argon-40:

$_0n^1$+ $_{18}Ar^{40}$ —— $_{18}Ar^{41}$+ γ

Argon-41 is a beta-gamma emitter with a half-life of 1.8 hours. Because argon constitute about 1% of air, radioactive argon-41 is going to be formed in whole places where air is exposed to neutrons.

4. As a final for instance, deal with the (n,γ) interaction of U-238 in the nuclear fuel:

$_0n^1$ + $_{92}U^{238}$ —— $_{92}U^{239}$ +γ

The yield U-239 is a β-,γ emitter with a half-life = 23 minutes.

$_{92}U^{239}$ —— $_{93}Np^{239}$ + β^-,γ

The daughter is an element of atomic number 93 named neptunium (Np) which does not exist in nature. Np-239 is besides a beta-gamma emitter and it has a half-life of 2.3 days:

$_{93}Np^{239}$ —— $_{94}Pu^{239}$ + β^-,γ

The daughter is plutonium-239, one more element which does not obtain generally. Pu-239 is a continuing alpha emitter. It has nuclear features partially identical to uranium-235, since neutrons may induce it to fission. Fuel that is in a performing reactor will progressively generate a few Pu-239 as a conclusion of the reactions over, and afterwards this Pu-239 will fission and produce heat similar to U-235.

Whereas there are several sources of neutrons at Ames, scientists should still have a usual familiarization with this type of radiation. Neutrons are given off by just the weightiest elements like uranium. These weighty particles are relatively great and have a tendency to split spontaneously down the medium producing two recent elements with nuclei that are the most closely same in magnitude. The ejected neutrons composes a small portion of the end product of splitted nucleuses. They possess enough energy to repeat a new splitting reaction if it is the vicinity of another large nucleus. The number of splitting nucleus can

increase rapidly by interacting with these ejected neutron. This process is called chain reaction if there are sufficient nuclei in the vicinity. These interactions are used in nuclear reactors to warmth water for producing electricity.

Neutrons are able to besides be syntheticly produced by equipments user alpha emitters, for example radium, if the alpha emitter is confined with by a metal like beryllium. The effect of the alpha particle on the beryllium nucleus is to cause it to split and emit a neutron in the progression. The neutron has no charge and thus can be most entering. The quantity of shielding essential for decreasing a neutron flow to a reliable state is immediately connected with the energy of the neutrons in the flow. Several centimeters of shielding will ensure enough prevention from slow neutrons; however a few feet of shielding may be essential for the very energetic neutrons. Shielding is very well carrying out by utilizing hydrogen wealth samples such as water, Plexiglas, or paraffin.

Associated with protons, neutrons generate the nucleus, keeep along with by the powerful force. The neutron is a baryon and is noted to be comprised of two down quarks and one up quark [141].

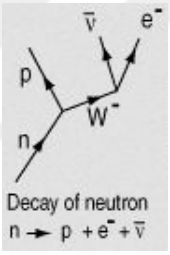

Figure 3.12: Decay process of neutron.

A free neutron will decay with a half-life of almost 10.3 minutes; however it is steady when jointed into a nucleus. The decay of the neutron includes the weak interaction as demonstrated in the Feynman diagram to the true. This actual is significant in samples of the early universe. The neutron is almost 0.2% more massive magnitude than a proton, which interpretations to an energy distinction of 1.29 MeV.

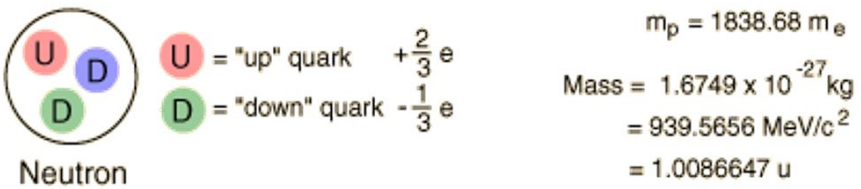

Figure 3.13: Feynman diagram.

The decay of the neutron is relevant to a quark conversion because of this a down quark is surrounded to an up by the weak interaction. The approximate half-life of 10.3 min/0.693 = 14.9 minutes is appallingly lengthy for an atom decays that product 1.29 MeV of energy. You would say that this decay is gradually "downwards" in energy and could be hoped for advance quickly. It is likely for a proton to be converted into a neutron; however you have to provide 1.29 MeV of energy to arrive the threshold for that conversion. In the many initial levels of the big bang if the thermal energy was higher than 1.29 MeV, we estimate that the conversion among protons and neutrons was progression smoothly in both positions such as there was an actually same number of protons and neutrons.

A free neutron having a half-life of about 10.3 minutes will decay if it is not captured by a nucleus. Beta decay with an emission of an electron and an electron antineutrino can be observed after the neutron capture. The decay of the neutron involves the weak interaction as indicated in the Feynman diagram to the right.

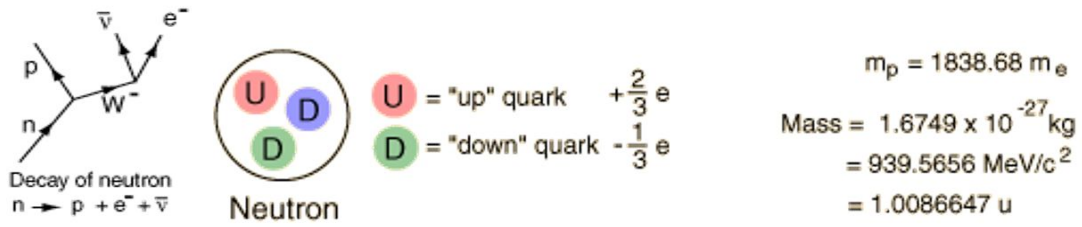

Figure 3.14: Feynman diagram.

A much particular diagram of the neutron's decay definitions it as the conversion of one of the neutron's down quarks into an up quark. It is an instance of the type of quark conversions that are included in very nuclear progression, involving beta decay [141].

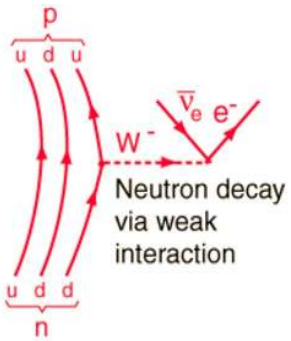

Figure 3.15: Neutron decay via weak interaction.

The decay of the neutron is a well instance of the investigation what causes the find out of the neutrino. An analysing of the energetics of the decay may be employed to exemplify the quandarys what compare to initial scientists of this progress.

Using the conception of binding energy, and to presenting the masses of the atoms by their remain mass energies, the energy product from neutron decay may be to take into account from the atom masses. The energy product is conservatively symbolized by the Q. Since energy and momentum need be protected in the decay, it will be indicate that the lighter electron will make away with very of the kinetic energy. With a kinetic energy of this size, the relativistic kinetic energy to explain need be used.

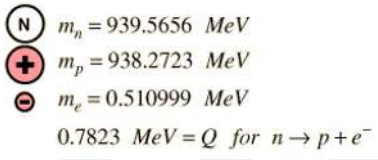

Figure 3.16: Rest mass energy of particles.

For the moment we assume indirectly that the decay includes only the proton and electron as yields. The energy product Q could then be subdivided among the proton and electron. The electron will obtain very of the kinetic energy and will be relativistic, however the proton is non-relativistic.

The energy equate is thus

$$Q = 0.7823\text{MeV} = \text{KE}_e + \frac{1}{2}m_p v_p^2 = \text{KE}_e + \frac{p_p^2 c^2}{2m_p c^2} \tag{3.1}$$

In the remain limits of the neutron, preservation of momentum necessarys

$$pc_{electron} = - pc_{proton}$$

and $\text{pc}_{electron}$ may be termed in conditions of the electron kinetic energy

$$(pc_{electron})^2 = KE_e^2 + 2KE_e.m_e c^2 \tag{3.2}$$

The energy equate thus occurs

$$0.7823\text{MeV} = \text{KE}_e + \frac{\text{KE}_e^2 + 2\text{KE}_e \cdot m_e c^2}{2m_p c^2} \tag{3.3}$$

If you subrogate the numbers for this value of Q, you see that the $\text{KE}_e{}^2$ expressed is insignificant, thus the necessary kinetic energy of the electron can be calculated. The necessary electron kinetic energy for this two-atom decay figure is

$$0.7823MeV = KE_e \left[1 + \frac{m_e}{m_p}\right]; \text{KE}_e = 0.7819\text{MeV} \tag{3.4}$$

In the same way, the momentum of the electron for this two atom decay is enforced to be

$$\text{pc}_{electron} = \sqrt{KE_e^2 + 2KE_e.m_e c^2} = 1.188\text{MeV} \tag{3.5}$$

The available momentum and energy dispersions for the electron are like indicate following [141].

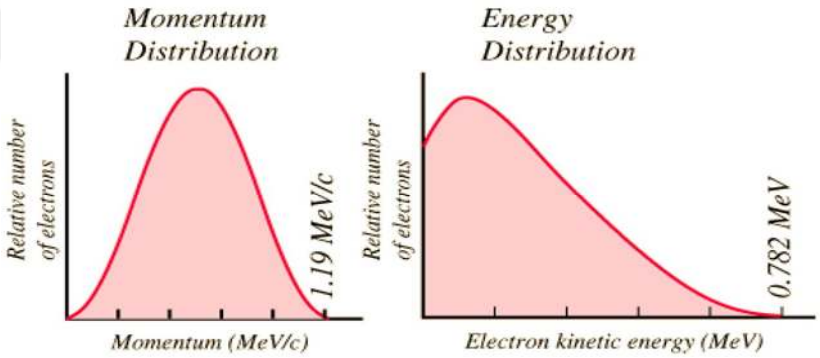

Figure 3.17: Momentum and energy distribution of electrons

The fact that the electrons produced from the neutron decay had continuous distributions of energy and momentum was a clear indication that there was another particle emitted along with the electron and proton. It had to be a neutral particle and in certain decays carried almost all the energy and momentum of the decay. This would not have been so extraordinary except for the fact that when the electron had its maximum kinetic energy, it accounted for all the energy Q available for the decay [141]. So there was no energy left over to account for the mass energy of the other emitted particle. The initial investigators were compared with the quandarys of an atom which could transport closely whole the energy and momentum of the decay; however what had no charge and seemingly no atomic mass.

The mysterious atom was named a neutrino, however it was 25 years before unambiguous empirical investigation of the neutrino was generated by Cowan and Reines. The available perceiving of the decay of the neutron is

$$\mathrm{n} \rightarrow \mathrm{p}{+}\mathrm{e}^{-} + \bar{\nu}_e \tag{3.6}$$

This decay illustrates some of the conservation laws which govern particle decays. The proton in the product satisfies the conservation of baryon number, but the emergence of the electron unaccompanied would violate conservation of lepton number. The third atom need be an electron antineutrino to permit the decay to gratify lepton number protection. The electron has lepton number 1, and the antineutrino has lepton number 1.

CHAPTER 4

MATERIALS AND METHODS

4.1 Materials

The synthesis of the compounds and the majority of the characterization in this study were held in Middle East Technical University, Faculty of Art and Sciences, Department of Chemistry. The syntheses of materials were done in solid-state chemistry laboratory. Thermoluminescence and sensitivity measurements of products against neutron dosimeters were held in Gaziantep University in the Department of Engineering Physics.

All materials and chemicals used in the experimental studies are analytical grade. LiB_3O_5, $Li_2B_4O_7$, BaB_4O_7, CaB_4O_7 and MgB_4O_7 were produced for to be used as neutron dosimeters by solid-state synthesis method and after the synthesizing process compounds were doped with metal ions by high temperature solid state method. The powder forms of Li_2CO_3, $MgCO_3$, $CaCO_3$, $BaCO_3$ and $H_3(^{10}B)O_3$ were used as starting materials for synthesis of LiB_3O_5, $Li_2B_4O_7$, BaB_4O_7, CaB_4O_7 and MgB_4O_7 powder compounds. Al_2O_3, $AgNO_3$, $CuCI_2$, $Ce(SO_4)_2.4H_2O$, $MnCI_2.4H_2O$, $MgSO_4$, Gd_2O_3, Eu_2O_3 and Dy_2O_3 compounds, which are metal sources, were utilized for doping of synthesized LiB_3O_5, $Li_2B_4O_7$, BaB_4O_7, CaB_4O_7 and MgB_4O_7 powder compounds.

4.2 Instrumentation

4.2.1 Powder X-Ray Diffractometer (XRD)

In this study, new dosimetric materials were analyzed by obtaining XRD pattern for determination of crystal lattice, unit cell structure, d-spacing, miller indices and crystal structure. The X-ray Diffractometer employed for the crystal

structure investigations was a Rigaku MiniFlex X-ray Diffractometer with a radiation source of Cu-Kα line (λ=1,54056 Å) to confirm phase purity. The scanning rate within a 2θ range of 3 to 90° is 2 °/min.

4.2.2 Furnace

The samples were heated in Protherm furnaces that are able to heat the samples up to 1500 °C and they have heating rate control parameters.

4.2.3 Fourier Transform Infrared Spectrometer (FT-IR)

The FTIR analysis of borate-based neutron dosimeters that developed in this study was measured vibrational frequencies of bonds between crystal lattice atoms/ions and obtained information about the functional groups in the molecule and observed the effects on the characteristics of the produced dosimeters. The vibrational modes of the produced materials were studied by VARIAN 1000 FTIR spectrometer between wave numbers 500 to 4000 cm^{-1} with 128 scans. The FTIR spectrometer is equipped with attenuated total reflectance (ATR). The resolution was chosen as 8 cm^{-1}.

4.2.4 Differential Thermal Analyzer (DTA) and Thermogravimetric Analyzer (TGA)

In thermal analysis, the physical property of a material was measured as a function of temperature. The chemical changes in the structure of the material were also observed from the physical measurement results. In this study, the physical properties of the borate compounds doped with metal ions were measured before and after the doping process to determine the melting points, the water outlet temperatures between the crystal layers of the dehydration event, the dehydration temperature and the mineral phase formation of the crystal structure water. In order to assess the thermal behavior of the samples as well as their chemical stability, the differential thermal analysis was carried out in an aluminum crucible at a heating rate of 10 °C/min in atmospheric condition using Pyris 1 Perkin Elmer DTA/TGA simultaneous a differential thermal analyzer and thermogravimetric analyzer. The heating interval was chosen between 30 °C and 930 °C.

4.2.5 Scanning Electron Microscope (SEM)

The SEM analyses were performed by using Zeiss SUPRA 50 VP with which has magnification range between 12-900000, variable pressure between 2 and 133 Pa, and acceleration voltage of 0.1-30 kV.

4.2.6 ^{252}Cf Neutron Source

^{252}Cf source was used for the production of neutron radiations. The samples were irradiated for 1 min at room temperature with a ^{252}Cf neutron+gamma source delivering about 0.08 Gy/min radiation. The all samples were exposed to neutron, ^{252}Cf radiations at room temperature. The average energy of the neutron source is around 2 MeV. The neutron source was purchaced from Eckert & Ziegler Isotope Products GmbH and its calibration was also done by the manufacturer on 01 March 2015.

Figure 4.1: ^{252}Cf neutron source.

4.2.7 Thermoluminescence Reader

The dosimetric properties of the samples were investigated by using Harshaw QS-3500 Manual type TL Reader interfaced to a PC where the TL signals were analyzed. This TL Reader is controlled by a computer simply by means of an RS-232 cable consisting of a temperature control unit, a heater tray, a photomultiplier, a high voltage source, signal amplifiers and translators connected in series to the system. Once the signal collection is done by the TL reader, it is transferred to the computer and controlled by winrems software program specially written under windows and the luminescence curves are taken by this

program. A detailed analysis of the TL luminescence curves gives many physical parameters of the dosimetry studied. With this program, not only the physical parameters of the developed dosimeters are obtained but also a lot of information about the dosimetric properties is obtained.

The glow curves were measured using a platinum planchet at a linear heating rate of 1 °C/s from room temperature (RT) up to 400 °C. To eliminate unwanted infrared lights emitted from heater, a standard clean glass filter always installed in the reader between sample and photomultiplier tube, which has the peak sensitivity of wavelength at ≈400 nm.

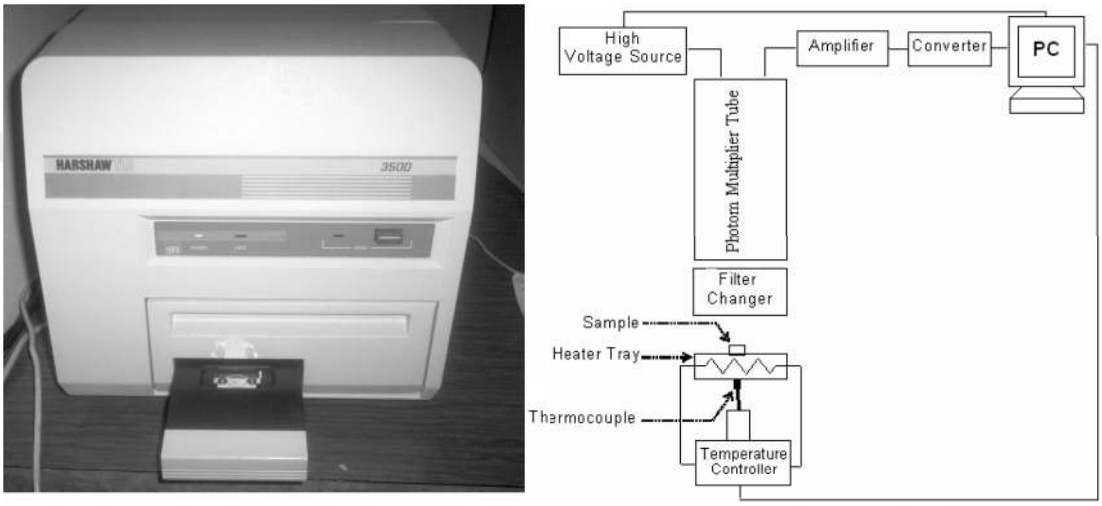

Figure 4.2: The Harshaw TLD system 3500 manual TL reader and the basic block diagram of this reader [142].

4.3 Experimental Procedure

Lithium tetraborate ($Li_2B_4O_7$), lithium triborate (LiB_3O_5), magnesium tetraborate (MgB_4O_7), calcium tetraborate (CaB_4O_7)and barium tetraborate (BaB_4O_7) compounds were synthesized by solid state high temperature method using ^{10}B isotope enriched boric acid (96.5% ^{10}B-$H_3(^{10}B)O_3$).

4.3.1 Synthesis of Lithium Triborate

Lithium triborate was synthesized previously in solid-state chemistry laboratories at Middle East Technical University [143]. The powder samples of undoped LiB_3O_5 were synthesized by high temperature solid state reaction method.

Li_2CO_3 (98.5% pure, Merck) and $H_3(^{10}B)O_3$ (99.5% pure, Merck) were mixed with stoichiometric amounts and 15.0 ml of distilled water was added to obtain of lithium triborate product. The mixture was heated and stirred on magnetic stirrer around 90 °C until a homogeneous mixture was obtained. The heating and stirring of the mixture continued till three four parts of water was evaporated. Then, highly viscous mixture was preheated in a muffle furnace up to 200 °C with 6 °C/min heating rate. It was kept at this temperature for 4 h in order to get rid of residual water in the mixture. After the preheating stage, the cooled sample re-grinded in agate mortar. Afterwards, the furnace was adjusted to heat the sample up to 750 °C with 6.0 °C/min heating rate and retention time was 4 h at this temperature. Intermittent grinding of the mixture facilitates discharge of gases properly while heating solid mixture. The expected reaction is given below.

$$Li_2CO_3 + 6H_3BO_3 \longrightarrow 2LiB_3O_5 + CO_2 + 9H_2O$$

Doping Procedure for Lithium Triborate

All samples were doped with metals according to wt/wt percentage. Synthesized lithium triborate samples were doped with Al_2O_3, $AgNO_3$, $CuCI_2.2H_2O$, $Ce(SO_4)_2.4H_2O$, $MnCI_2.4H_2O$, $MgSO_4$, Gd_2O_3, Eu_2O_3 and Dy_2O_3. 1.0 gram of lithium triborate and certain amounts of dopants were blended in agate mortar. Subsequently, powder form of mixture was placed in porcelain crucible and it was heated up to 750 °C with 4.0 °C/min heating rate in furnace. The retention time was 14 h at that temperature. After heating stage, sample was slowly cooled down room temperature. Metal concentrations and dopant combinations are given in the Tables 4.1 - 4.9.

An example calculation of the mass in grams for 0.1% aluminium (Al) doped compound is given below.

Molecular weight (MA) for Al_2O_3=101.96128 g/mole

MA for Al=26.98153 g/mole

$$\%0.1 \text{ for Al} \rightarrow \frac{10^{-3}\text{g}}{\text{MA for Al}} = \frac{10^{-3}\text{ g}}{26.98153\text{ g/mole}} = 3.706 \times 10^{-5}\text{ mole}$$

Since there are two Al_2O_3

$$\frac{3.706 \times 10^{-5}}{2}\text{ mole} = 1.853 \times 10^{-5}\text{mole} \times 101.96\frac{\text{g}}{\text{mole}} = 1.88 \times 10^{-3}\text{g}$$

Table 4.1: Aluminum Doping Scheme.

LiB_3O_5 Weight (g)	**Aluminum (Al) wt %**	**Al_2O_3 (g)**
1.0	0.1	0.00188
1.0	0.5	0.094 0
1.0	1	0.0188

Table 4.2: Silver Doping Scheme.

LiB_3O_5 Weight (g)	**Silver (Ag) wt %**	**$AgNO_3$ (g)**
1.0	0.1	0.00154
1.0	0.5	0.0077
1.0	1	0.0154

Table 4.3: Cerium Doping Scheme.

LiB_3O_5 Weight (g)	**Cerium (Ce) wt %**	**$Ce(SO_4)_2.4H_2O$(g)**
1.0	0.1	0.0028
1.0	0.5	0.0144
1.0	1	0.028

Table 4.4: Copper Doping Scheme.

LiB_3O_5 Weight (g)	**Copper (Cu) wt %**	**$CuCI_2.2H_2O$ (g)**
1.0	0.1	0.0026
1.0	0.5	0.013
1.0	1	0.026

Table 4.5: Dysprosium Doping Scheme.

LiB_3O_5 Weight (g)	**Dysprosium (Dy) wt %**	**Dy_2O_3 (g)**
1.0	0.1	0.00114
1.0	0.5	0.0057
1.0	1	0.0114

Table 4.6: Europium Doping Scheme.

LiB_3O_5 Weight (g)	**Europium (Eu) wt %**	**Eu_2O_3 (g)**
1.0	0.1	0.001157
1.0	0.5	0.00578
1.0	1	0.01157

Table 4.7: Gadolinium Doping Scheme.

LiB_3O_5 Weight (g)	**Gadolinium (Gd) wt %**	**Gd_2O_3 (g)**
1.0	0.1	0.00059
1.0	0.5	0.0029
1.0	1	0.0059

Table 4.8: Manganese Doping Scheme.

LiB_3O_5 Weight (g)	**Manganese (Mn) wt %**	**$MnCI_2.4H_2O$ (g)**
1.0	0.1	0.02
1.0	0.5	0.1
1.0	1	0.2

Table 4.9: Magnesium Doping Scheme.

LiB_3O_5 Weight (g)	**Magnesium (Mg) wt %**	**$MgSO_4$ (g)**
1.0	0.1	0.0036
1.0	0.5	0.018
1.0	1	0.036

4.3.2 Synthesis of Lithium Tetraborate

Lithium tetraborate was synthesized previously in solid-state chemistry laboratories at Middle East Technical University [144-146].

The powder samples of undoped $Li_2B_4O_7$ were synthesized high temperature solid state reaction method. Li_2CO_3 (98.5% pure, Merck) and $H_3(^{10}B)O_3$ (99.5% pure, Merck) were mixed with stoichiometric amounts and 15.0 ml of distilled water was added to obtain of lithium tetraborate product. The mixture was

heated and stirred on magnetic stirrer around 90 °C until a homogeneous mixture was obtained. The heating and stirring of the mixture continued till three four parts of water was evaporated.

Then, highly viscous mixture was preheated in a muffle furnace up to 150 °C with 6.6 °C/min heating rate. It was kept at this temperature for 4 h in order to get rid of residual water in the mixture. After the preheating stage, the cooled sample re-grinded in agate mortar. Afterwards, the furnace was adjusted to heat the sample up to 750°C with 4 °C/min heating rate and retention time was 4 h at this temperature. Intermittent grinding of the mixture facilitates discharge of gases properly while heating solid mixture. The expected reaction is given below.

$$Li_2CO_3 + 4H_3BO_3 \longrightarrow Li_2B_4O_7 + CO_2 + 6H_2O$$

Doping Procedure for Lithium Tetraborate

All samples were doped with metals according to wt/wt percentage. The synthesized lithium tetraborate samples were used Al_2O_3, $AgNO_3$, $CuCI_2.2H_2O$, $Ce(SO_4)_2.4H_2O$, $MnCI_2.4H_2O$, $MgSO_4$, Gd_2O_3, Eu_2O_3 and Dy_2O_3 metal sources. 1.0 gram lithium tetraborate and the dopants (chosen upon doping combination) were stirred in 15.0 ml of distilled water to form suspension by heating and stirring with magnetic stirrer at 90 °C for 30 min. The suspension in a crucible was put into the furnace to heat up to 150°C with heating rate 6.6 °C/min and kept at this temperature for 3 h. After intermittent grinding of the mixture was performed, the furnace was adjusted to heat the sample up to 700 °C with 4.0 °C/min heating rate and the retention time was 2 h at this temperature. The dopants and their amounts used in single doping system are also given in Tables 4.1 - 4.9.

4.3.3 Synthesis of Magnesium Tetraborate

The powder samples of undoped MgB_4O_7 were also synthesized high temperature solid state reaction method. $MgCO_3$ (98.5% pure, Merck) and $H_3(^{10}B)O_3$ (99.5% pure, Merck) were mixed with stoichiometric amounts and 15.0 ml of distilled water was added to obtain of magnesium tetraborate product. The mixture was heated and stirred on magnetic stirrer around 90 °C until a homogeneous mixture was obtained. The heating and stirring of the mixture continued till three four parts of water was evaporated. Then, highly viscous mixture was preheated

in a muffle furnace up to 400 °C with 4 °C/min heating rate. It was kept at this temperature for 4 h in order to get rid of residual water in the mixture. After the preheating stage, the cooled sample re-grinded in agate mortar. Afterwards, the furnace was adjusted to heat the sample up to 850 °C with 2 °C/min heating rate and retention time was 12 h at this temperature. Intermittent grinding of the mixture facilitates discharge of gases properly while heating solid mixture. The expected reaction is given below.

$$MgCO_3 + 4H_3BO_3 \longrightarrow MgB_4O_7 + CO_2 + 6H_2O$$

Doping Procedure for Magnesium Tetraborate

All samples were doped with metals according to wt/wt percentage. Cu-doped MgB_4O_7, Dy-doped MgB_4O_7, Eu-doped MgB_4O_7 and Gd-doped MgB_4O_7 samples were prepared by taking the starting material in stoichiometric ratio and adding desired amount of $CuCI_2.2H_2O$, Gd_2O_3, Eu_2O_3 and Dy_2O_3 metal source in the mixture. The metal ion doping of the magnesium tetraborate compound was carried out by the magnesium tetraborate synthesis described above. The dopants and their amounts used in single doping system are given Tables 4.4 - 4.7.

4.3.4 Synthesis of Calcium Tetraborate

The powder samples of undoped CaB_4O_7 were synthesized high temperature solid state reaction method. $CaCO_3$ (98.5% pure, Merck) and $H_3(^{10}B)O_3$ (99.5% pure, Merck) were mixed with stoichiometric amounts and 15.0 ml of distilled water was added to obtain of calcium tetraborate product. The mixture was heated and stirred on magnetic stirrer around 90 °C until a homogeneous mixture was obtained. The heating and stirring of the mixture continued till three four parts of water was evaporated. Then, highly viscous mixture was preheated in a muffle furnace up to 750 °C with 4 °C/min heating rate. It was kept at this temperature for 4 h in order to get rid of residual water in the mixture. After the preheating stage, the cooled sample re-grinded in agate mortar. Afterwards, the furnace was adjusted to heat the sample up to 850 °C with 4.0 °C/min heating rate and retention time was 10 h at this temperature. Intermittent grinding of the mixture facilitates discharge of gases properly while heating solid mixture. The expected reaction is given below.

$$CaCO_3 + 4H_3BO_3 \longrightarrow CaB_4O_7 + CO_2 + 6H_2O$$

Doping Procedure for Calcium Tetraborate

All samples were doped with metals according to wt/wt percentage. Dy-doped CaB_4O_7, Eu-doped CaB_4O_7 and Gd-doped CaB_4O_7 samples were prepared by taking the starting material in stoichiometric ratio and adding desired amount of Gd_2O_3, Eu_2O_3 and Dy_2O_3 metal source in the mixture. The metal ion doping of the calcium tetraborate compound was carried out by the calcium tetraborate synthesis described above. The dopants and their amounts used in single doping system are given Tables 4.5 - 4.7.

4.3.5 Synthesis of Barium Tetraborate

The powder samples of undoped BaB_4O_7 were synthesized high temperature solid state reaction method. $BaCO_3$ (98.5% pure, Merck) and $H_3(^{10}B)O_3$ (99.5% pure, Merck) were mixed with stoichiometric amounts and 15.0 ml of distilled water was added to obtain of barium tetraborate product. The mixture was heated and stirred on magnetic stirrer around 90 °C until a homogeneous mixture was obtained. The heating and stirring of the mixture continued till three four parts of water was evaporated. Then, highly viscous mixture was preheated in a muffle furnace up to 400°C with 4 °C/min heating rate. It was kept at this temperature for 4 h in order to get rid of residual water in the mixture. After the preheating stage, the cooled sample re-grinded in agate mortar. Afterwards, the furnace was adjusted to heat the sample up to 800°C with 2.0 °C/min heating rate and retention time was 12 h at this temperature. Intermittent grinding of the mixture facilitates discharge of gases properly while heating solid mixture. The expected reaction is given below.

$$BaCO_3 + 4H_3BO_3 \longrightarrow BaB_4O_7 + CO_2 + 6H_2O$$

Doping Procedure for Barium Tetraborate

All samples were doped with metals according to wt/wt percentage. Dy-doped BaB_4O_7, Eu-doped BaB_4O_7 and Gd-doped BaB_4O_7 samples were prepared by taking the starting material in stoichiometric ratio and adding desired amount of Gd_2O_3, Eu_2O_3 and Dy_2O_3 metal source in the mixture. The metal ion doping of the barium tetraborate compound was carried out by the barium tetraborate synthesis described above. The dopants and their amounts used in single doping system are given tables Tables 4.5 - 4.7.

CHAPTER 5

EXPERIMENTAL RESULTS AND DISCUSSIONS

5.1 Characterization of Materials

As mentioned in chapter 4, the synthesized all materials such as lithium tetraborate, lithium triborate, magnesium tetraborate, calcium tetraborate and barium tetraborate compounds were characterized by X-ray Diffraction (XRD), Fourier Transform Infrared Spectroscopy (FT-IR), Scanning Electron Microscopy (SEM) and Differential Thermal Analysis (DTA) and Thermogravimetric Analysis (TGA) to determine structural and morphological properties. The thermoluminescence (TL) properties of lithium tetraborate, lithium triborate, magnesium tetraborate, calcium tetraborate; and barium tetraborate compounds samples were studied to examine the radiation dosimetric properties of them.

5.1.1 X-Ray Diffraction (XRD) Results

XRD results for Lithium Triborate

The powder X-ray diffraction method has been employed to determine whether the lithium triborate material is correctly produced or not. Besides, this method helps us to examine the effects of dopants on the crystal structure of host materials. The XRD patterns of LiB_3O_5 and metal doped LiB_3O_5 compounds are given in Figures 5.2 - 5.10. The X-ray diffraction patterns are shown with Miller indices (hkl) of synthesized materials and they are well matched with corresponding reference data (JCDPS No: 70-0735) which is shown Figure 5.1. The crystal structure of lithium triborate is showing orthorhombic crystal system with space group $Pna2_1$, unit cell parameters are: a = 8.456 Å, b = 5.133 Å and c = 7.386 Å [147]. When the peak positions of the XRD patterns of undoped and doped lithium triborate samples in the figures from 5.2 up to 5.10 were compared

to each others, no extra peaks detected due to the dopants. However, it was observed that the Al doped lithium triborate compound has extra peaks. It is thought that these extra peaks are due to Al doping.

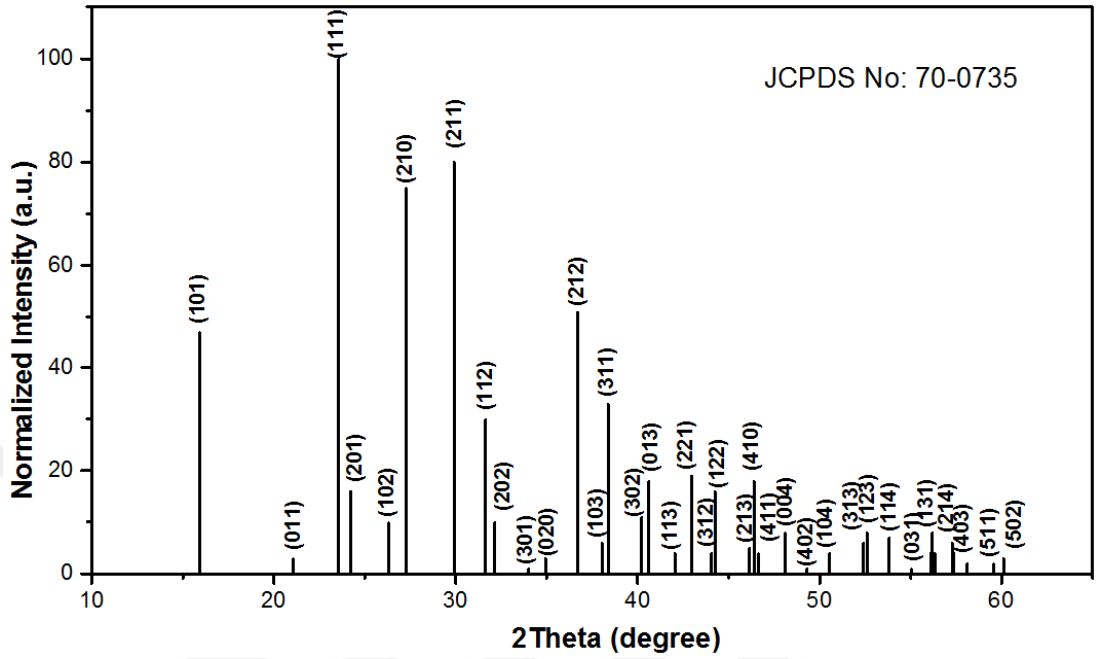

Figure 5.1: XRD Pattern of Lithium Triborate (JCDPS No: 70-0735).

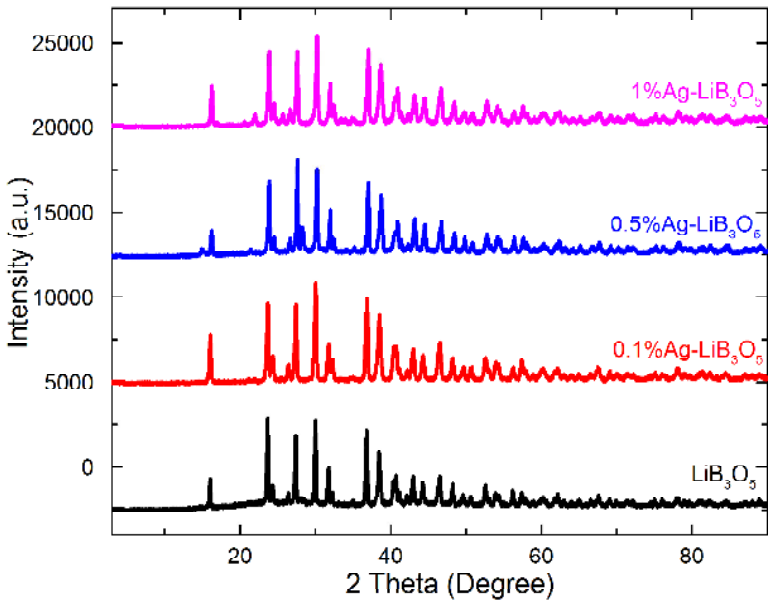

Figure 5.2: XRD pattern of Ag-doped LiB_3O_5 sample.

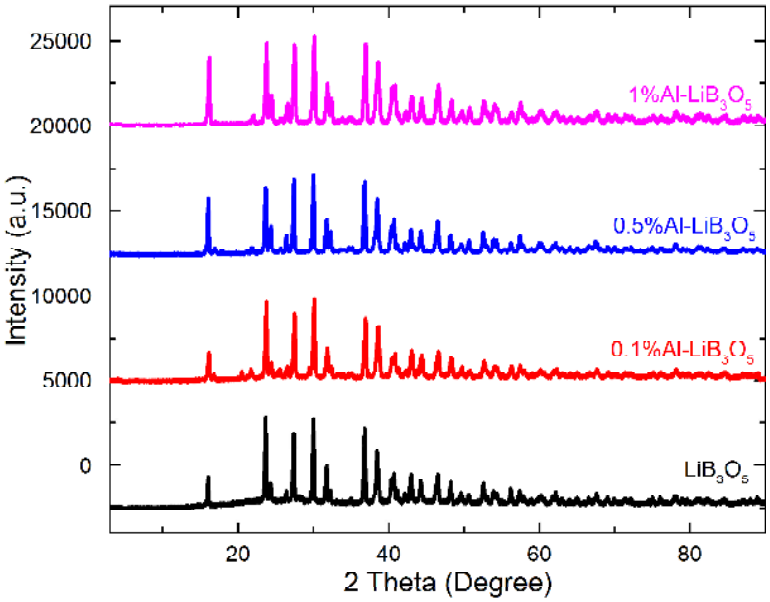

Figure 5.3: XRD pattern of Al-doped LiB_3O_5 sample.

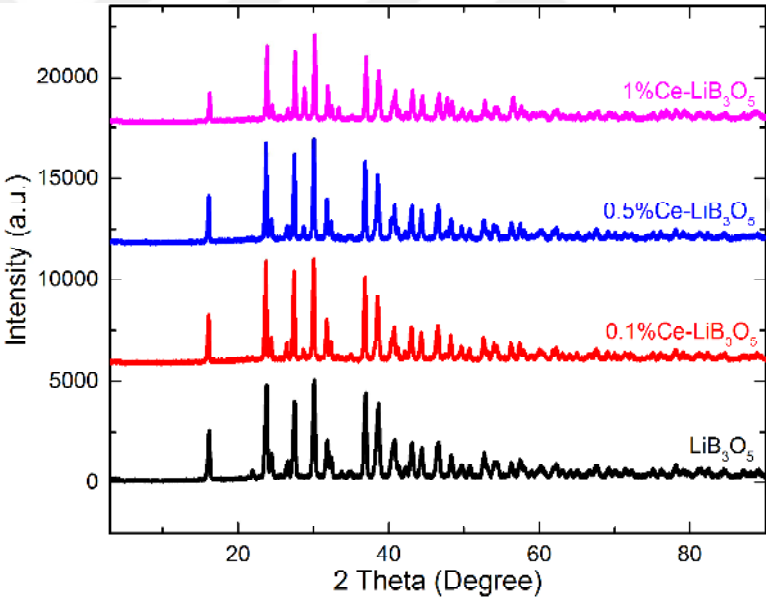

Figure 5.4: XRD pattern of Ce-doped LiB_3O_5 sample.

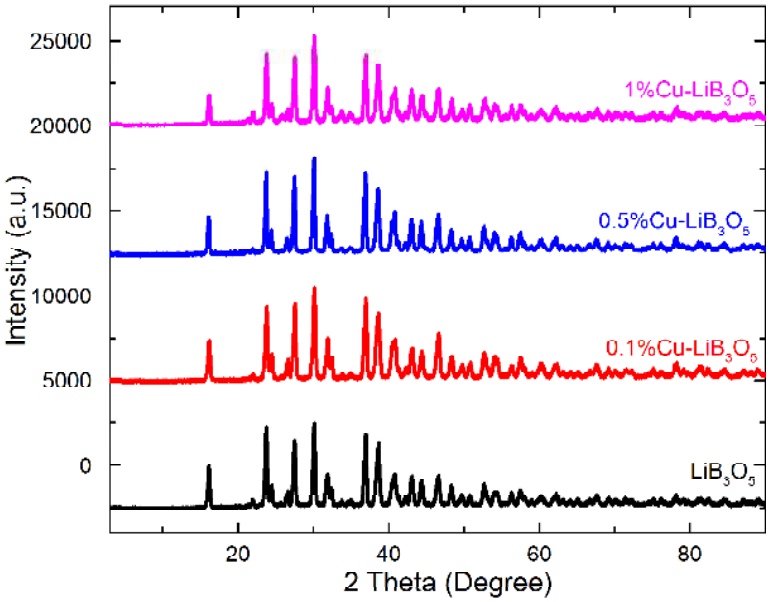

Figure 5.5: XRD pattern of Cu-doped LiB_3O_5 sample.

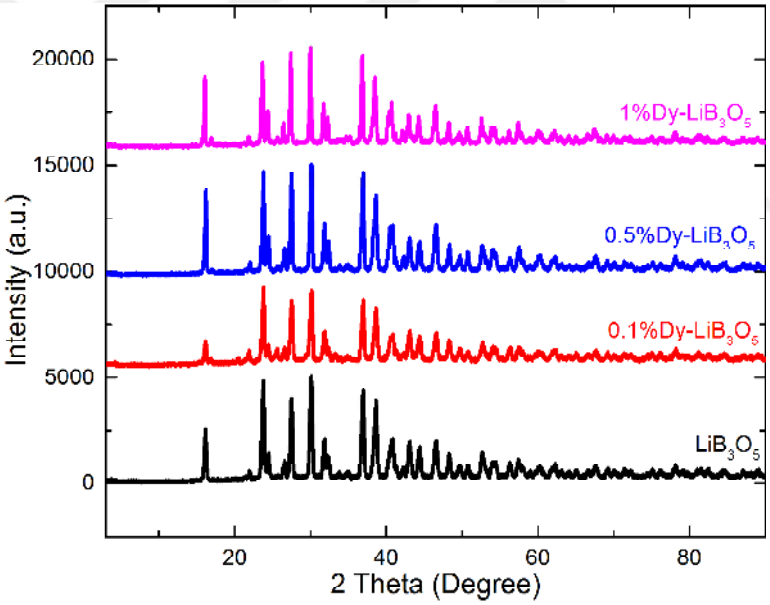

Figure 5.6: XRD pattern of Dy-doped LiB_3O_5 sample.

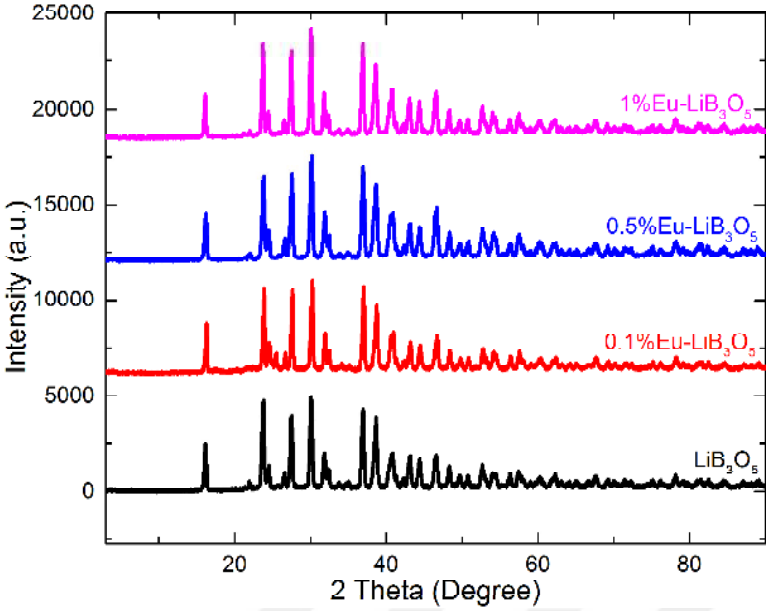

Figure 5.7: XRD pattern of Eu-doped LiB_3O_5 sample.

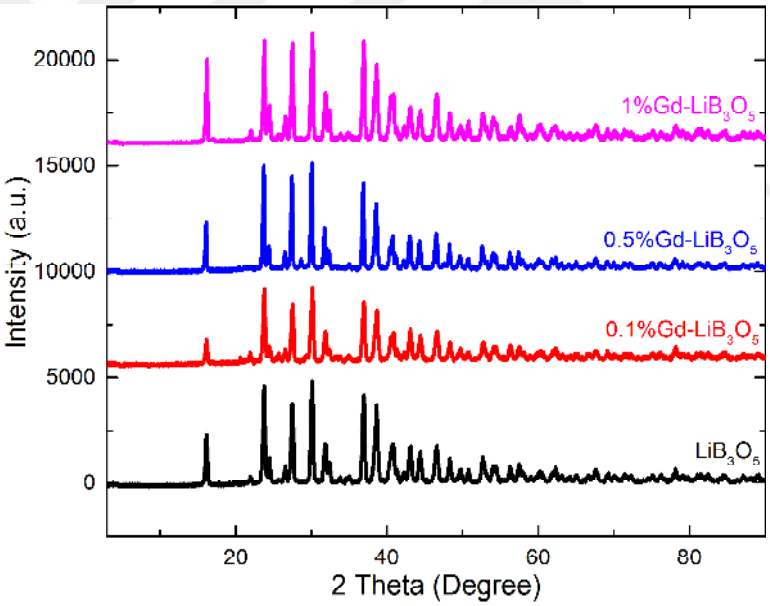

Figure 5.8: XRD pattern of Gd-doped LiB_3O_5 sample.

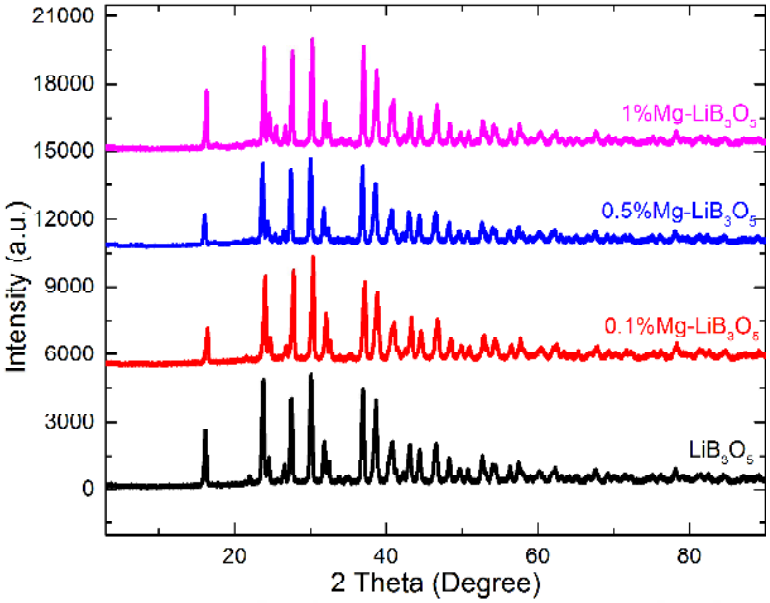

Figure 5.9: XRD pattern of Mg-doped LiB_3O_5 sample.

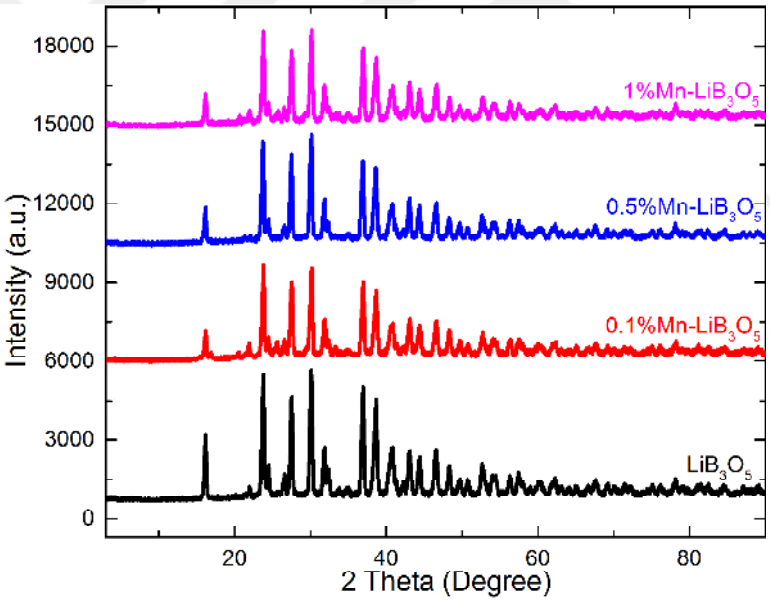

Figure 5.10: XRD pattern of Mn-doped LiB_3O_5 sample.

XRD results for Lithium Tetraborate

The lithium tetraborate crystal consists of two BO_4 tetrahedral units and two BO_3triangles. Two boron atoms and one oxygen atom in tetragonal group are shared by two six membered rings that are two non-planar. The three-dimensional form of lithium tetraborate is constructed by the basic repeating structural block

$(B_4O_9)^{6-}$. In this structure, crystallographically, two inequivalent boron sites and four inequivalent oxygen sites are exist. All of the lithium sites are identical [148].

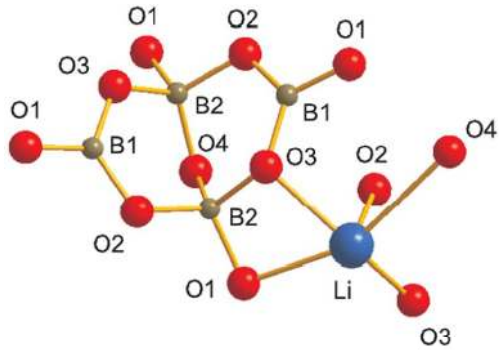

Figure 5.11: Schematic representation of a portion of the $Li_2B_4O_7$ crystal. The five oxygen ions surrounding a lithium site are illustrated along with the basic B_4O_9 group. This view is along an arbitrary direction [148].

The XRD patterns of $Li_2B_4O_7$ and metal doped $Li_2B_4O_7$ compounds are given in Figures 5.13 - 5.21. The X-ray diffraction patterns are shown with Miller indices (hkl) of synthesized materials and they are well matched with corresponding reference data (JCDPS No: 18-0717) which is shown in Figure 5.12. The lithium tetraborate crystallizes in the tetragonal structure. The unit cell parameters are a = 9.477 Å b = 9.477 Å and c = 10.286 Å. The phase composition of the lithium tetraborate samples has been synthesized and consequently characterized and crystal structures of the samples were determined. According to the XRD results, most of the peaks at the diffractogram were found to show overlaps with the JCPDS (Card No.: 18-0717) card. As shown in the diffractograms of the lithium tetraborate samples doped using the solution method, it is observed that there is no change in the structure of lithium tetraborate after doping process. Additionally, the peak intensities of %1 Ce and Eu doped lithium tetraborate samples generally decreased with respect to peak intensity of un-doped lithium tetraborate.

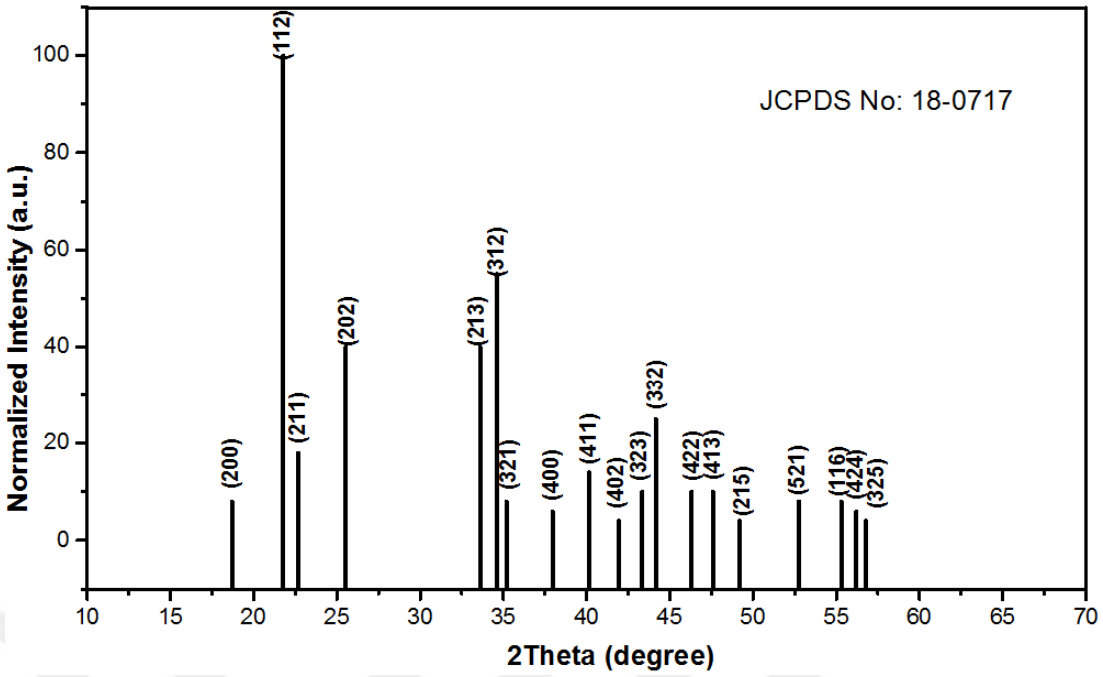

Figure 5.12: XRD Pattern of Lithium Tetraborate (JCDPS No: 18-0717).

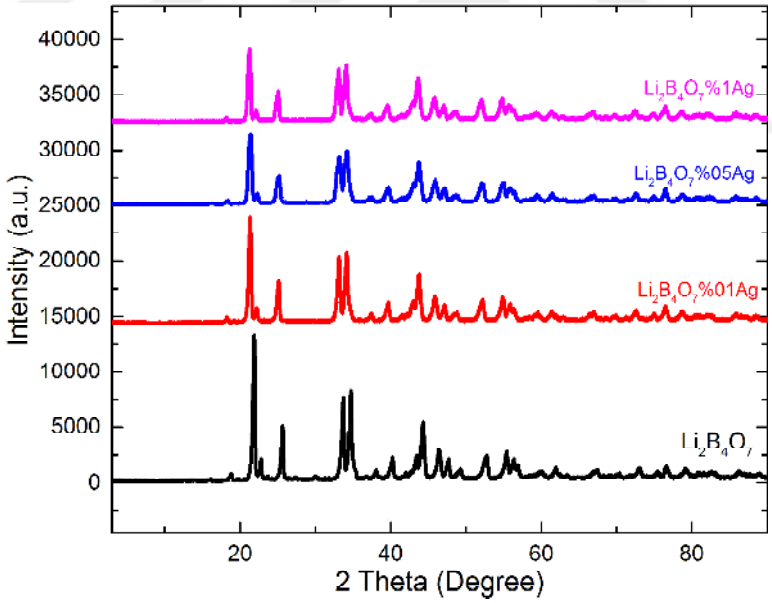

Figure 5.13: XRD pattern of Ag-doped $Li_2B_4O_7$ sample.

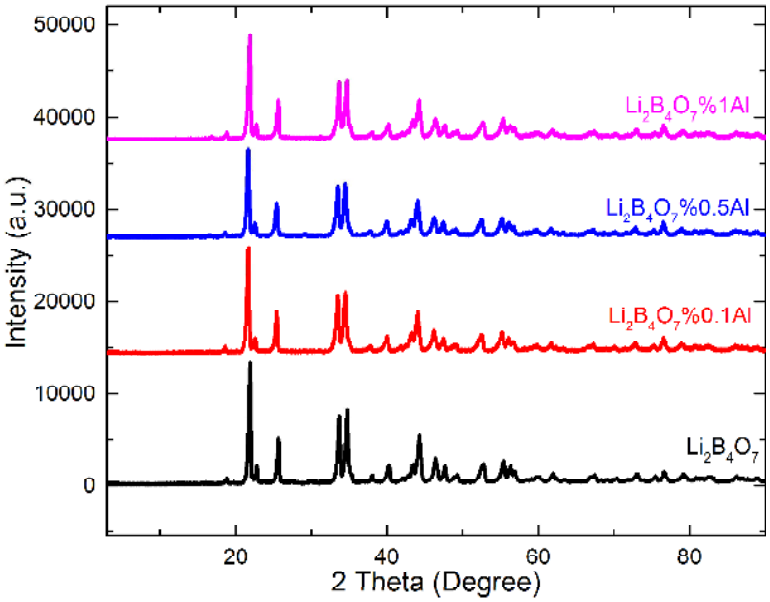

Figure 5.14: XRD pattern of Al-doped $Li_2B_4O_7$ sample.

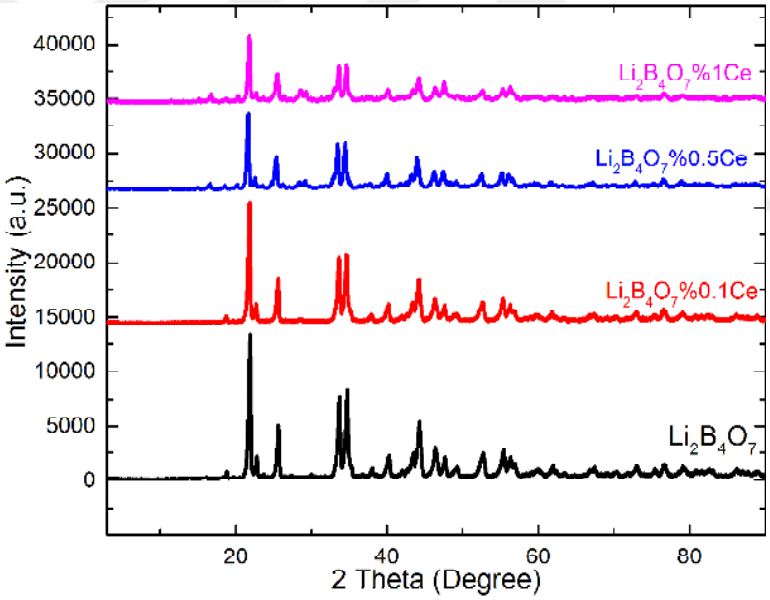

Figure 5.15: XRD pattern of Ce-doped $Li_2B_4O_7$ sample.

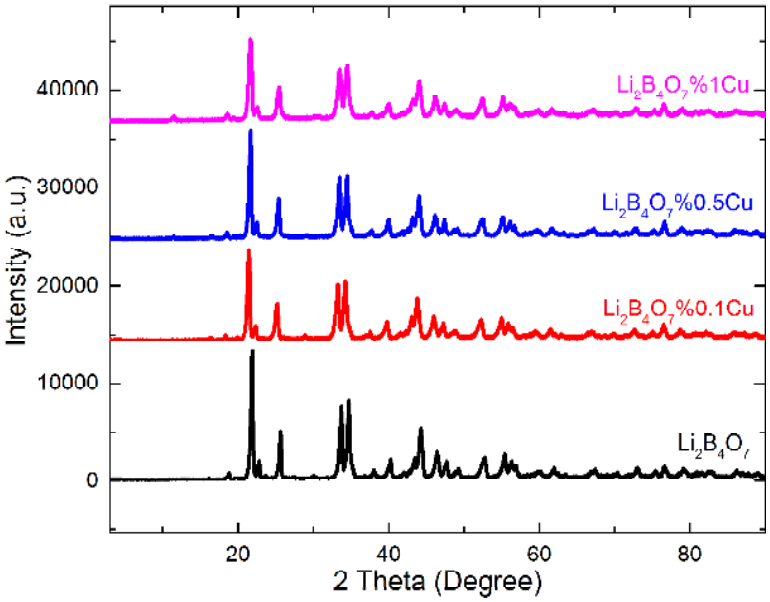

Figure 5.16: XRD pattern of Cu-doped $Li_2B_4O_7$ sample.

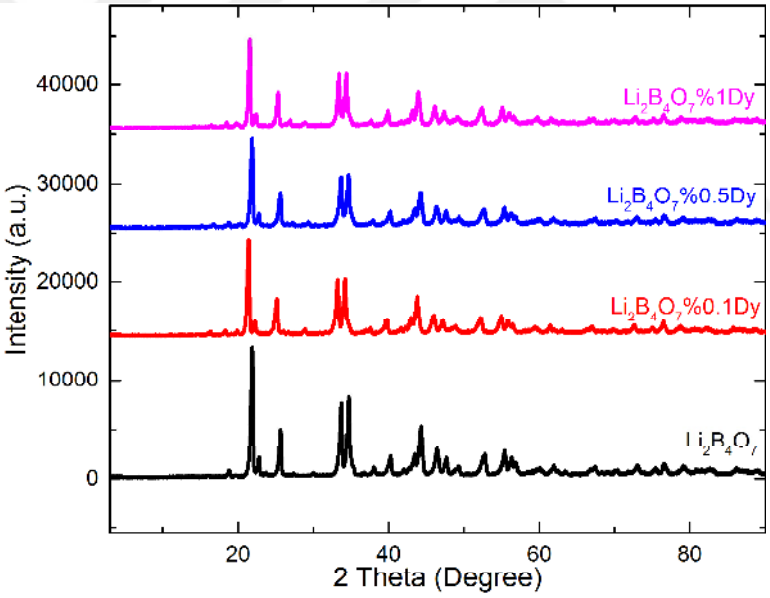

Figure 5.17: XRD pattern of Dy-doped $Li_2B_4O_7$ sample.

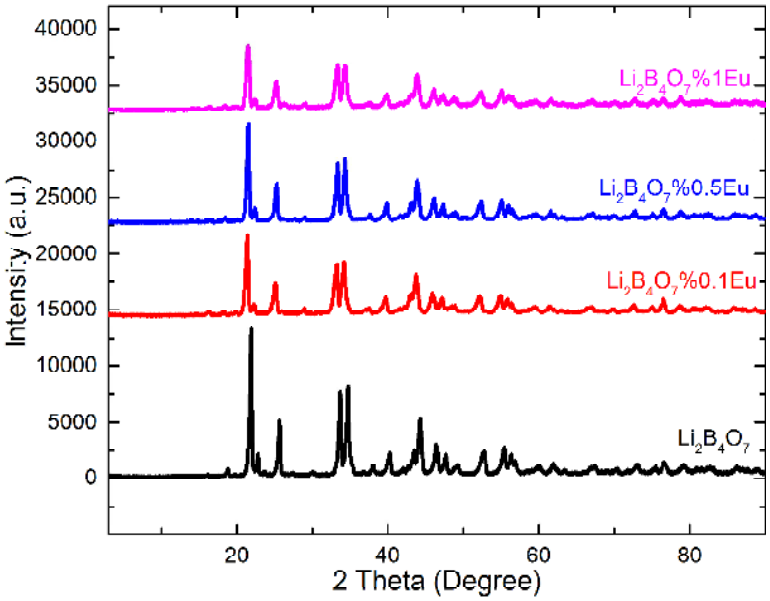

Figure 5.18: XRD pattern of Eu-doped $Li_2B_4O_7$ sample.

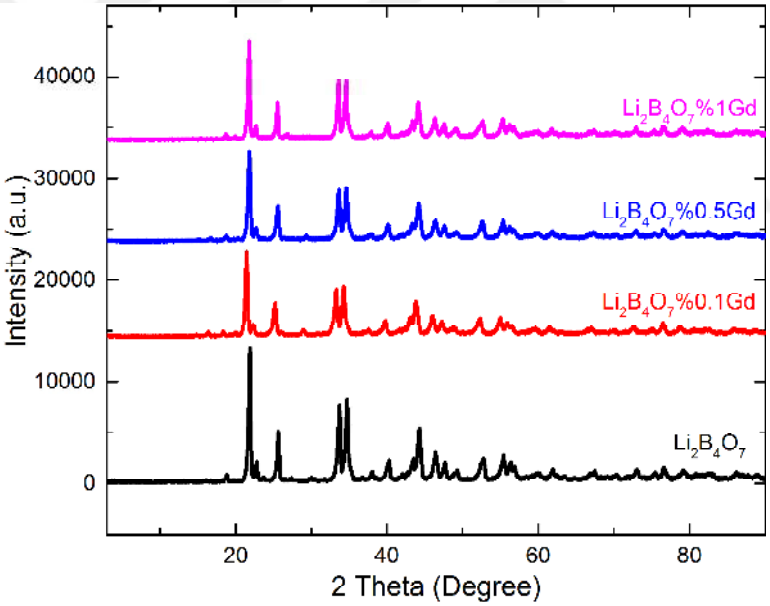

Figure 5.19: XRD pattern of Gd-doped $Li_2B_4O_7$ sample.

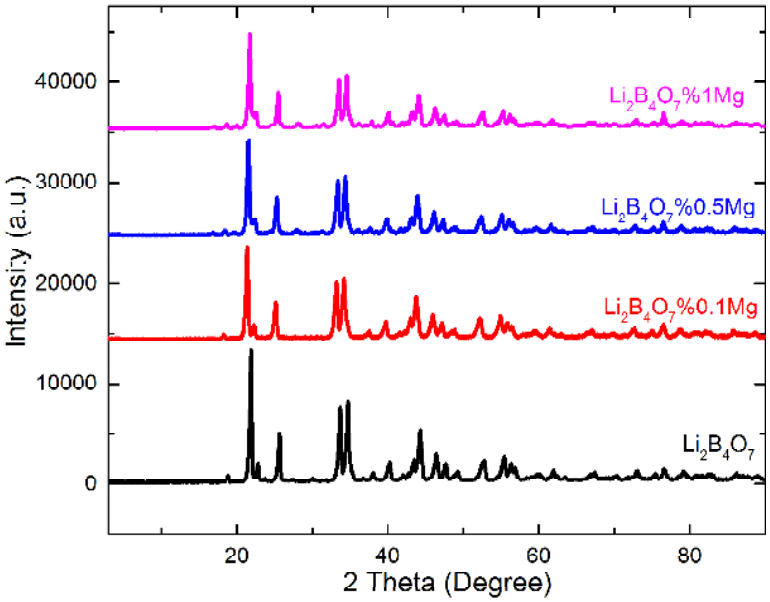

Figure 5.20: XRD pattern of Mg-doped $Li_2B_4O_7$ sample.

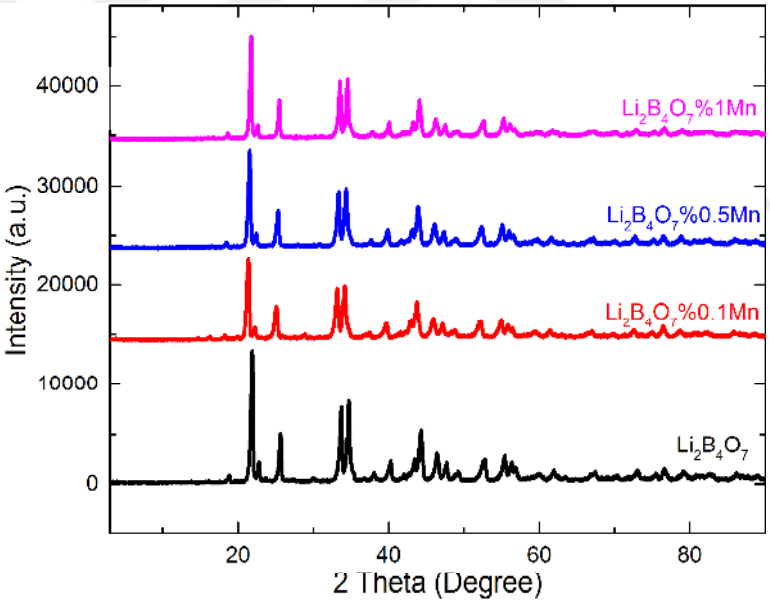

Figure 5.21: XRD pattern of Mn-doped $Li_2B_4O_7$ sample.

XRD results for Magnesium Tetraborate

The XRD patterns of MgB_4O_7 and metal doped MgB_4O_7 compounds are given in Figures 5.23 - 5.26. The X-ray diffraction patterns are shown with Miller indices (hkl) of synthesized materials and they are well matched with corresponding reference data (JCDPS No: 31-0787) which is shown Figure 5.22. The

magnesium tetraborate indicates an orthorhombic structure. The unit cell parameters are a = 8.596 Å b = 13.729 Å and c = 7.956 Å. The XRD measurements were performed to determine the phase composition of the magnesium tetraborate compounds which has been synthesized by the solid state high temperature method. According to the XRD results, most of the peaks in the diffractogram were overlapped with JCPDS (Card No: 31-0787) card.

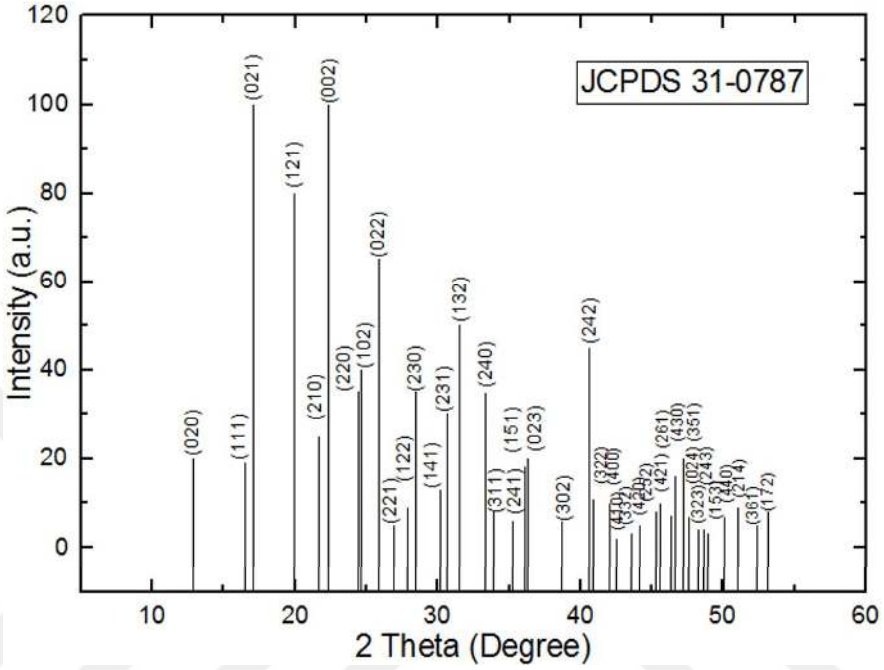

Figure 5.22: XRD Pattern of Magnesium Tetraborate (JCDPS No: 31-0787).

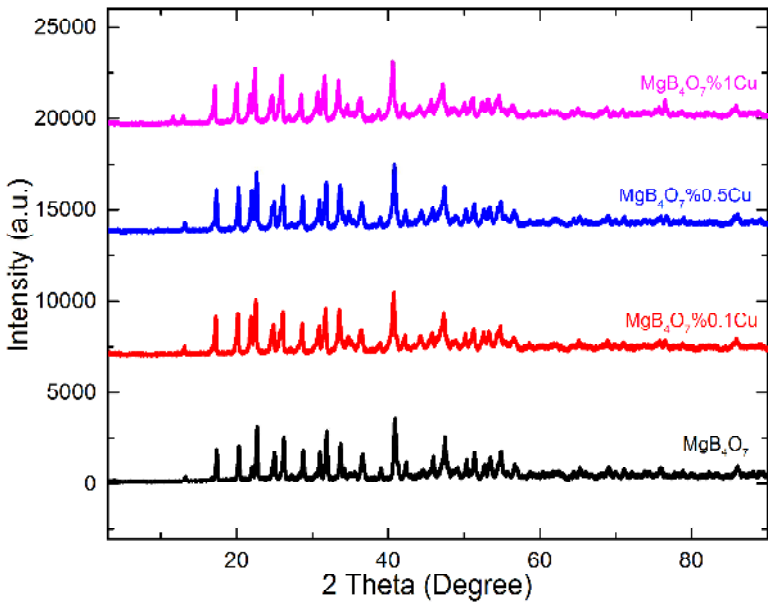

Figure 5.23: XRD pattern of Cu-doped MgB_4O_7 sample.

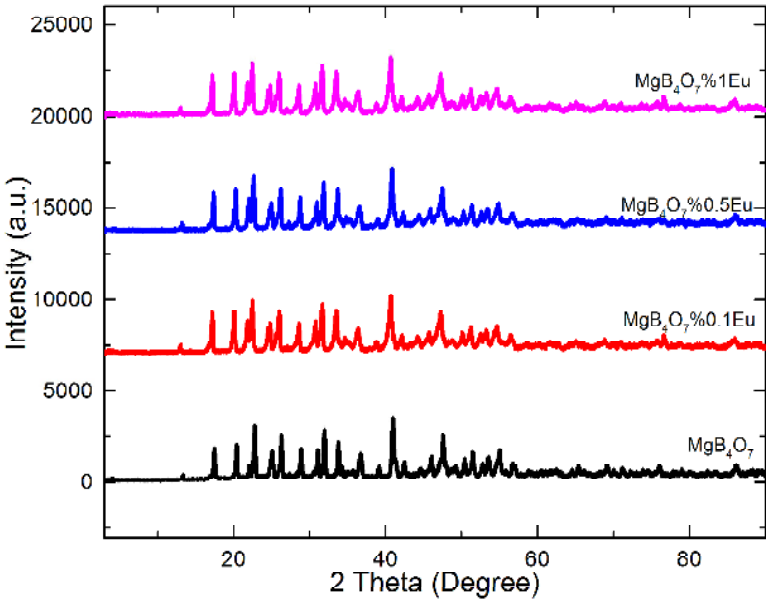

Figure 5.24: XRD pattern of Eu-doped MgB_4O_7 sample.

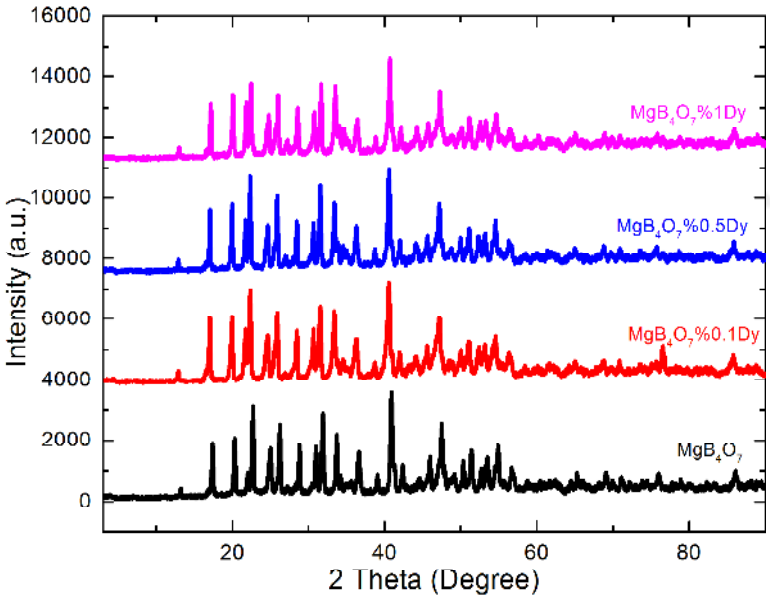

Figure 5.25: XRD pattern of Dy-doped MgB_4O_7 sample.

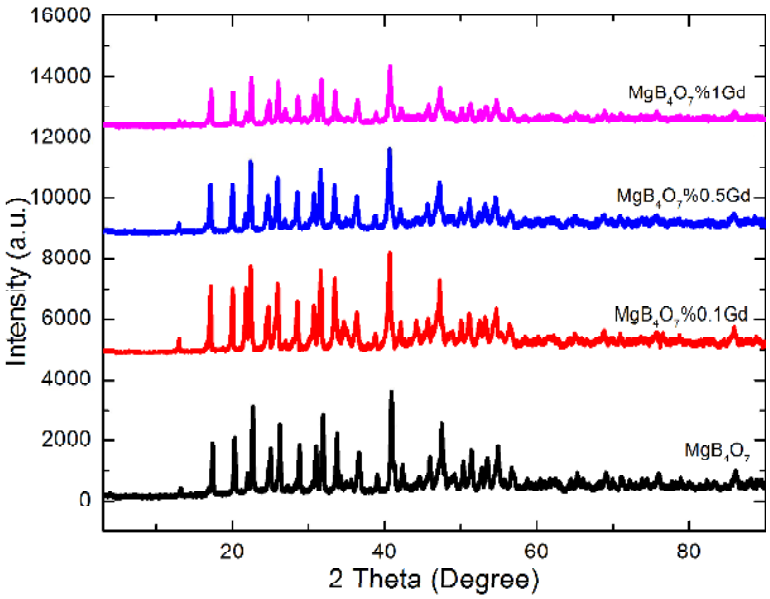

Figure 5.26: XRD pattern of Gd-doped MgB_4O_7 sample.

XRD results for Calcium Tetraborate

The XRD patterns of CaB_4O_7 and metal doped CaB_4O_7 compounds are given in Figure 5.28. The X-ray diffraction patterns are shown with Miller indices (hkl) of synthesized materials and they are well matched with corresponding reference data (JCDPS No: 31-0253) which is shown Figure 5.27. The calcium tetraborate specifies a monoclinic structure. The unit cell parameters are a = 12.264 Å, b = 9.895 Å and c = 7.796 Å. The phase composition of the calcium tetraborate samples synthesized and then characterized for investigation of crystal structures of the samples. According to the XRD results, most of the peaks in the diffractogram were overlapped with JCPDS (Card No: 31-0253) card. As shown in the diffractograms of the calcium tetraborate, the samples doped by adding metal ions to the initial materials, it was observed that there was no change in the structure of calcium tetraborate after doping process. Additionally, the peak intensities of Cu, Dy, Gd and Eu doped calcium tetraborate samples generally increased with respect to peak intensity of un-doped calcium tetraborate.

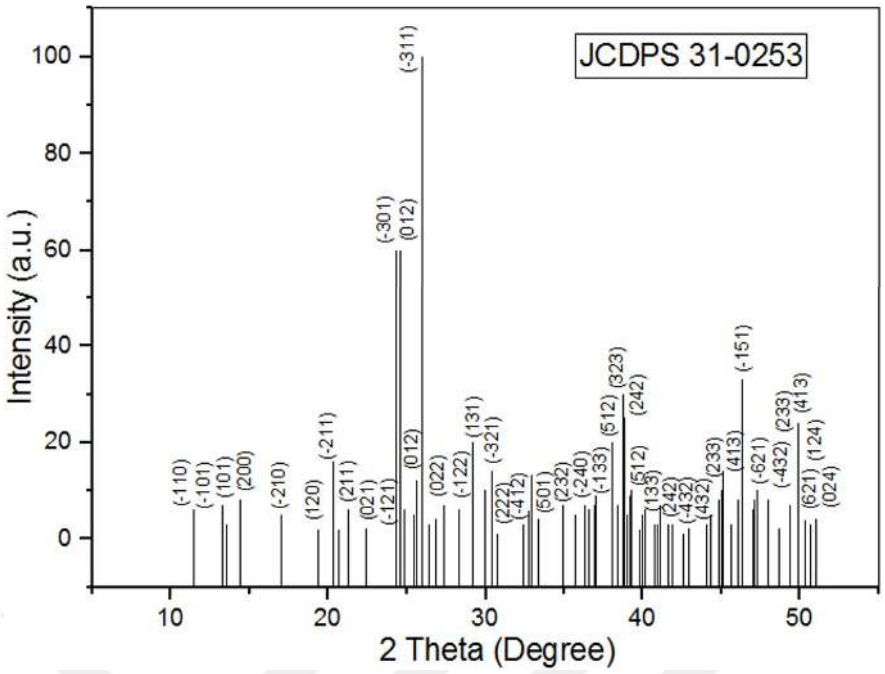

Figure 5.27: XRD Pattern of Calcium Tetraborate (JCDPS No: 31-0253).

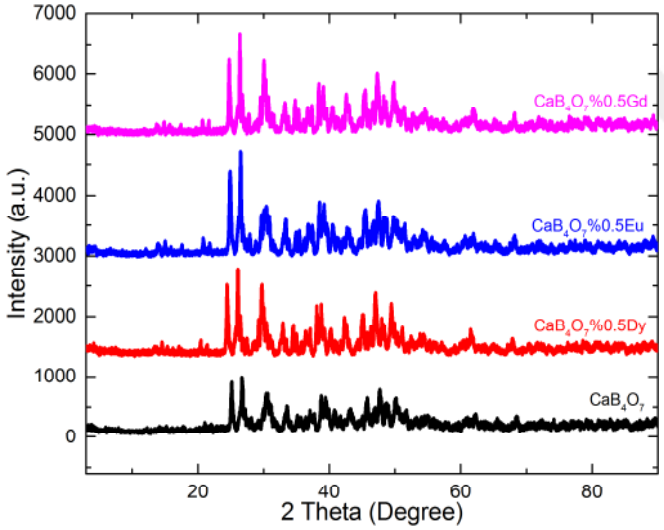

Figure 5.28: XRD pattern of 5% Eu, Gd and Dy doped CaB_4O_7 samples.

XRD results for Barium Tetraborate

The XRD patterns of BaB_4O_7 and metal doped BaB_4O_7 compounds are given in Figures 5.30. The X-ray diffraction patterns are shown with Miller indices (hkl) of synthesized materials and they are well matched with corresponding reference data (JCDPS No: 73-1333) that is shown Figure 5.29.

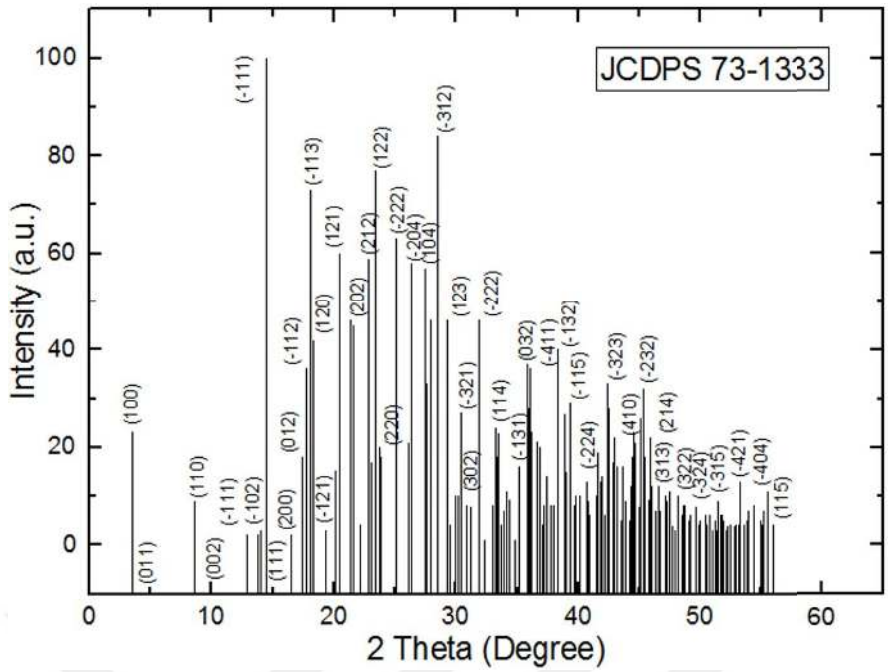

Figure 5.29: XRD Pattern of Barium Tetraborate (JCDPS No: 73-1333).

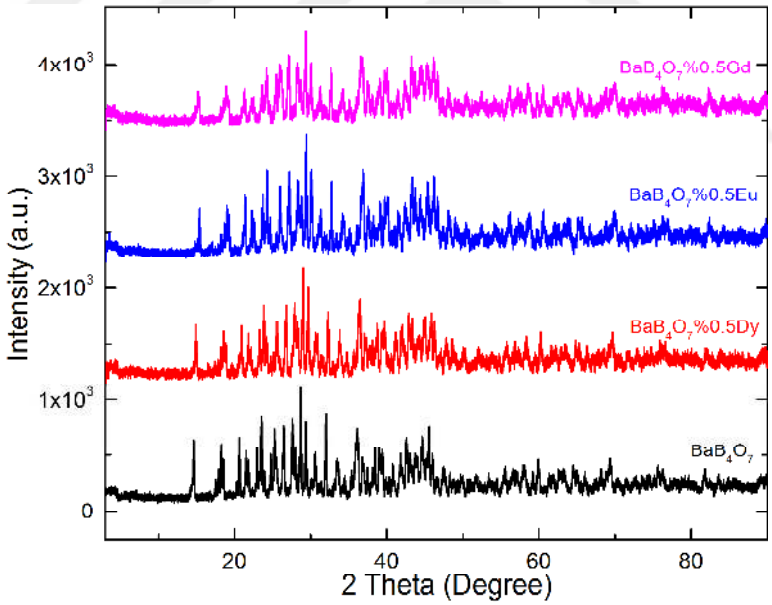

Figure 5.30: XRD pattern of 5% Eu, Gd and Dy doped BaB_4O_7 samples.

The barium tetraborate has a monoclinic structure. The unit cell parameters a = 10.560 Å, b = 8.200 Å and c = 13.010 Å. The phase composition of barium tetraborate samples synthesized and subsequently characterized to study about crystal structures of the samples. According to the XRD results, most of the peaks in the diffractogram were found to overlap with the JCPDS (Card No.

73-1333) card. As shown in the diffractograms of the barium tetraborate samples doped with metal ions to the initial materials, it was observed that the barium tetraborate structure did not cause any change after doping process.

Fourier Transform Infrared Spectroscopy (FTIR) results

The fourier transform infrared spectroscopy was employed to determine chemical bonding of synthesized un-doped and doped lithium triborate, lithium tetraborate, magnesium tetraborate, calcium tetraborate and barium tetraborate samples. Besides, FTIR was utilized to see the spectra differences of various synthesized samples and metal doped borate compound samples after the dopant addition. The fourier transform infrared spectroscopy of borate samples are shown in Figures 5.31 and 5.54 and they were performed to determine chemical bonding of borate compounds. The FTIR spectra were fitted with the literature values for BO_3 and BO_4 ring structure vibrations between 600 cm^{-1} and 1600 cm^{-1} [149-153]. In addition, the formation of new vibrational band was not detected after the addition of dopants into borate samples. The characteristic vibrational modes of borate compounds could be given as follows: the asymmetric stretching vibration band of B-O in BO_3 unit at ∼1432 and ∼1344 cm^{-1}, an asymmetric stretching band of B-O in BO_4unit assigned at ∼1130 cm^{-1}, the broad bands at ∼944 and ∼826 cm^{-1} assigned as symmetric stretching of B-O in BO_4 and BO_3rings; respectively. The weak band was observed at ∼710 cm^{-1} which is assigned as, out of plane bending of B-O in BO_3unit [154]. The absorption peaks attribute to borate network according to Table 1.

The vibration modes of the borate network are mainly active in three FTIR spectra region: 850–1100 cm^{-1} associated with the B–O stretching of tetrahydral BO^{4-} units, and 600–800 cm^{-1} associated with bending vibrations of various borate segments and a band at around 700 cm^{-1}, which corresponds to band bending of B–O–B bridges in the boron-oxygen network [150-155]. According to the results of FT-IR spectroscopy measurements, the locations of the vibration bands of borate compounds before and after doping are the same. No new bond formation has been observed due to the added metals.

Frequencies (cm^{-1})	Assigment	Reference
$\sim$ 685	B-O-B bending vibration	[150]
$\sim$ 700	B-O-B bending vibration in borate ring	[150, 151, 153]
850-1100	B-O stretching of tetrahydral BO_4^-	[150, 151, 153]
600-800	Bending vibrations of various borate	[151, 153]
$\sim$ 907	B-O stretching vibration of BO_4 units in tri, tetra and pantaborate groups	[150, 152]
$\sim$ 1400	B-O stretching trigonal BO_3 units	[150, 151, 153, 155]

Table 5.1: Frequencies and their assignments for FTIR spectra of borate compounds

FTIR results for Lithium Triborate

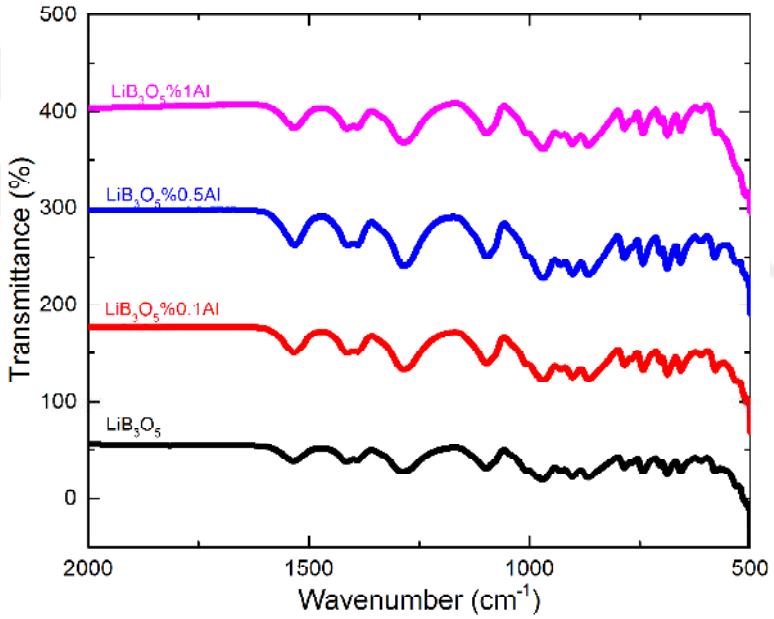

Figure 5.31: FTIR spectra of synthesized and Al-doped Lithium Triborate samples.

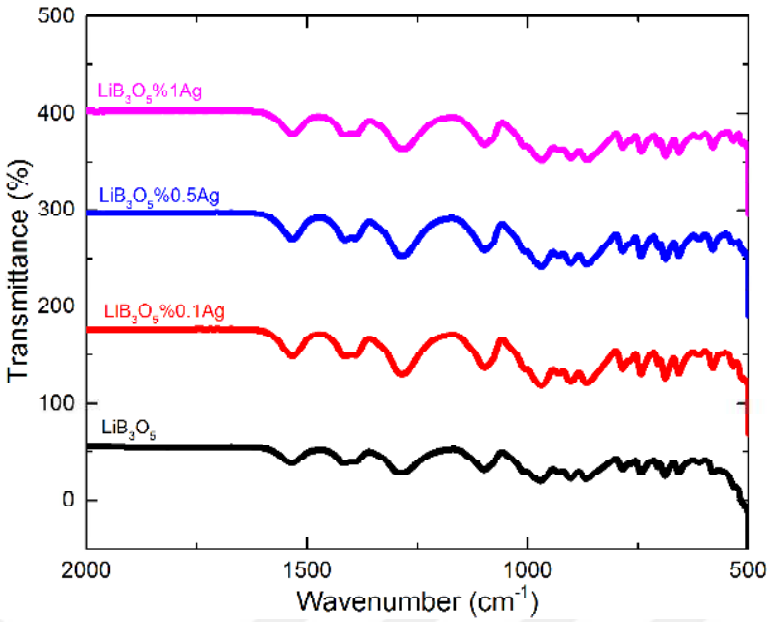

Figure 5.32: FTIR spectra of synthesized and Ag-doped Lithium Triborate samples.

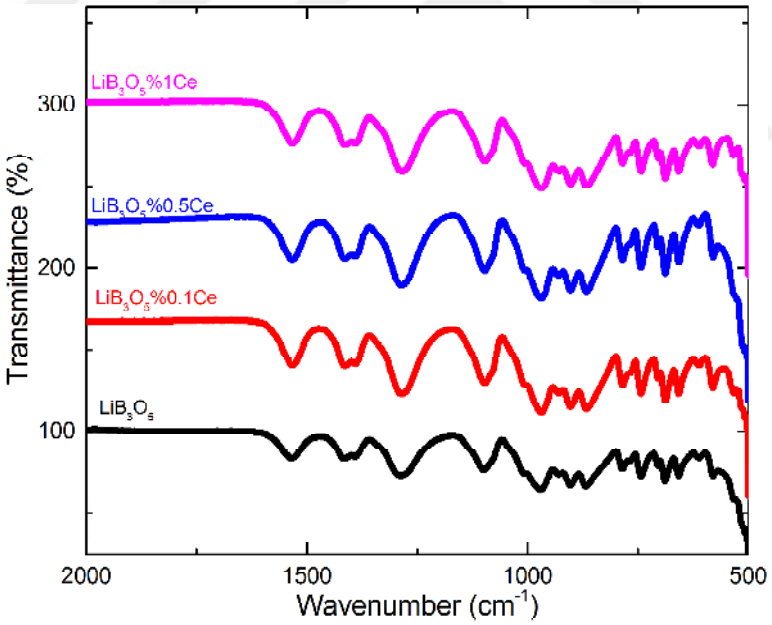

Figure 5.33: FTIR spectra of synthesized and Ce-doped Lithium Triborate samples.

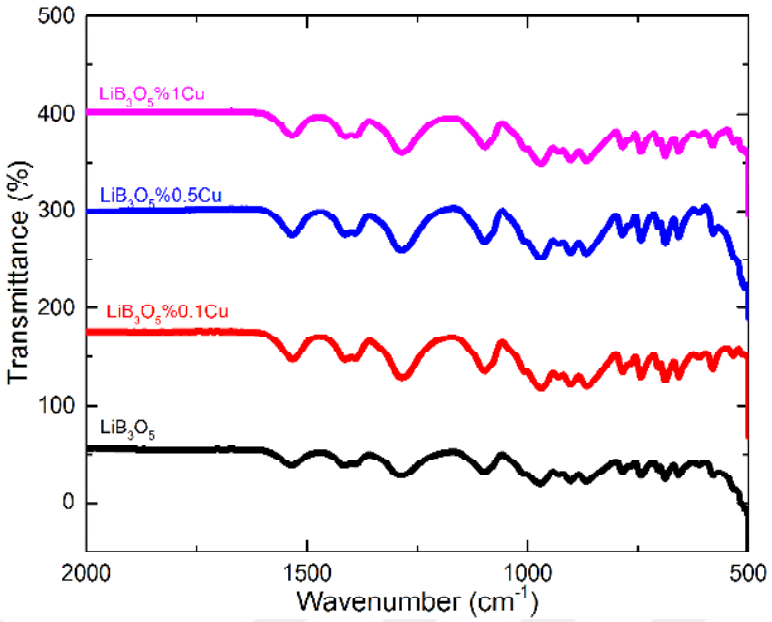

Figure 5.34: FTIR spectra of synthesized and Cu-doped Lithium Triborate samples.

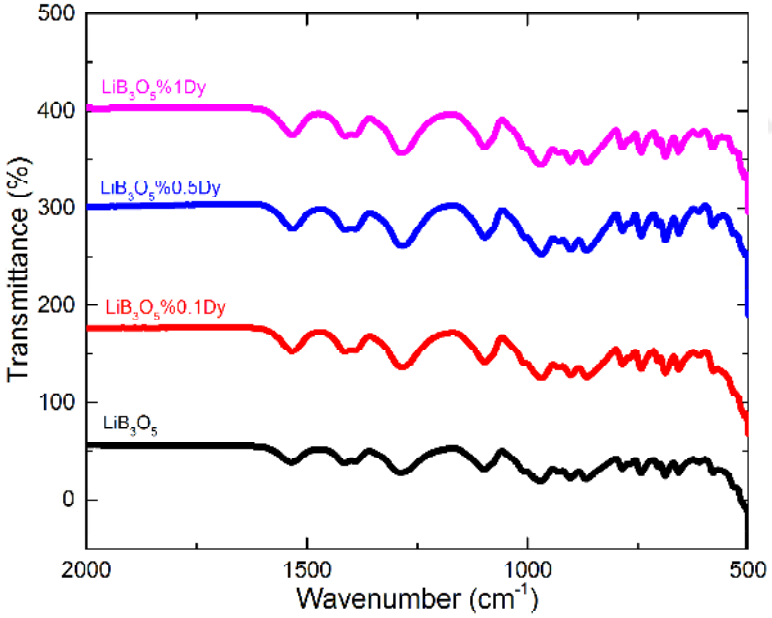

Figure 5.35: FTIR spectra of synthesized and Dy-doped Lithium Triborate samples.

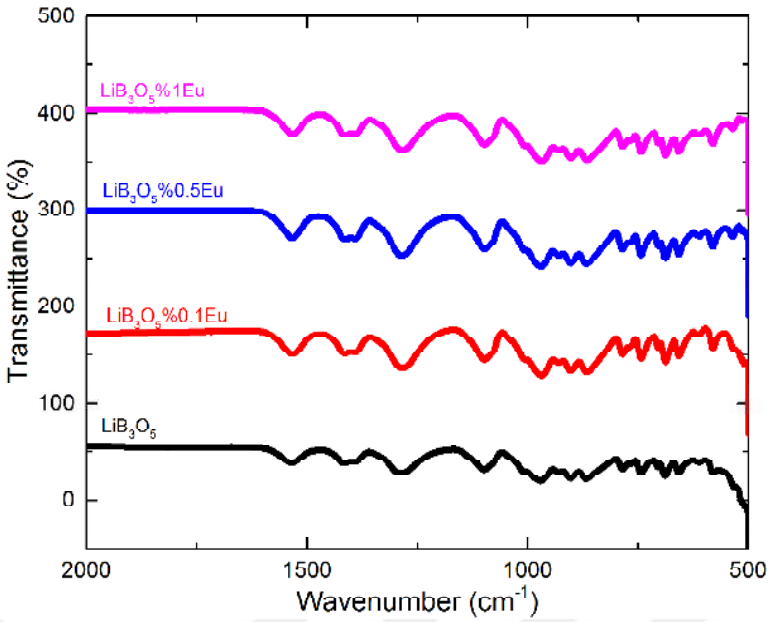

Figure 5.36: FTIR spectra of synthesized and Eu-doped Lithium Triborate samples.

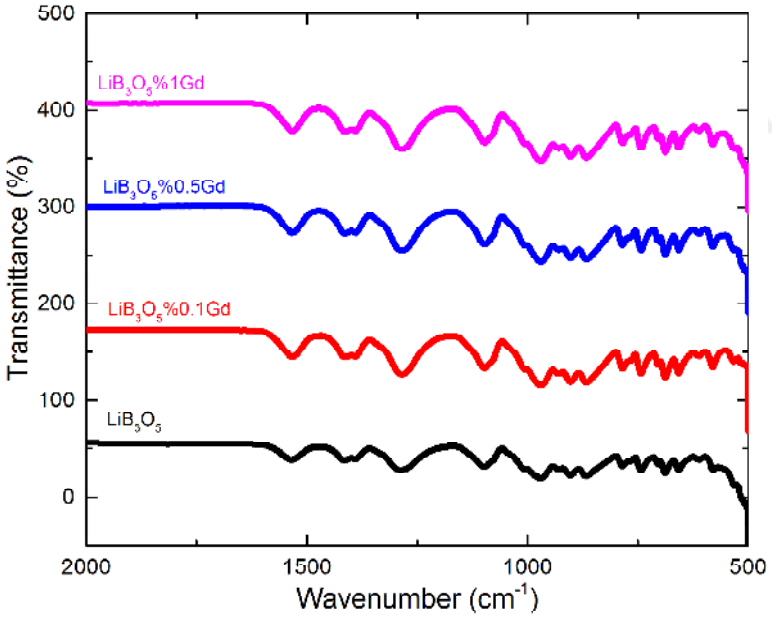

Figure 5.37: FTIR spectra of synthesized and Gd-doped Lithium Triborate samples.

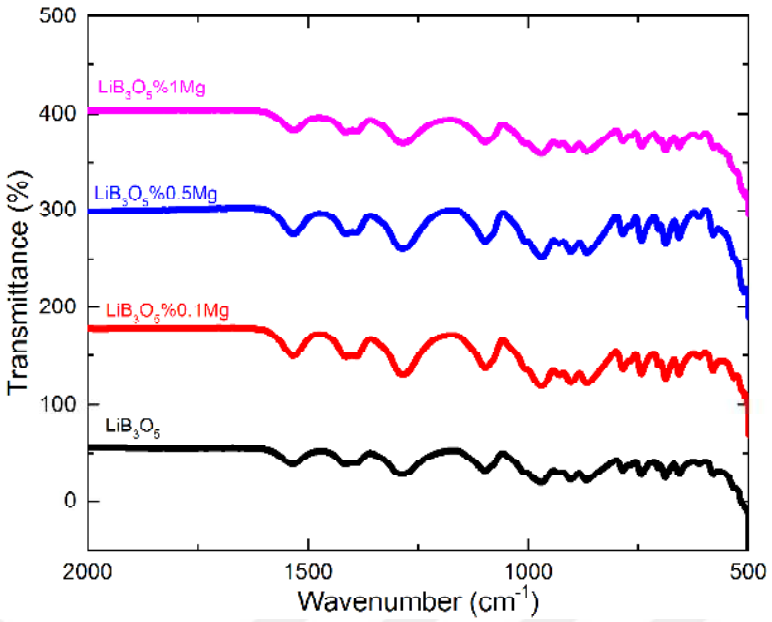

Figure 5.38: FTIR spectra of synthesized and Mg-doped Lithium Triborate samples.

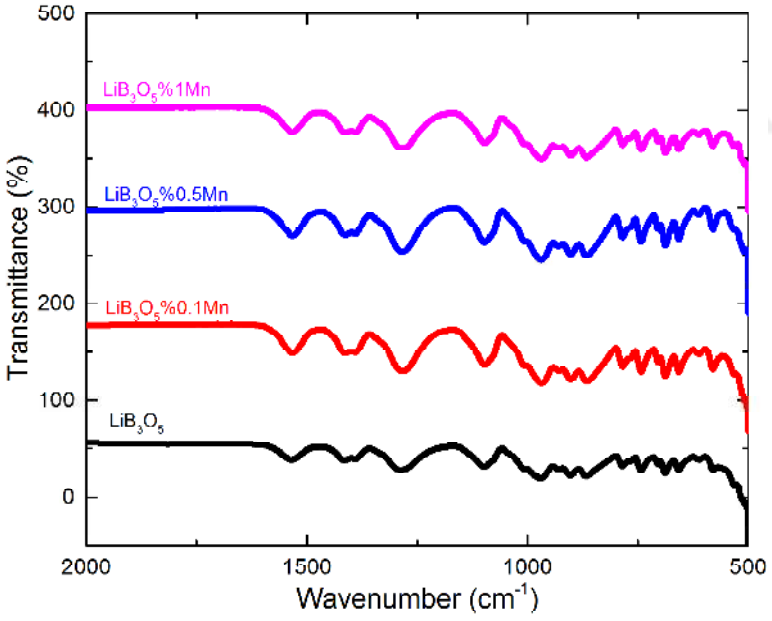

Figure 5.39: FTIR spectra of synthesized and Mn-doped Lithium Triborate samples.

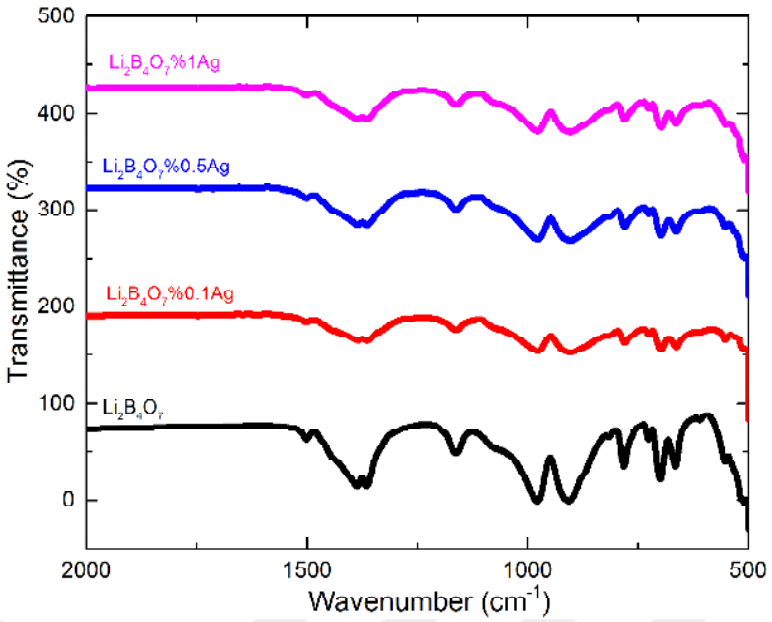

Figure 5.40: FTIR spectra of synthesized and Ag-doped Lithium Tetraborate samples.

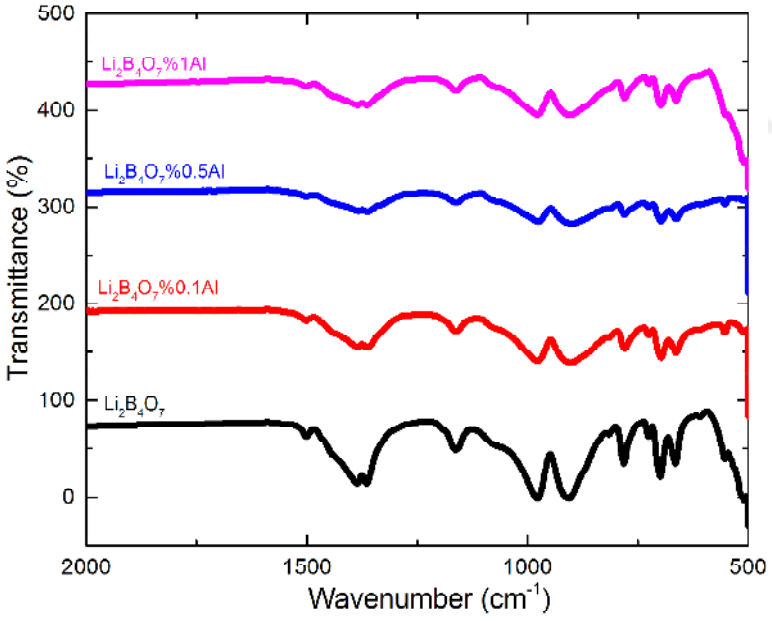

Figure 5.41: FTIR spectra of synthesized and Al-doped Lithium Tetraborate samples.

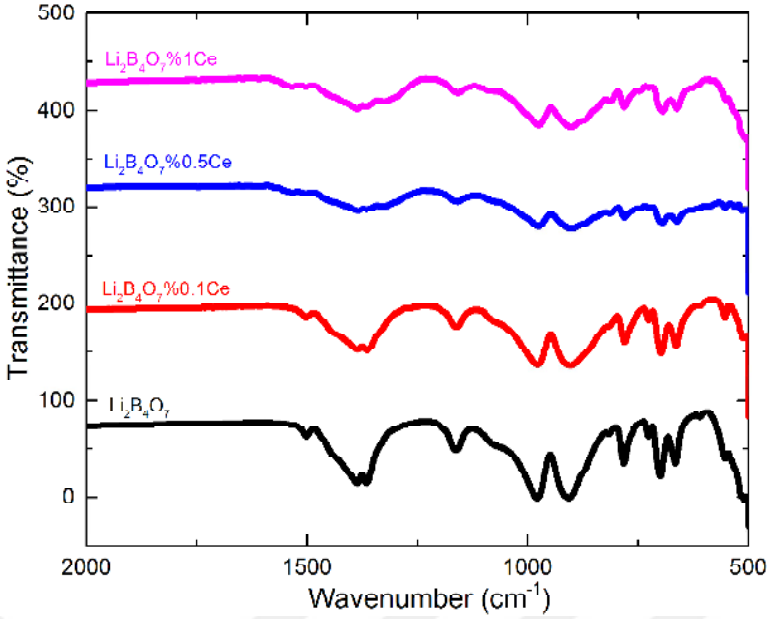

Figure 5.42: FTIR spectra of synthesized and Ce-doped Lithium Tetraborate samples.

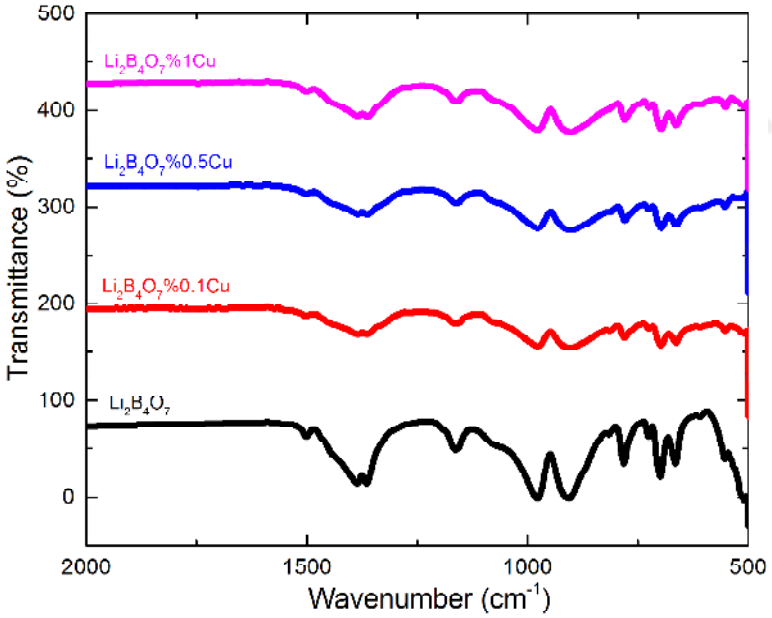

Figure 5.43: FTIR spectra of synthesized and Cu-doped Lithium Tetraborate samples.

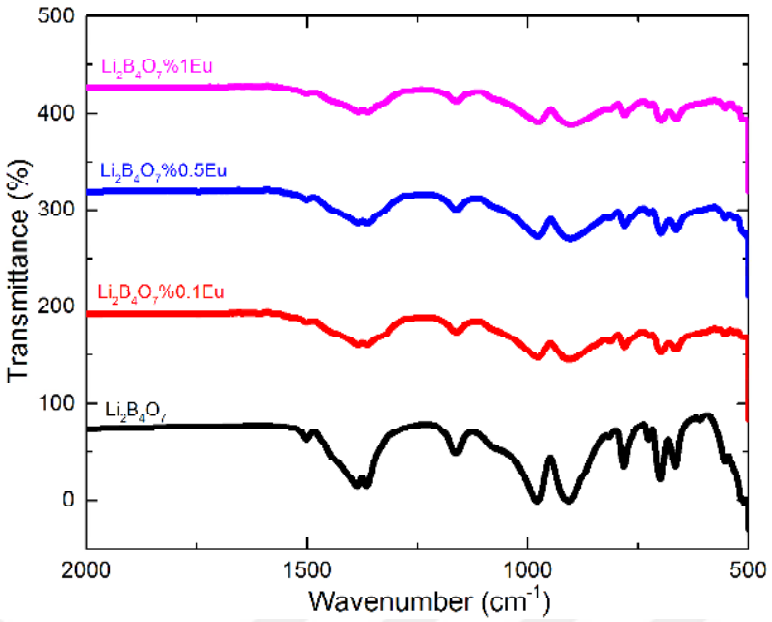

Figure 5.44: FTIR spectra of synthesized and Eu-doped Lithium Tetraborate samples.

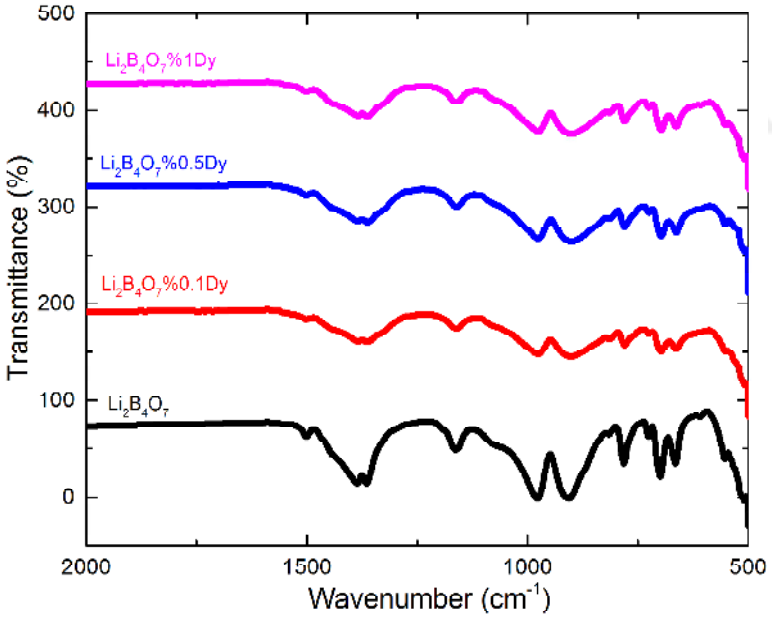

Figure 5.45: FTIR spectra of synthesized and Dy-doped Lithium Tetraborate samples.

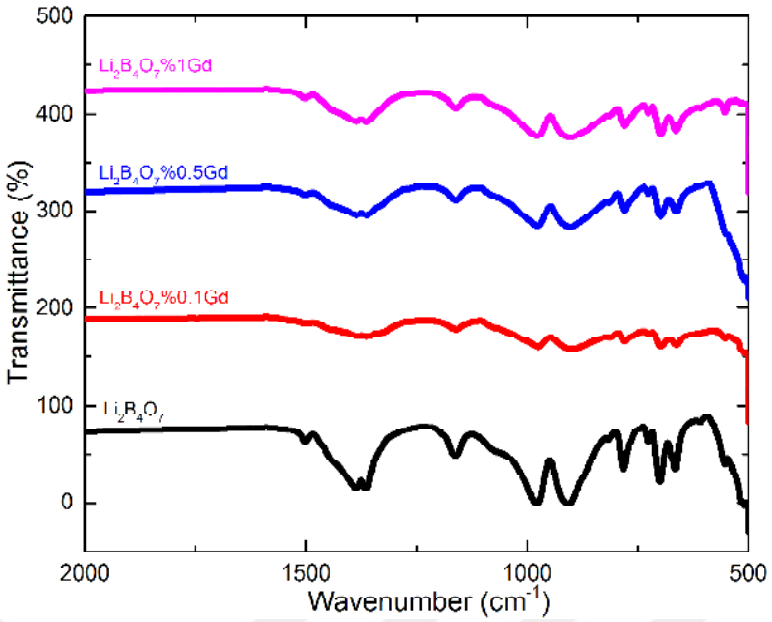

Figure 5.46: FTIR spectra of synthesized and Gd-doped Lithium Tetraborate samples.

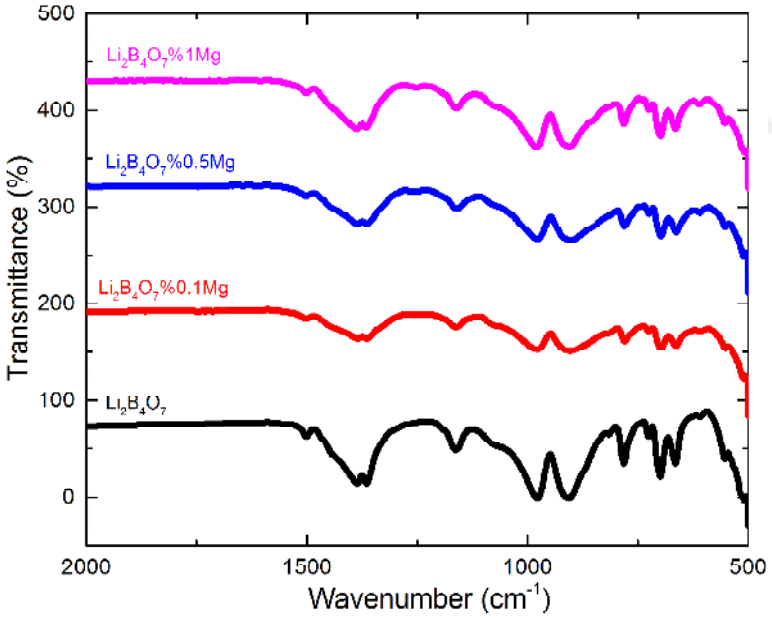

Figure 5.47: FTIR spectra of synthesized and Mg-doped Lithium Tetraborate samples.

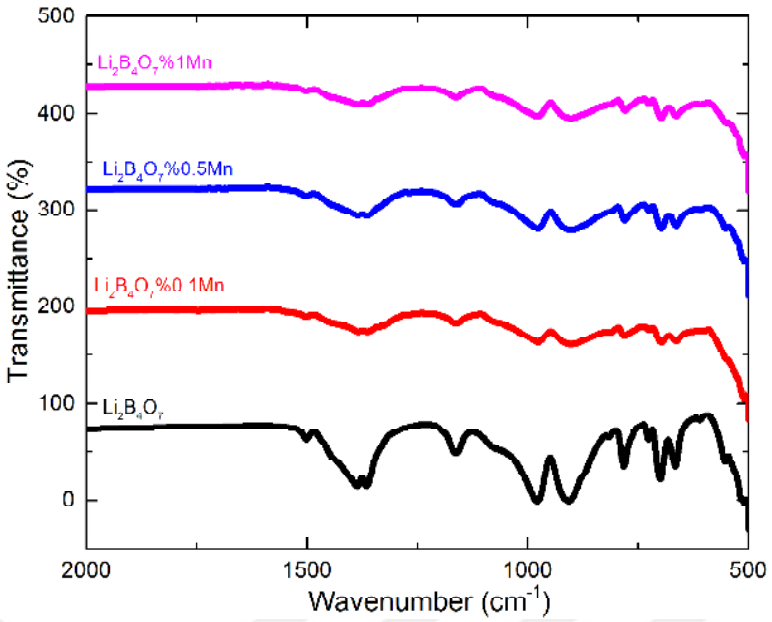

Figure 5.48: FTIR spectra of synthesized and Mn-doped Lithium Tetraborate samples.

FTIR results for Magnesium Tetraborate

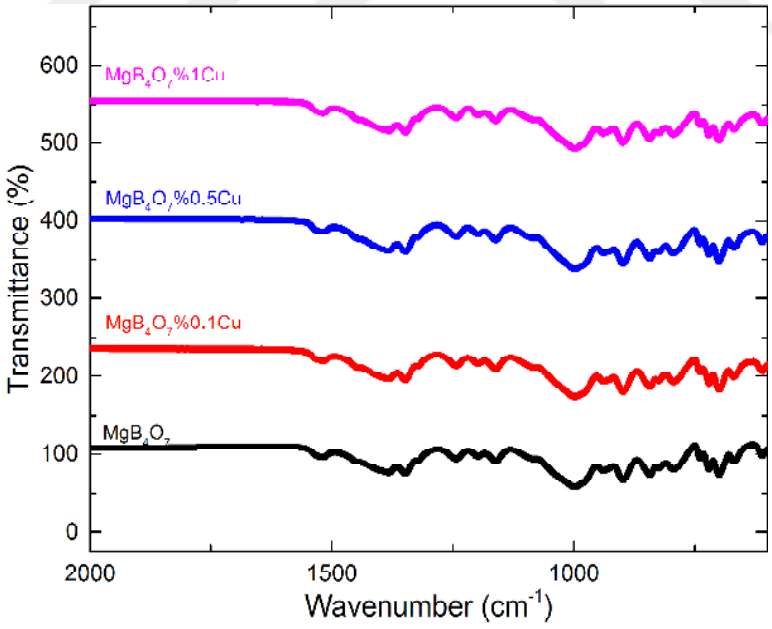

Figure 5.49: FTIR spectra of synthesized and Cu-doped Magnesium Tetraborate samples.

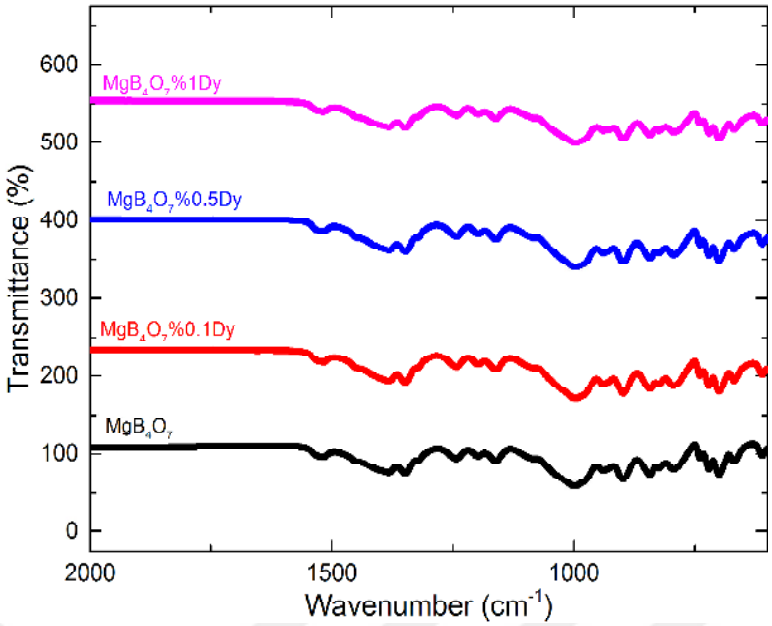

Figure 5.50: FTIR spectra of synthesized and Dy-doped Magnesium Tetraborate samples.

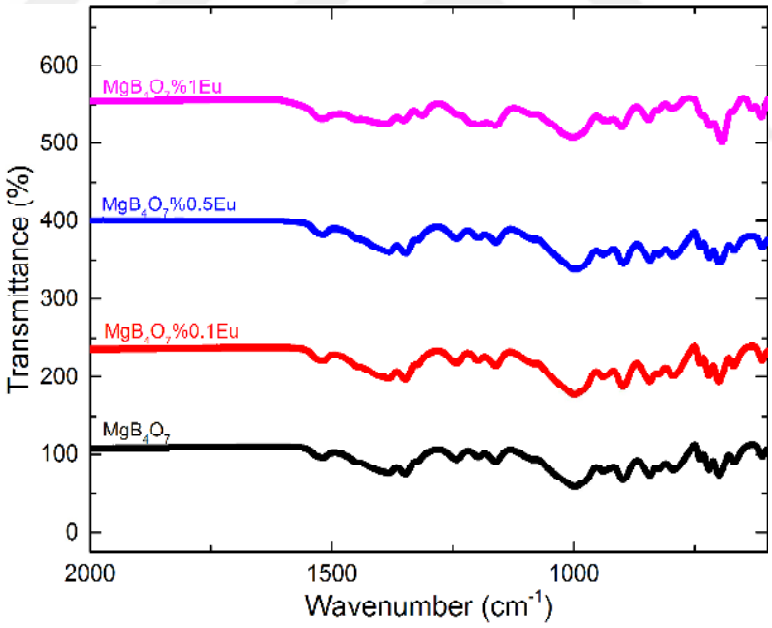

Figure 5.51: FTIR spectra of synthesized and Eu-doped Magnesium Tetraborate samples.

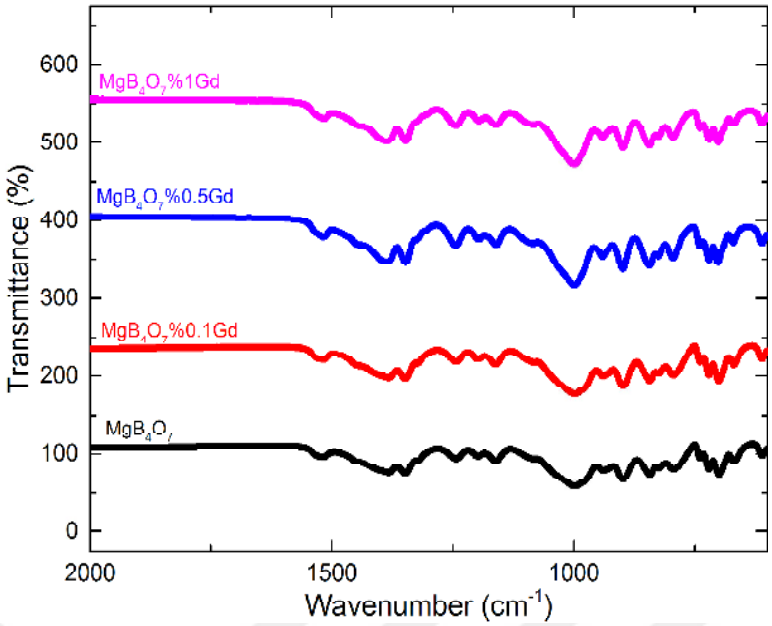

Figure 5.52: FTIR spectra of synthesized and Gd-doped Magnesium Tetraborate samples.

FTIR results for Calcium Tetraborate

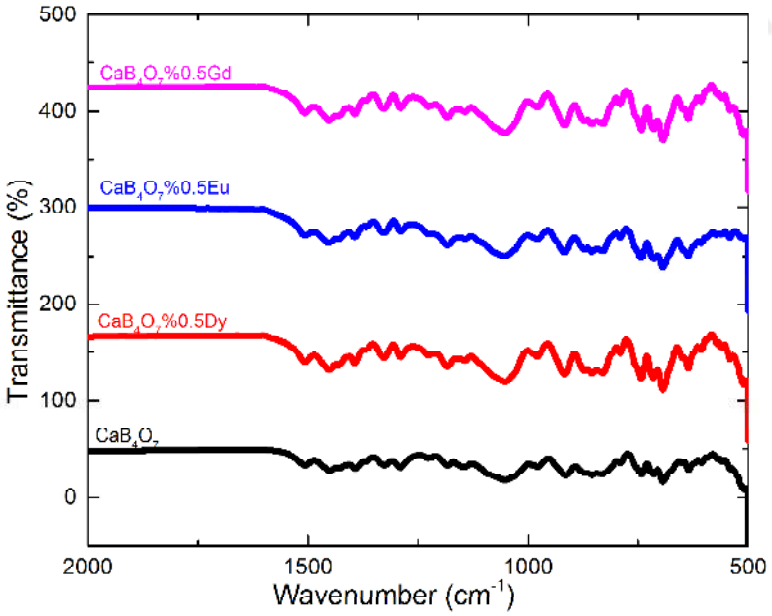

Figure 5.53: FTIR spectra of synthesized and 5% Gd, Eu and Dy doped Calcium Tetraborate samples.

FTIR results for Barium Tetraborate

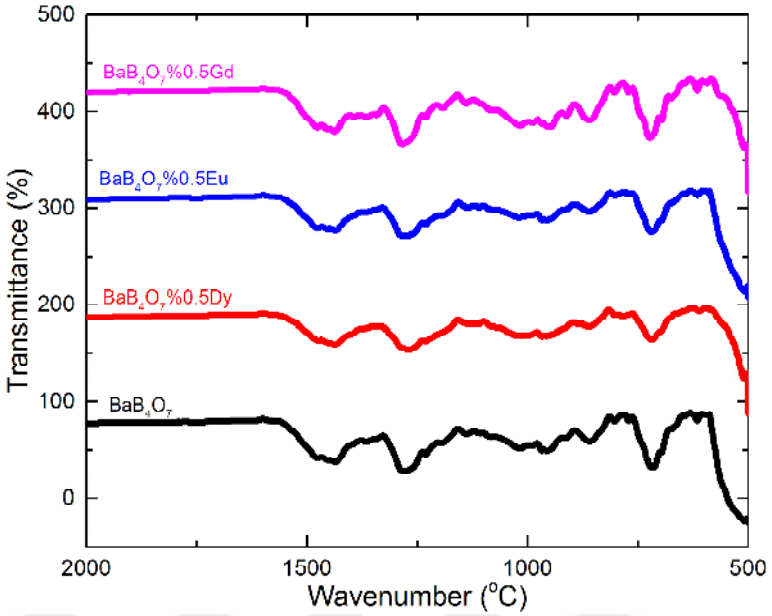

Figure 5.54: FTIR spectra of synthesized and 5% Gd, Eu and Dy doped Barium Tetraborate samples.

5.1.2 Thermoluminescence Results

The thermoluminescence measurements were taken after XRD characterization and FT-IR spectroscopy measurements of synthesized borate compounds by metal ion doped. The radiation dosimetric performance of a TL materials is highly depends upon shape of its glow curve intensity and peak temperatures of the glow peaks. The thermoluminesce glow curves of synthesized lithium tetraborate, lithium triborate, magnesium tetraborate, calcium tetraborate and barium tetraborate samples were utilized to determine whether those samples show ideal TL glow curve structure and the TL intensity for neutron measurements or not. The samples that have sufficient TL intensity and proper TL structure were analyzed for further dosimetric measurements such as dose-response and heating rate. The ^{252}Cf neutron source was used for thermoluminescence measurements made with the aim of developing neutron dosimetry. The average energy of the neutron source is around 2 MeV. The neutron dose which the neutron source is spread over 1 hour is 5 Gy. The background TL measurements were taken for each borate compound before each irradiation. The samples had 25-35 mg weight in all measurements. Measurements were made at a heating rate of 1 °C/s at 50-40 °C. After thermoluminescence measurements, it was observed that borate compounds were not sensitive to neutron. After annealing the compounds

for 1 hour at 600 °C, the neutron sensitivity of borate compounds were obtained. Therefore; each compound was annealed at 600 °C for 1 hour before each thermoluminescence measurement. The XRD measurements of annealed compounds were also taken after annealing processes. According to the XRD measurement results, no change in the structure of the compounds was observed after annealing processes. The dose-response and heating rate measurements of the obtained borate compounds were also performed.

Termoluminescence Dose-Response Results

The characterizations of the dose response graphs of the synthesized borate compounds are given in Figures 5.55 - 5.74. The 0.1 %, 0.5 %, 1 % Dy, Ag, Eu-doped, 0.1 %, 0.5 % Cu-doped, 0.1 % of Mg, Gd-doped of lithium tetraborate, un-doped magnesium tetraborate and 0.1 %, 0.5 %, 1 % Dy-doped magnesium tetraborate, 1 % Cu-doped lithium triborate, and un-doped calcium tetraborate and 0.5 % Dy-doped calcium tetraborate are exhibiting sensitivity to neutron radiation. The borate compounds, which are sensitive to neutron, show a linear increase in all compounds compared to increasing doses relative to the dose response results. No significant change in maximum peak temperatures versus increasing dose amount of borate compounds has been observed.

Figures 5.57, 5.61 and 5.65 show a single peak according to the dose response results of the Ag-doped lithium tetraborate compounds. The maximum peak temperatures of 0.1 %, 0.5 % and 1 % Ag-doped tetra borate compounds were observed at ≈271 °C, ≈271 °C and ≈278 °C, respectively. The peak temperature of 1 % Ag-doped was found to be higher than 0.1 % and 0.5 % Ag-doped lithium tetraborate compounds. Figures 5.60 and 5.62 show that 0.1 % and 0.5 % Cu-doped lithium tetraborate compounds have two glow peaks according to their dose response graphs. The maximum peak temperatures of both glow peaks of 0.1 % Cu-doped tetraborate were obsrerved at ≈169 °C and ≈254 °C, respectively. On the other hand, the maximum peak temperatures of these peaks of the 0.5 % Cu-doped tetraborate were observed at ≈166 °C and ≈265 °C, respectively. Figure 5.59, 5.63 and 5.67 show that the compounds according to the dose response graphs of 0.1 %, 0.5 % and 1 % with Eu-doped lithium tetraborate compounds have a single peak. The maximum peak temperatures of 0.1 %, 0.5 % and 1 % with Eu-doped lithium tetraborate compounds were measured at ≈266 °C, ≈260 °C and ≈267 °C, respectively. A single peak was observed according to dose response graphs of 0.1 %, 0.5 % and 1 % with Dy-doped lithium tetraborate compounds and they are shown in Figures 5.55, 5.56 and 5.66, respectively. In addition, the

peak temperatures of lithium tetraborate compounds doped with 0.1 %, 0.5 % and 1 % Dy were observed at ≈272 °C, ≈293 °C and ≈280 °C, respectively. Figures 5.58 and 5.64 show that the peak temperatures of this glow peak are seen at ≈267 °C and 271 °C for 0.1% Mg and 0.1% Gd doped lithium tetraborate compounds, respectively. A single peak was observed according to dose response graphs of un-doped and 0.1 %, 0.5 % and 1 % Dy-doped magnesium tetraborate compounds are given in Figures 5.68 - 5.71. The maximum peak temperatures of un-doped and 0.1 %, 0.5 %, 1 % Dy-doped magnesium tetraborate compounds were recorded at ≈243 °C, ≈250 °C, ≈234 °C and ≈256 °C, respectively. It is observed that 1 % Cu-doped lithium triborate compound has a single peak at ≈162 °C which is shown in Figure 5.74. Figures 5.72 and 5.73 show that the un-doped calcium tetraborate and 0.5 % Dy-doped calcium tetraborate compounds have a single peak compared to the dose response graphs. The maximum peak temperatures of un-doped calcium tetraborate and 0.5 % Dy doped calcium tetraborate were recorded at ≈178 °C and ≈180 °C, respectively.

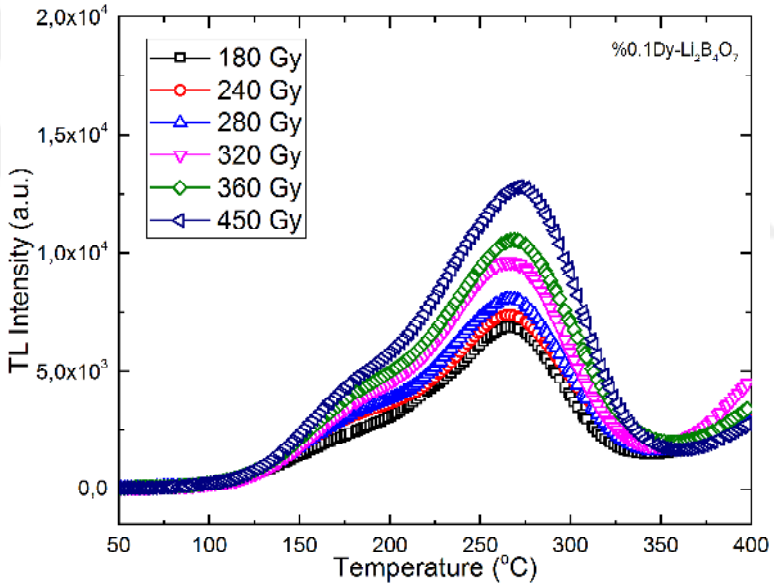

Figure 5.55: The glow curves of 0.1 % Dy-doped lithium tetraborate compound corresponding to various radiation doses using ^{252}Cf neutron source with a heating rate of 1 °C/s.

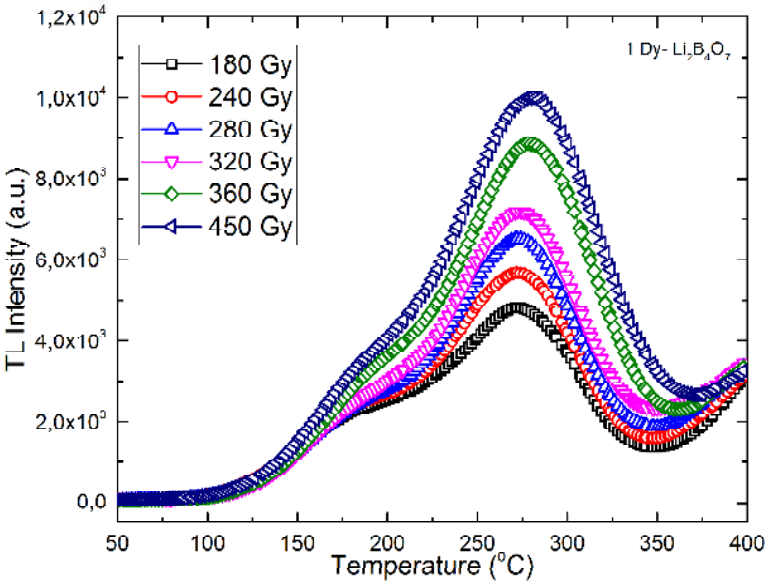

Figure 5.56: The glow curves of 1 % Dy-doped lithium tetraborate compound corresponding to various radiation doses using ^{252}Cf neutron source with a heating rate of 1 °C/s.

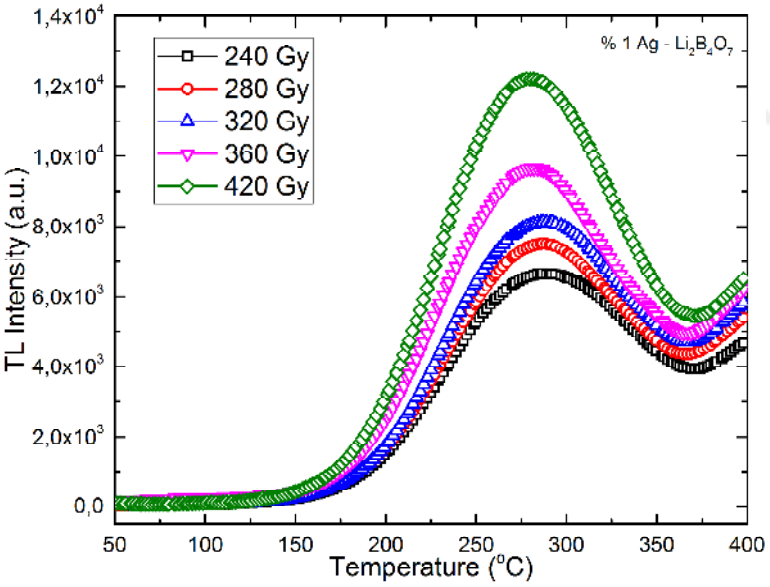

Figure 5.57: The glow curves of 1 % Ag-doped lithium tetraborate compound corresponding to various radiation doses using ^{252}Cf neutron source with a heating rate of 1 °C/s.

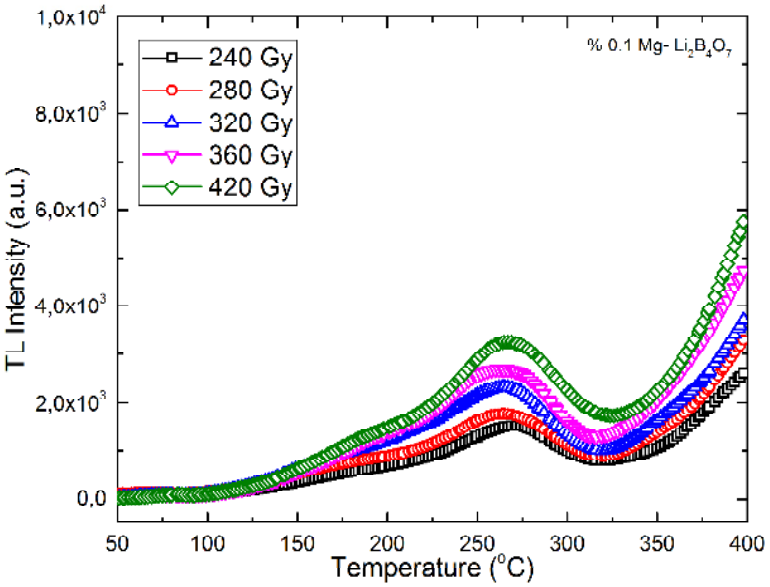

Figure 5.58: The glow curves of 0.1 % Mg-doped lithium tetraborate compound corresponding to various radiation doses using ^{252}Cf neutron source with a heating rate of 1 °C/s.

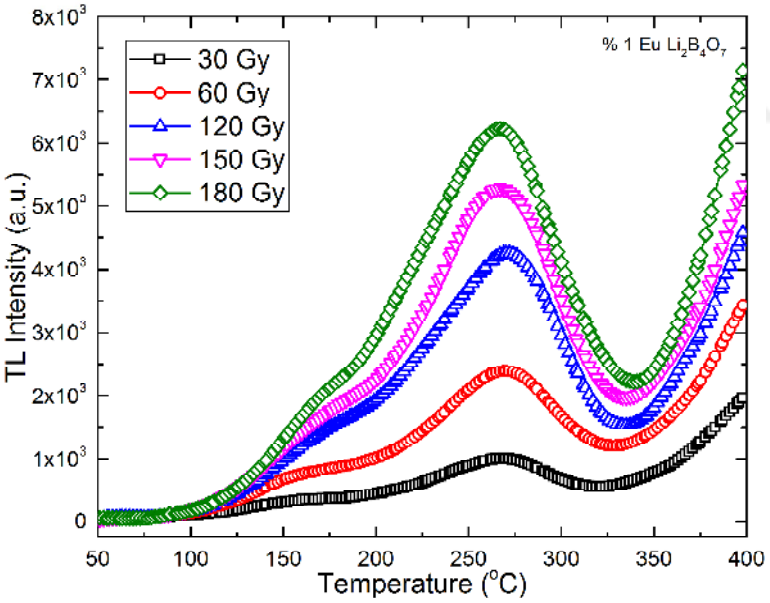

Figure 5.59: The glow curves of 1 % Eu-doped lithium tetraborate compound corresponding to various radiation doses using ^{252}Cf neutron source with a heating rate of 1 °C/s.

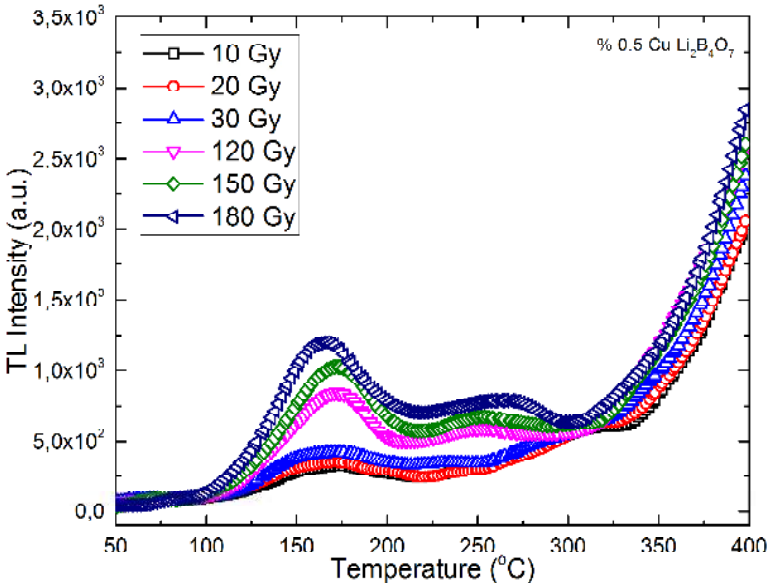

Figure 5.60: The glow curves of 0.5 % Cu-doped lithium tetraborate compound corresponding to various radiation doses using ^{252}Cf neutron source with a heating rate of 1 °C/s.

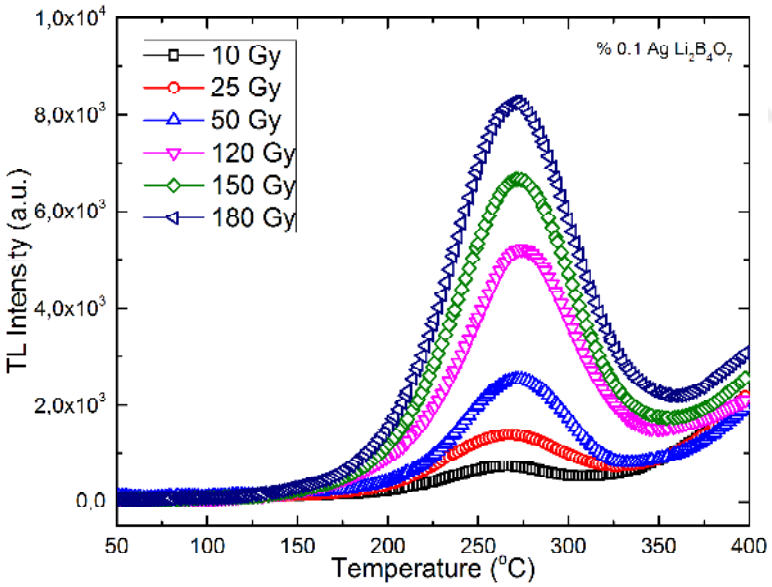

Figure 5.61: The glow curves of 0.1 % Ag-doped lithium tetraborate compound corresponding to various radiation doses using ^{252}Cf neutron source with a heating rate of 1 °C/s.

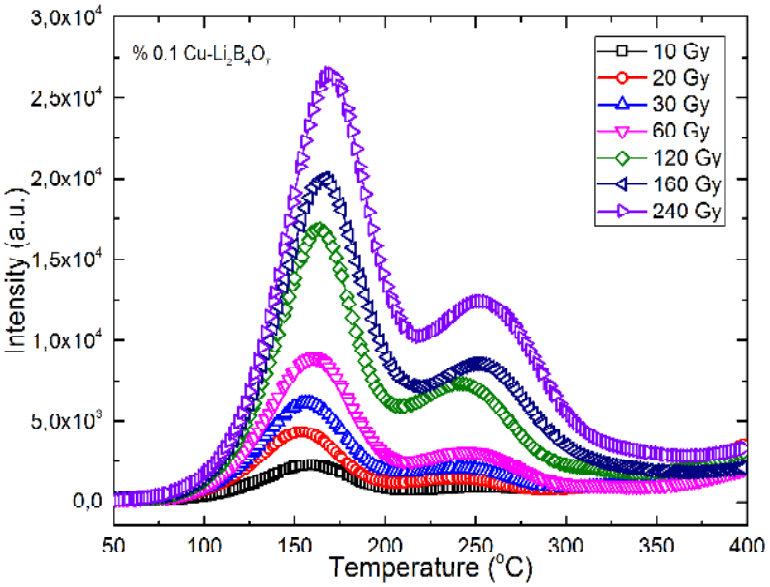

Figure 5.62: The glow curves of 0.1 % Cu-doped lithium tetraborate compound corresponding to various radiation doses using ^{252}Cf neutron source with a heating rate of 1 °C/s.

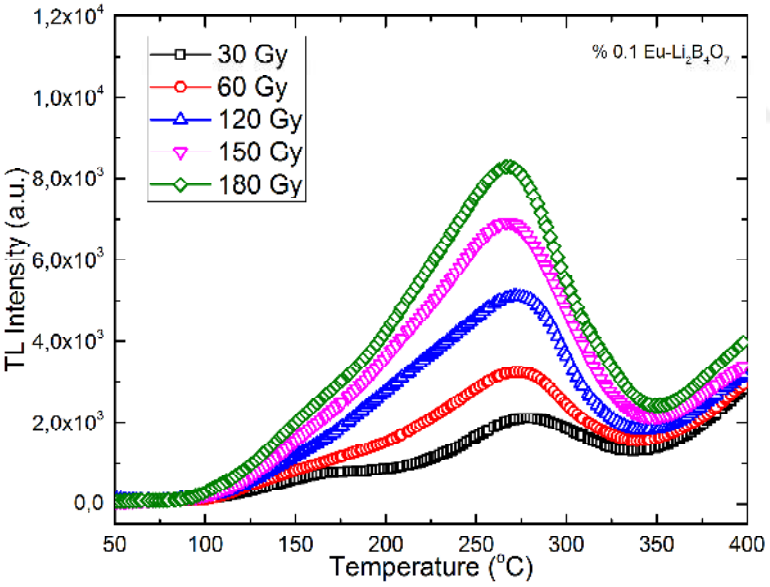

Figure 5.63: The glow curves of 0.1 % Eu-doped lithium tetraborate compound corresponding to various radiation doses using ^{252}Cf neutron source with a heating rate of 1 °C/s.

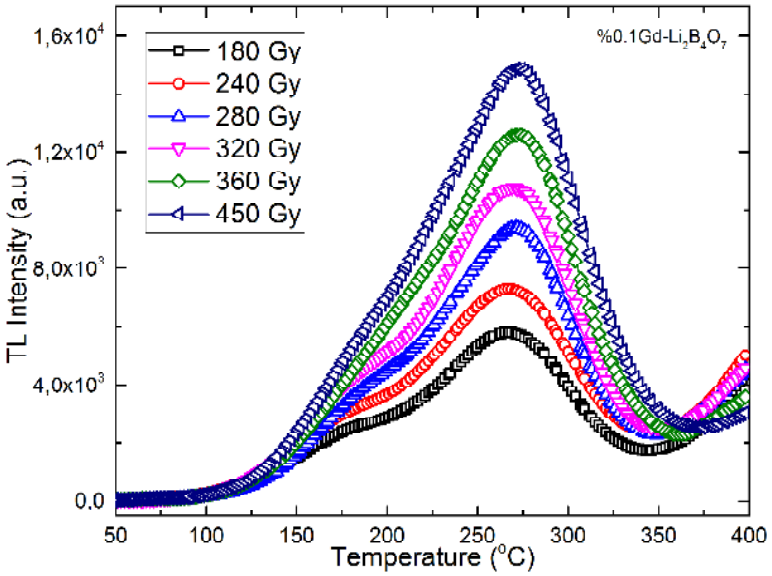

Figure 5.64: The glow curves of 0.1 % Gd-doped lithium tetraborate compound corresponding to various radiation doses using ^{252}Cf neutron source with a heating rate of 1 °C/s.

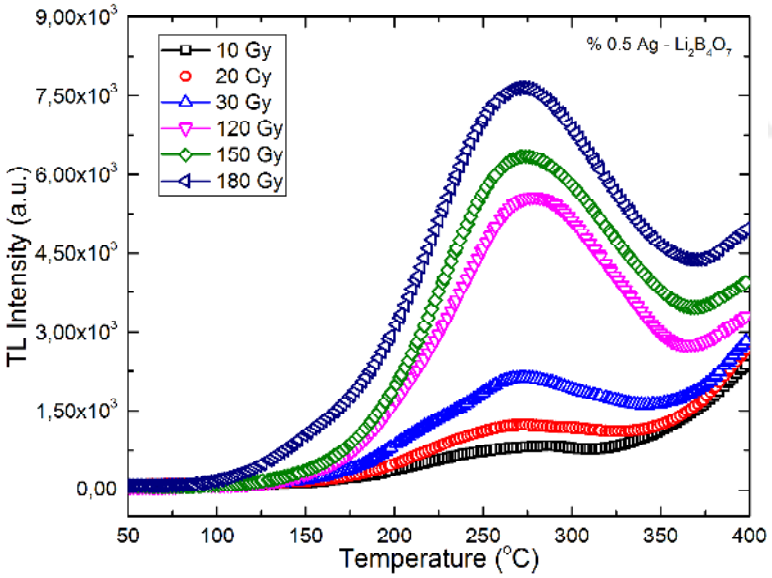

Figure 5.65: The glow curves of 0.5 % Ag-doped lithium tetraborate compound corresponding to various radiation doses using ^{252}Cf neutron source with a heating rate of 1 °C/s.

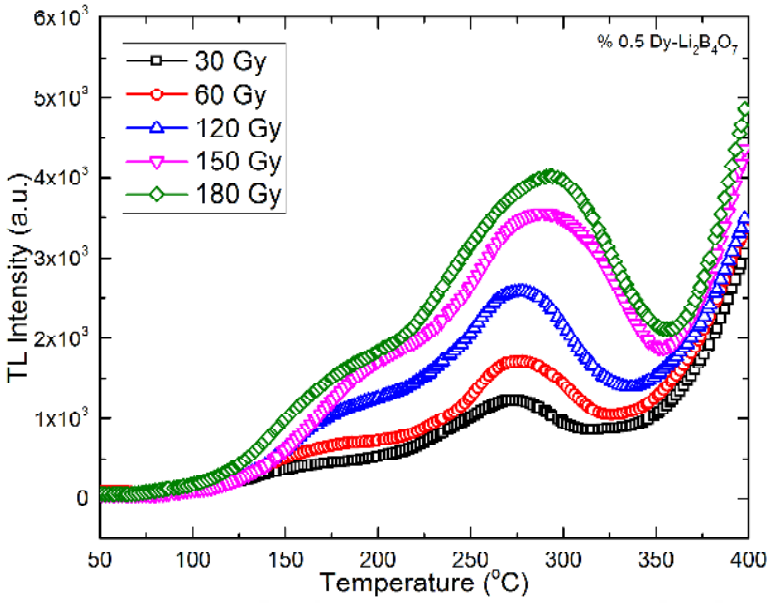

Figure 5.66: The glow curves of 0.5 % Dy-doped lithium tetraborate compound corresponding to various radiation doses using ^{252}Cf neutron source with a heating rate of 1 °C/s.

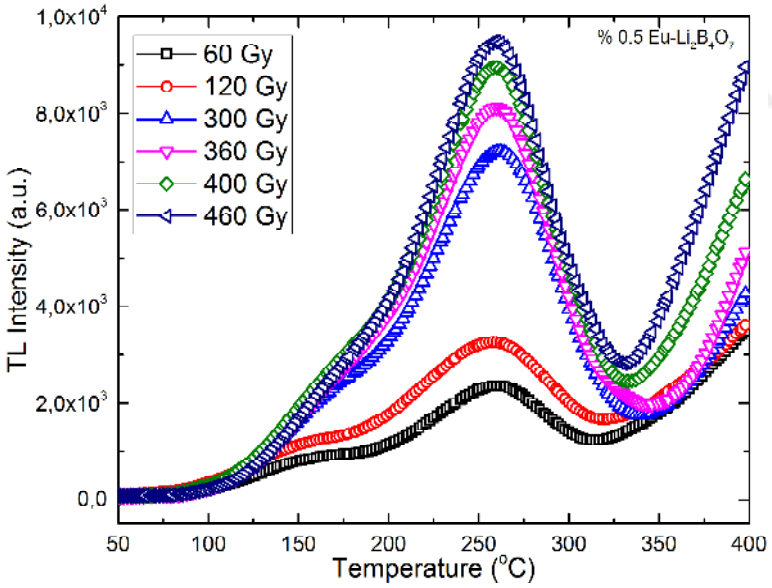

Figure 5.67: The glow curves of 0.5 % Eu-doped lithium tetraborate compound corresponding to various radiation doses using ^{252}Cf neutron source with a heating rate of 1 °C/s.

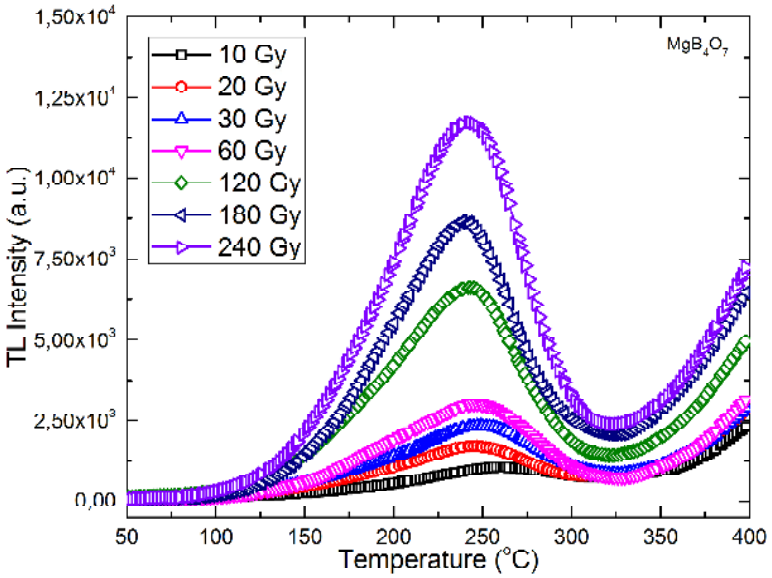

Figure 5.68: The glow curves of magnesium tetraborate compound corresponding to various radiation doses using ^{252}Cf neutron source with a heating rate of 1 °C/s.

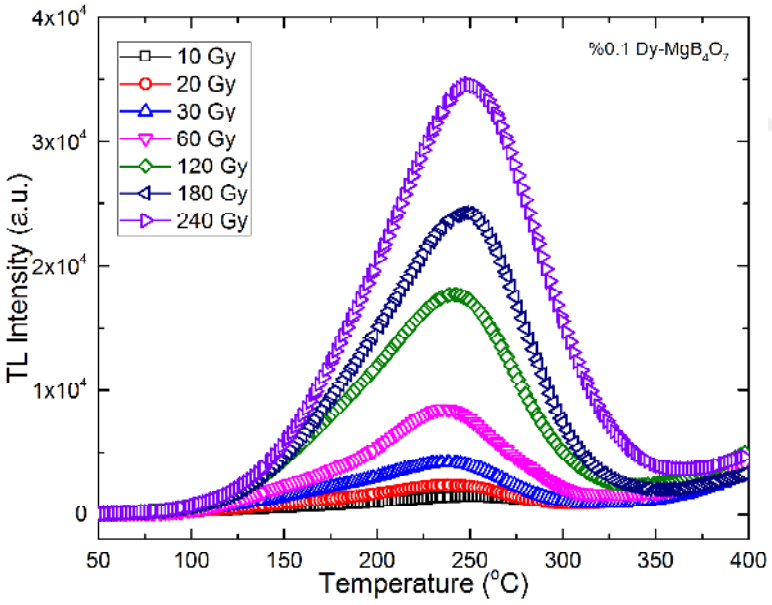

Figure 5.69: The glow curves of 0.1 % Dy-doped magnesium tetraborate compound corresponding to various radiation doses using ^{252}Cf neutron source with a heating rate of 1 °C/s.

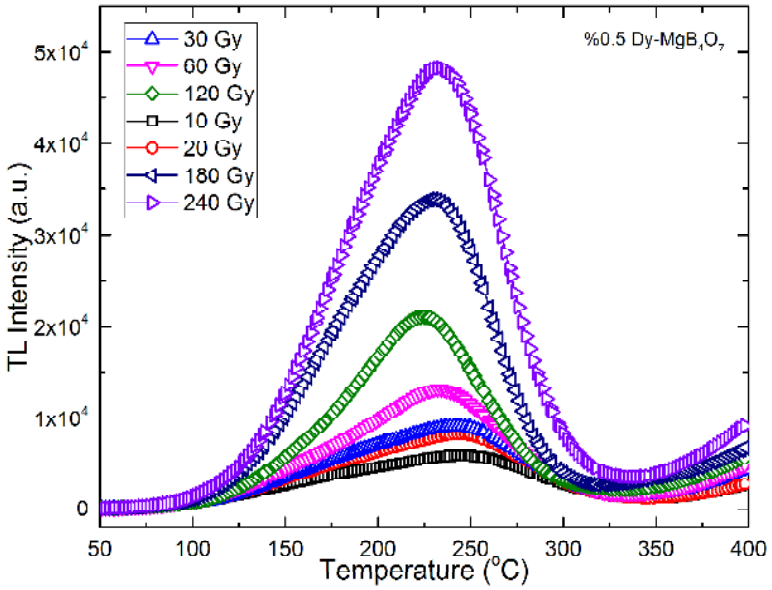

Figure 5.70: The glow curves of 0.5 % Dy-doped magnesium tetraborate compound corresponding to various radiation doses using ^{252}Cf neutron source with a heating rate of 1 °C/s.

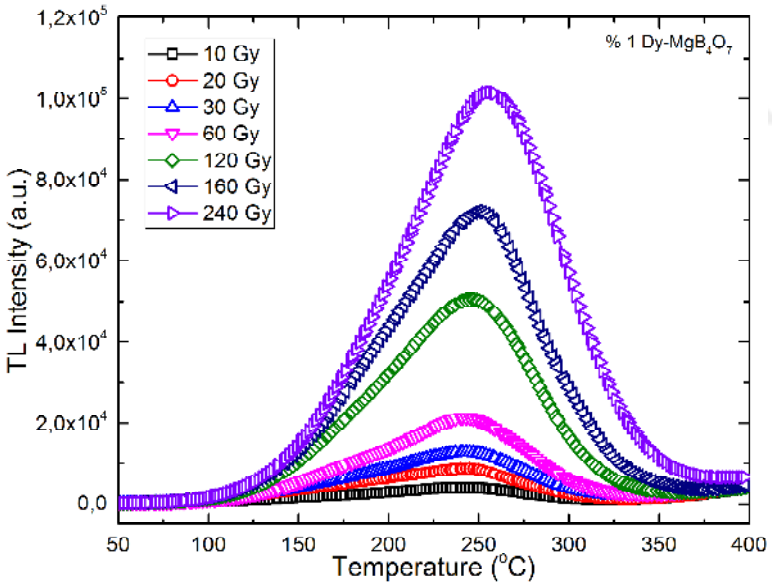

Figure 5.71: The glow curves of 1 % Dy-doped magnesium tetraborate compound corresponding to various radiation doses using ^{252}Cf neutron source with a heating rate of 1 °C/s.

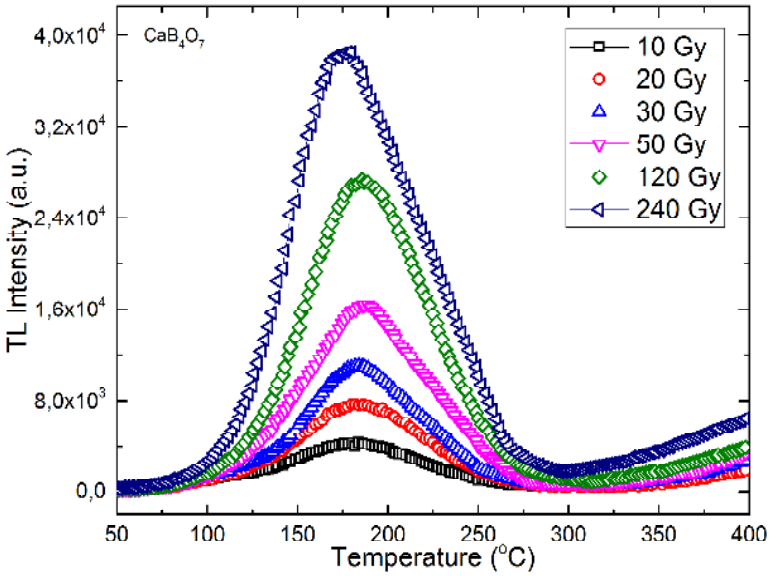

Figure 5.72: The glow curves of calcium tetraborate compound corresponding to various radiation doses using ^{252}Cf neutron source with a heating rate of 1 °C/s.

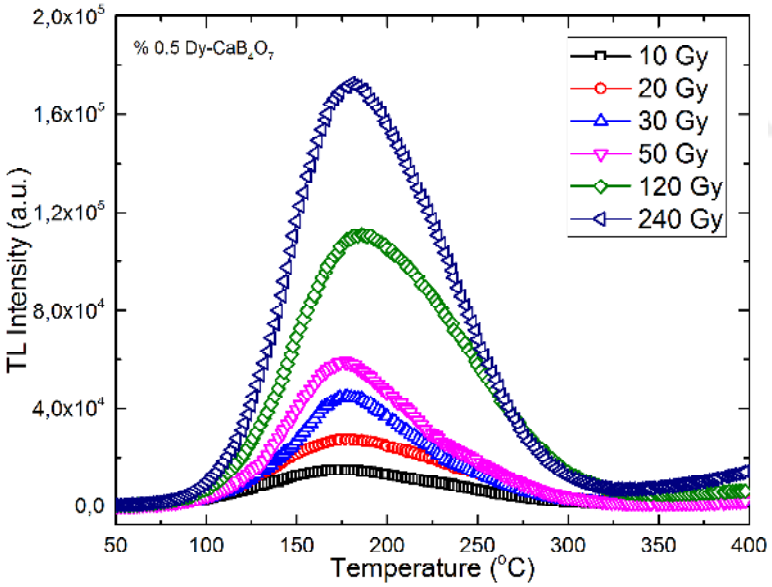

Figure 5.73: The glow curves of 0.5 % Dy-doped calcium tetraborate compound corresponding to various radiation doses using ^{252}Cf neutron source with a heating rate of 1 °C/s.

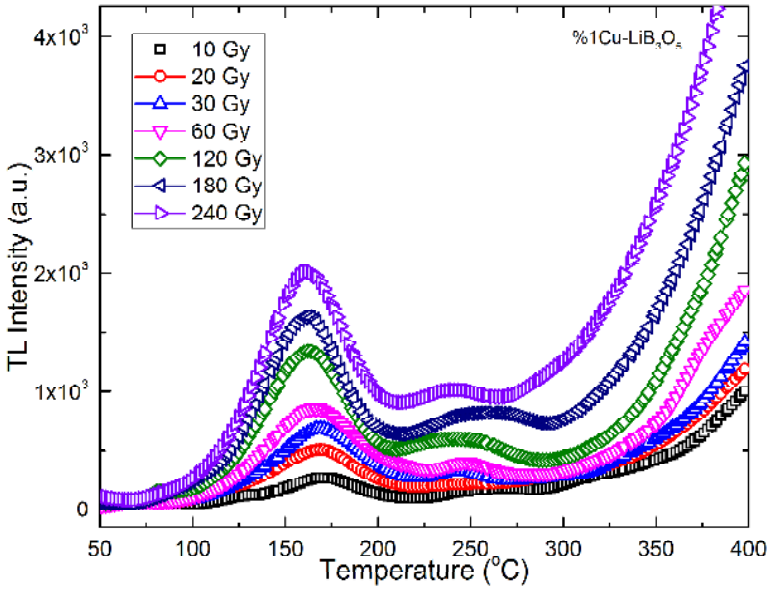

Figure 5.74: The glow curves of 1 % Cu-doped lithium triborate compound corresponding to various radiation doses using ^{252}Cf neutron source with a heating rate of 1 °C/s.

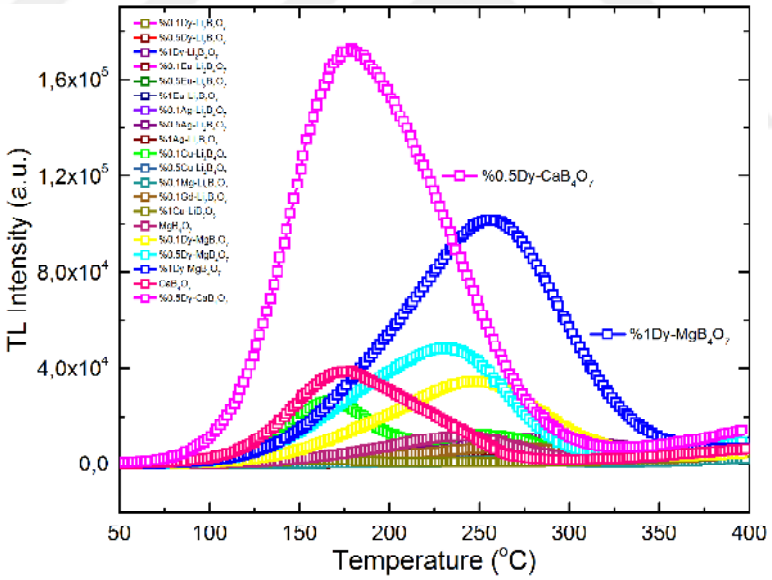

Figure 5.75: The comparison of dose response glow curves of borate compounds.

Figure 5.75 shows a comparison of thermoluminescent results of some borate compounds that are sensitive to neutron radiation. As seen, 0.5 % Dy-doped calcium tetraborate compound has the highest TL intensity of among all borate compounds. The thermoluminescence measurement were done after exposure to the 240 Gy neutron dose.

Termoluminescence Heating Rate Results

It is well known that the heating rate is an important experimental parameter on the glow peak intensities and peak temperatures of many TL dosimetric materials [156-158]. In general, the peak intensity decreases with the increasing heating rate due to thermal quenching [159]. The TL glow curve readout was carried out on a platinum planchet at a linear heating rate 1 °C/s up to 400 °C/s, except for the heating rate experiments. In the variable heating rate (VHR) experiments; to observe the changes in the glow curve structures, to check the glow peak intensities and dose dependence effects of the peak positions as a function of exposed dose levels; the heating rates were changed between 1 °C/s and 9 °C/s. The effects of heating rates on the glow curves of the synthesized lithium tetraborate, lithium triborate, magnesium tetraborate, calcium tetraborate and barium tetraborate compounds were observed after the irradiation by ^{252}Cf neutron source at doses 240 Gy. All of the recorded TL glow curves after various heating rates are shown in Figures 5.76 - 5.95 for all borate compounds. It is clearly seen from these figure that the maximum peak temperatures of all glow peaks shift to high temperature side while the corresponding TL intensities and the total areas under the glow curves of borate compounds decrease with the increasing heating rates.

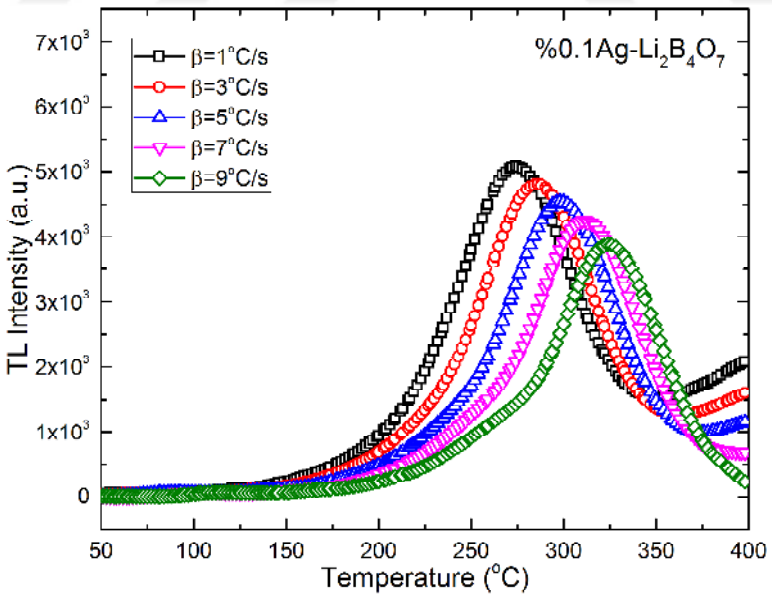

Figure 5.76: The TL glow curves of 0.1 % Ag-doped lithium tetraborate compound measured after various heating rates between 1 and 9 °C/s. Measurements are taken after irradiation of 240 Gy using ^{252}Cf neutron source.

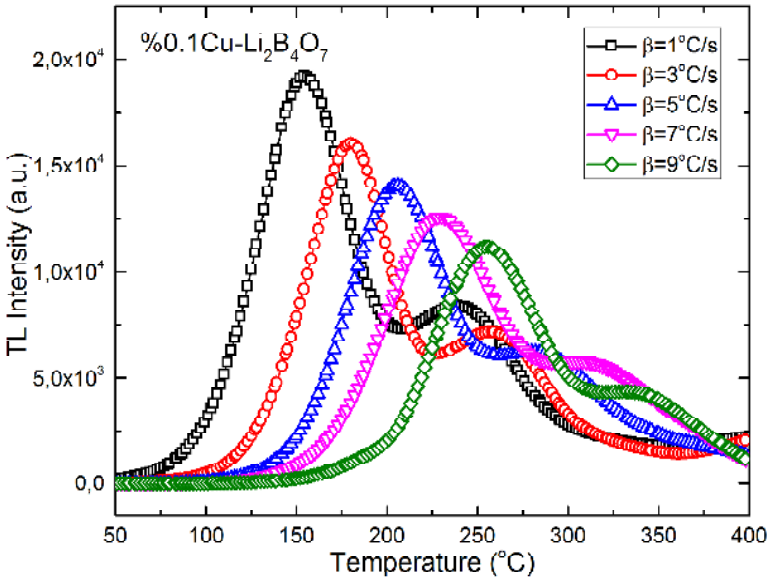

Figure 5.77: The TL glow curves of 0.1 % Cu-doped lithium tetraborate compound measured after various heating rates between 1 and 9 °C/s. Measurements are taken after irradiation of 240 Gy using ^{252}Cf neutron source.

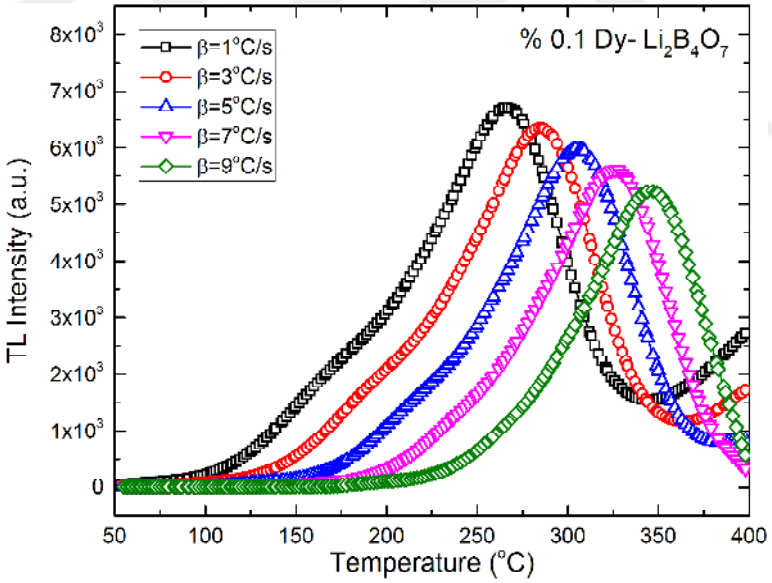

Figure 5.78: The TL glow curves of 0.1 % Dy-doped lithium tetraborate compound measured after various heating rates between 1 and 9 °C/s. Measurements are taken after irradiation of 240 Gy using ^{252}Cf neutron source.

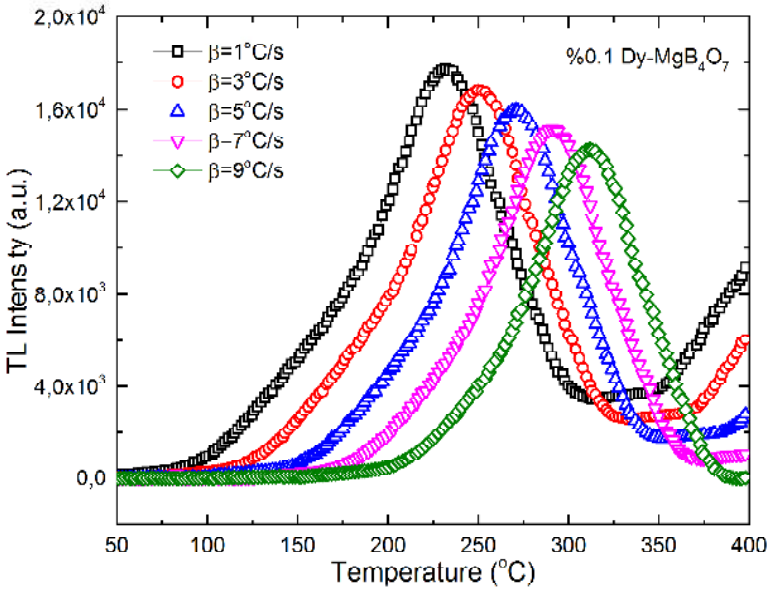

Figure 5.79: The TL glow curves of 0.1 % Dy-doped magnesium tetraborate compound measured after various heating rates between 1 and 9 °C/s. Measurements are taken after irradiation of 240 Gy using ^{252}Cf neutron source.

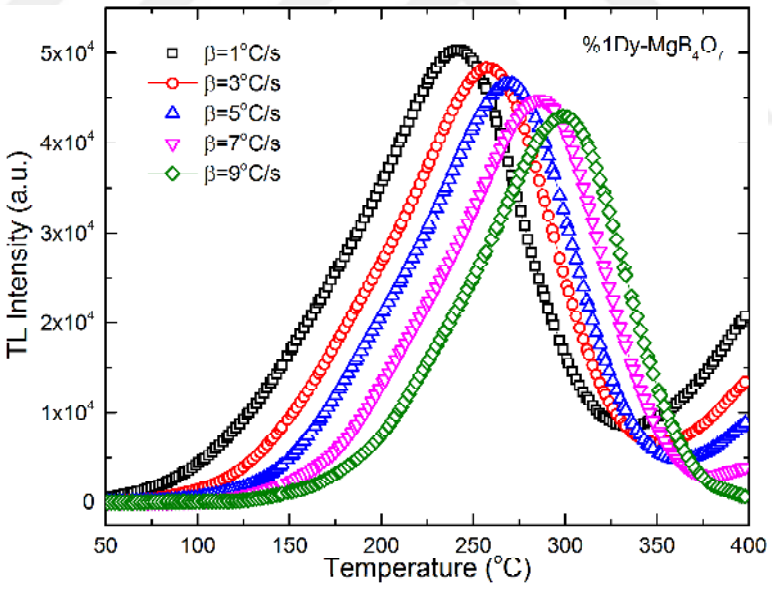

Figure 5.80: The TL glow curves of 1 % Dy-doped magnesium tetraborate compound measured after various heating rates between 1 and 9 °C/s. Measurements are taken after irradiation of 240 Gy using ^{252}Cf neutron source.

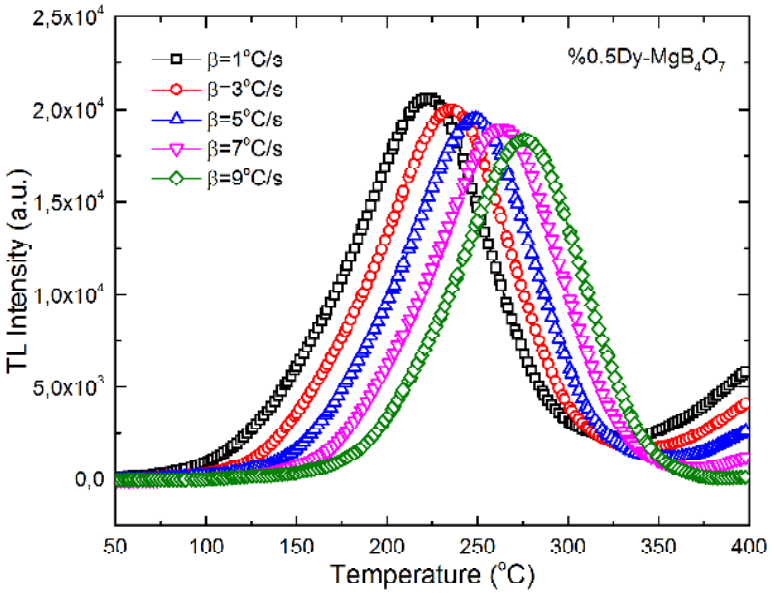

Figure 5.81: The TL glow curves of 0.5 % Dy-doped magnesium tetraborate compound measured after various heating rates between 1 and 9 °C/s. Measurements are taken after irradiation of 240 Gy using ^{252}Cf neutron source.

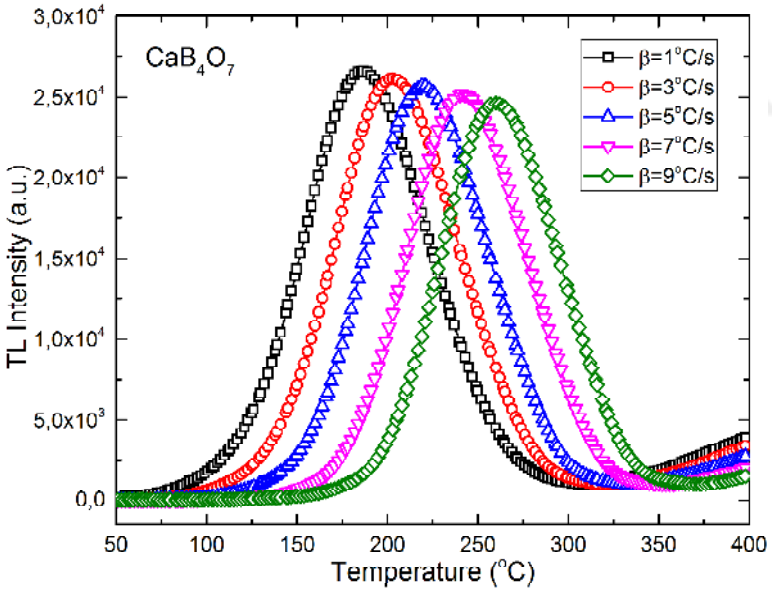

Figure 5.82: The TL glow curves of calcium tetraborate compound measured after various heating rates between 1 and 9 °C/s. Measurements are taken after irradiation of 240 Gy using ^{252}Cf neutron source.

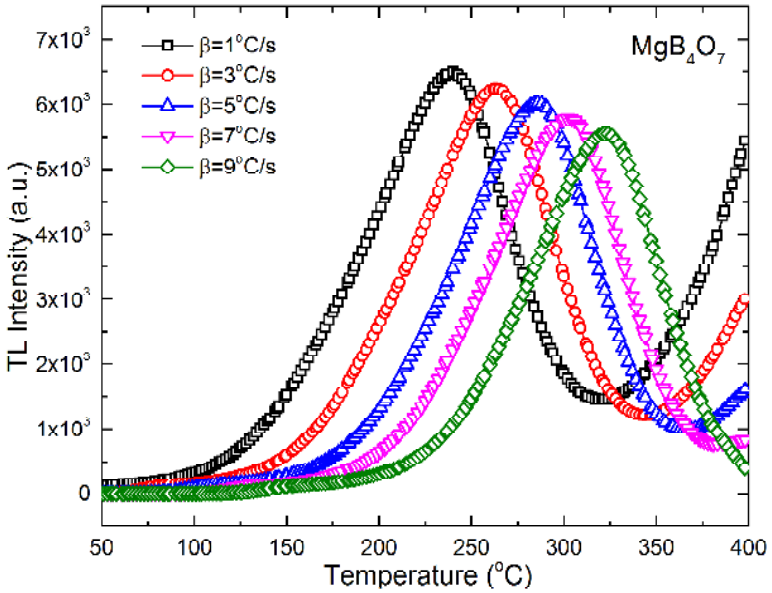

Figure 5.83: The TL glow curves of magnesium tetraborate compound measured after various heating rates between 1 and 9 °C/s. Measurements are taken after irradiation of 240 Gy using ^{252}Cf neutron source.

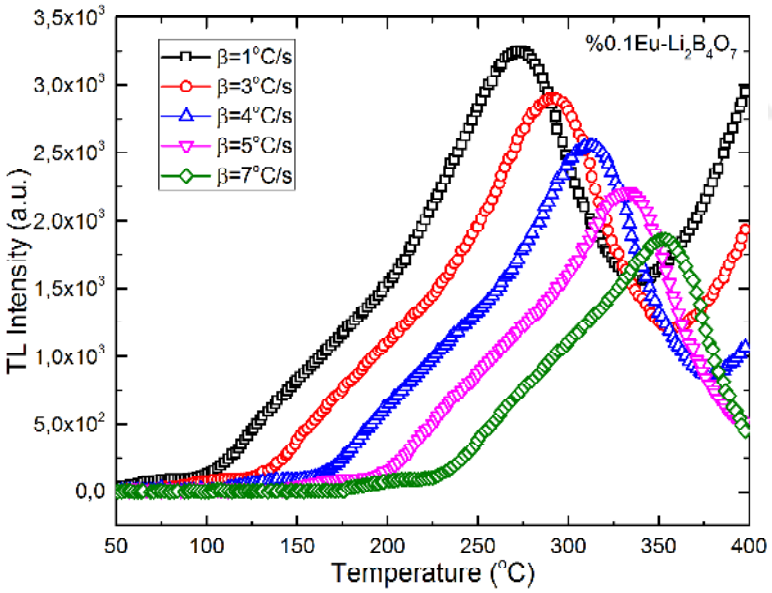

Figure 5.84: The TL glow curves of 0.1 % Eu-doped lithium tetraborate compound measured after various heating rates between 1 and 9 °C/s. Measurements are taken after irradiation of 240 Gy using ^{252}Cf neutron source.

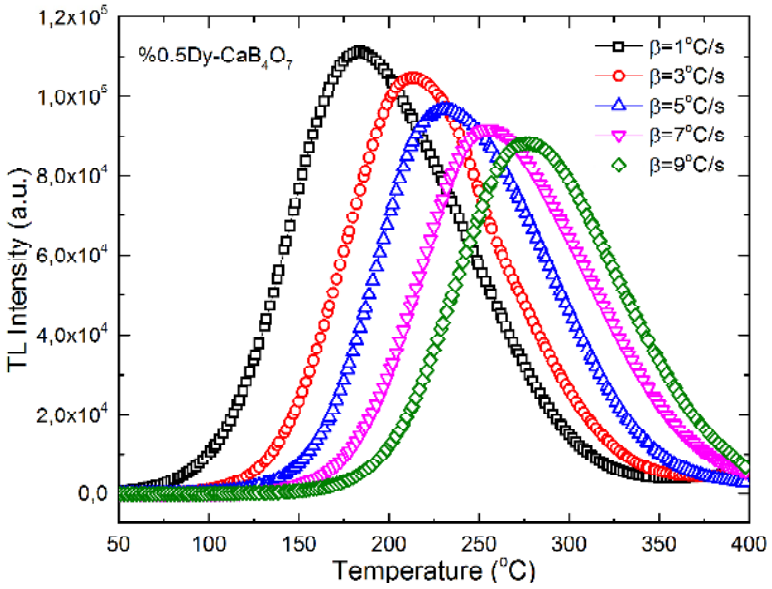

Figure 5.85: The TL glow curves of 0.5 % Eu-doped calcium tetraborate compound measured after various heating rates between 1 and 9 °C/s. Measurements are taken after irradiation of 240 Gy using ^{252}Cf neutron source.

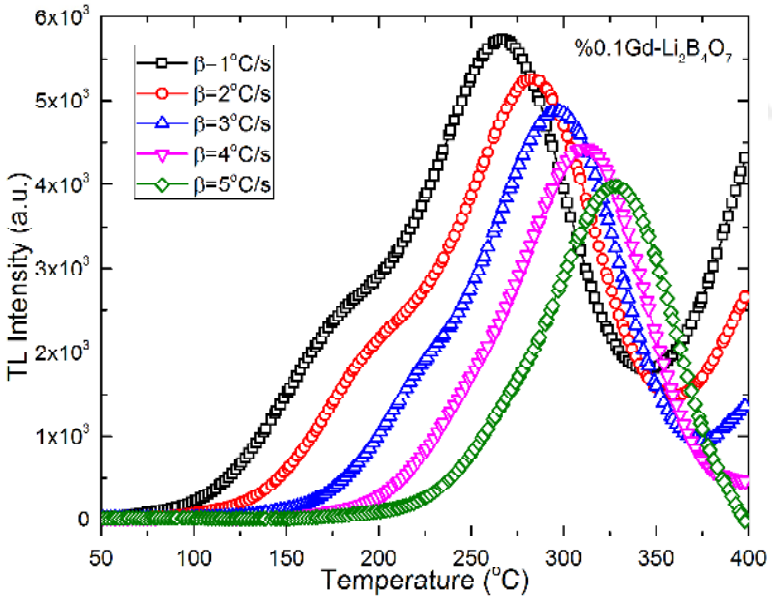

Figure 5.86: The TL glow curves of 0.1 % Gd-doped lithium tetraborate compound measured after various heating rates between 1 and 9 °C/s. Measurements are taken after irradiation of 240 Gy using ^{252}Cf neutron source.

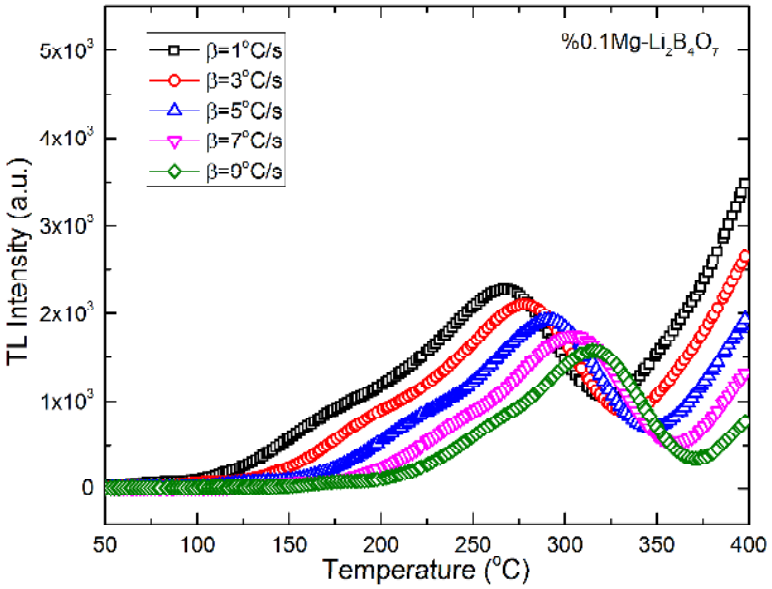

Figure 5.87: The TL glow curves of 0.1 % Mg-doped lithium tetraborate compound measured after various heating rates between 1 and 9 °C/s. Measurements are taken after irradiation of 240 Gy using ^{252}Cf neutron source.

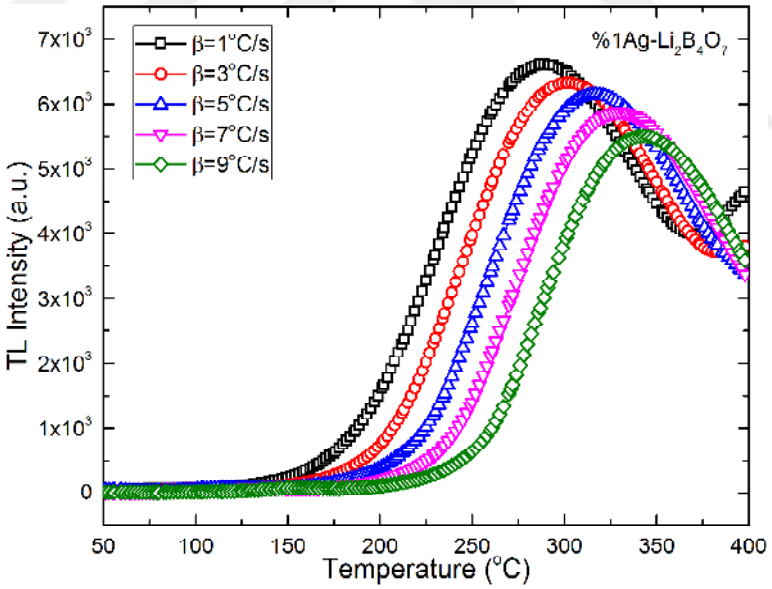

Figure 5.88: The TL glow curves of 1 % Ag-doped lithium tetraborate compound measured after various heating rates between 1 and 9 °C/s. Measurements are taken after irradiation of 240 Gy using ^{252}Cf neutron source.

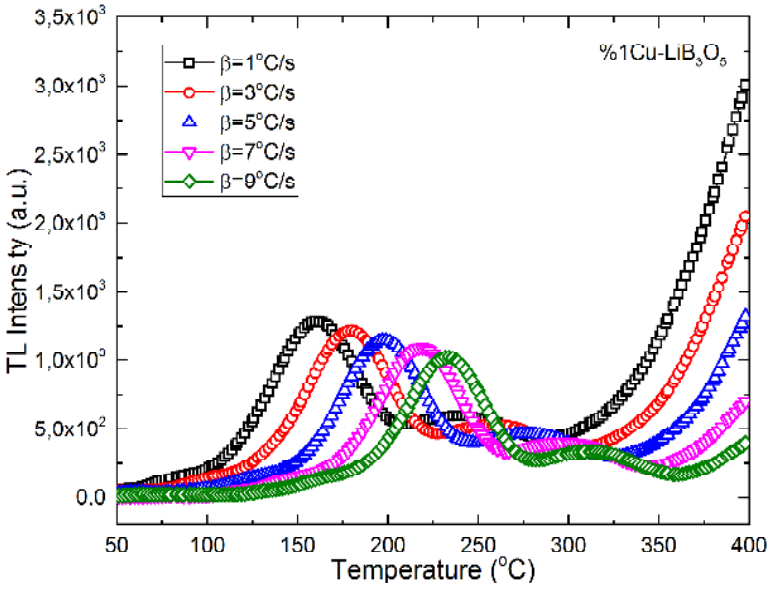

Figure 5.89: The TL glow curves of 1 % Cu-doped lithium triborate compound measured after various heating rates between 1 and 9 °C/s. Measurements are taken after irradiation of 240 Gy using ^{252}Cf neutron source.

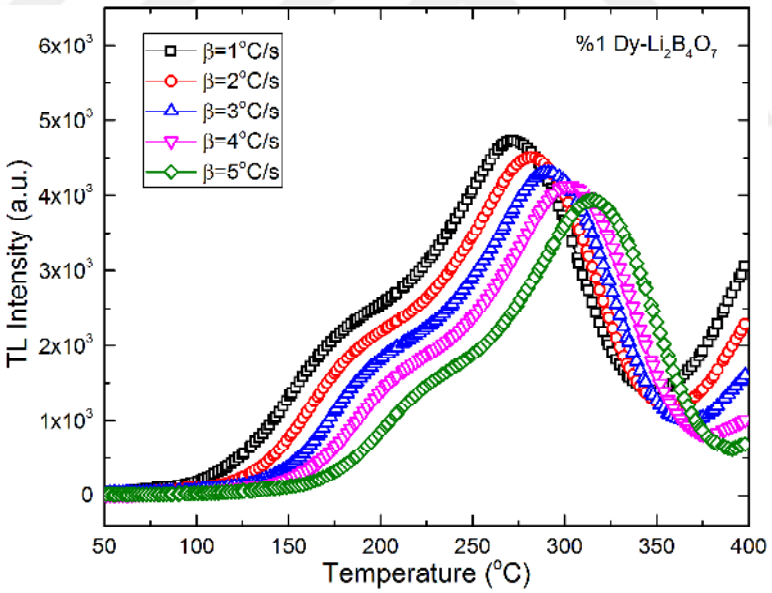

Figure 5.90: The TL glow curves of 1 % Dy-doped lithium tetraborate compound measured after various heating rates between 1 and 9 °C/s. Measurements are taken after irradiation of 240 Gy using ^{252}Cf neutron source.

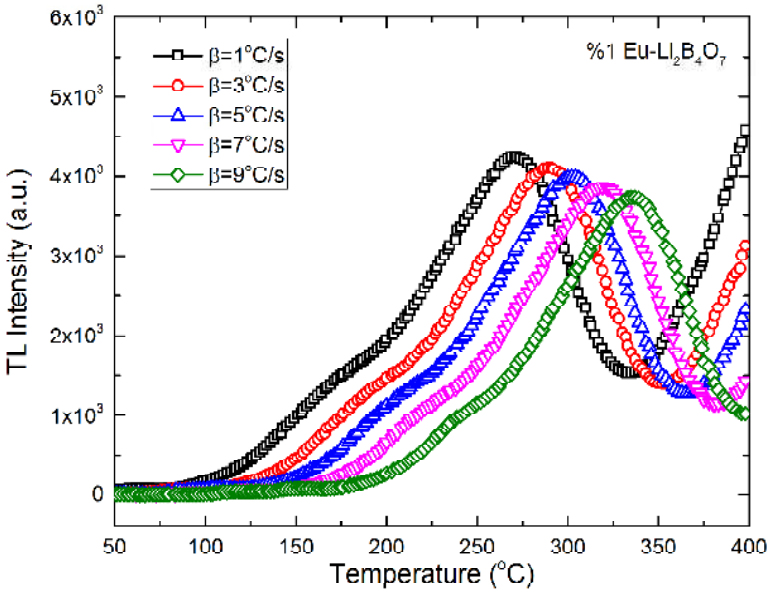

Figure 5.91: The TL glow curves of 1 % Eu-doped lithium tetraborate compound measured after various heating rates between 1 and 9 °C/s. Measurements are taken after irradiation of 240 Gy using ^{252}Cf neutron source.

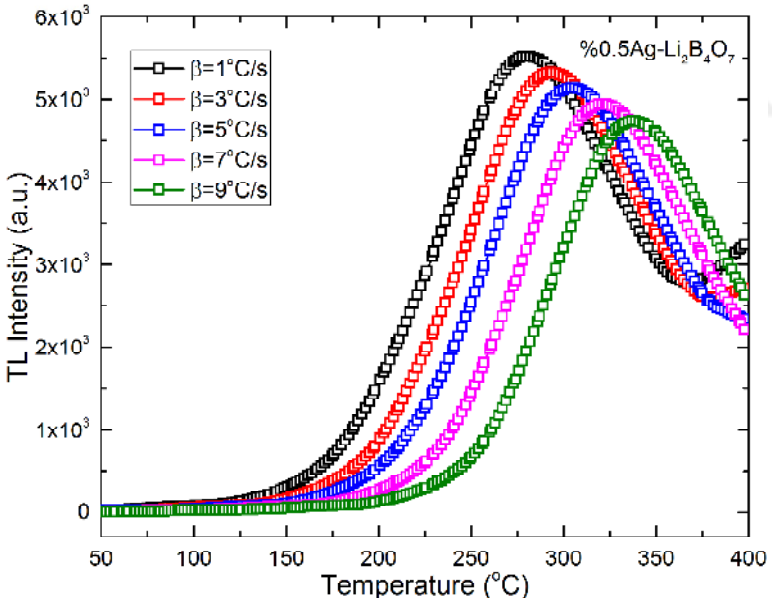

Figure 5.92: The TL glow curves of 0.5 % Ag-doped lithium tetraborate compound measured after various heating rates between 1 and 9 °C/s. Measurements are taken after irradiation of 240 Gy using ^{252}Cf neutron source.

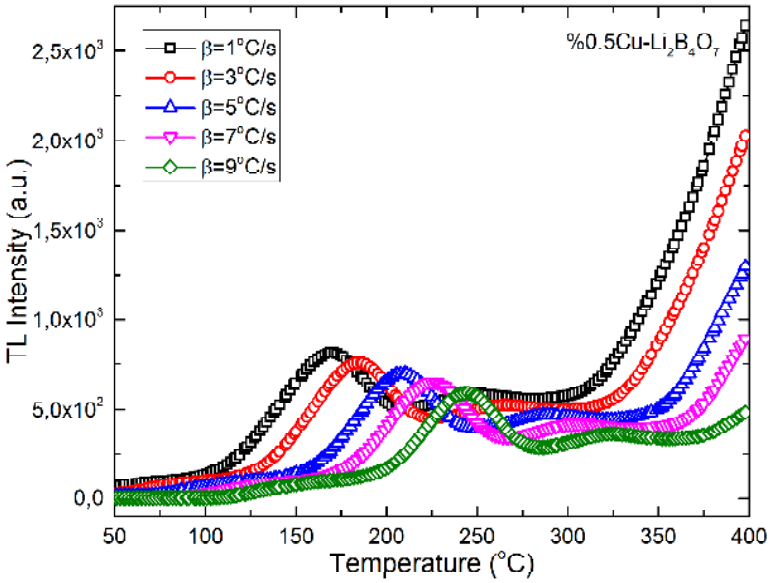

Figure 5.93: The TL glow curves of 0.5 % Cu-doped lithium tetraborate compound measured after various heating rates between 1 and 9 °C/s. Measurements are taken after irradiation of 240 Gy using ^{252}Cf neutron source.

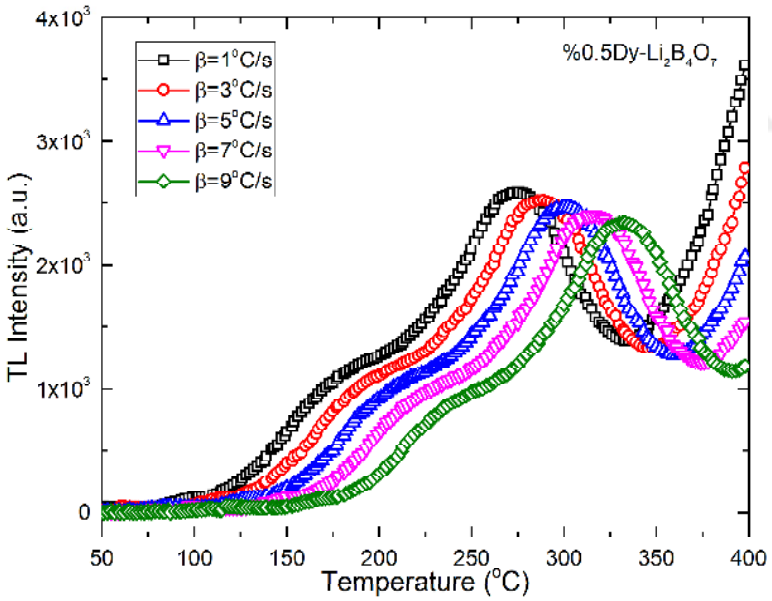

Figure 5.94: The TL glow curves of 0.5 % Dy-doped lithium tetraborate compound measured after various heating rates between 1 and 9 °C/s. Measurements are taken after irradiation of 240 Gy using ^{252}Cf neutron source.

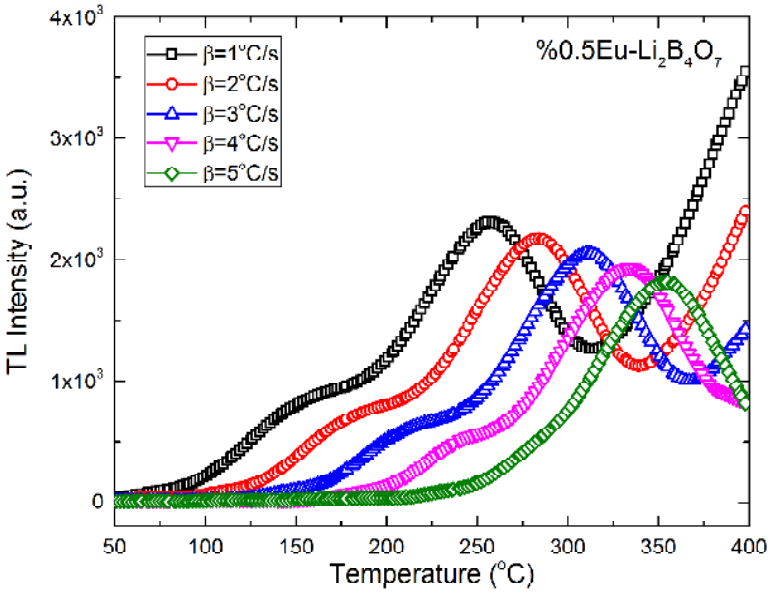

Figure 5.95: The TL glow curves of 0.5 % Eu-doped lithium tetraborate compound measured after various heating rates between 1 and 9 °C/s. Measurements are taken after irradiation of 240 Gy using ^{252}Cf neutron source.

5.1.3 Differential Thermal Analysis (DTA) and Thermogravimetric Analysis (TGA) Results

The temperature dependence to mass change and thermal stability of the synthesized compounds have been studied by using Pyris 1 Perkin Elmer DTA / TGA Analyzer. The measurement was carried out at nitrogen atmosphere at the range of 30 °C and 930 °C. The heating rate was 10 °C/s. The DTA and TGA results of un-doped and doped borate compounds are illustrated in Figures 5.96 and 5.115. In all figures, it is observed that all samples were thermally stable in the particular desired range.

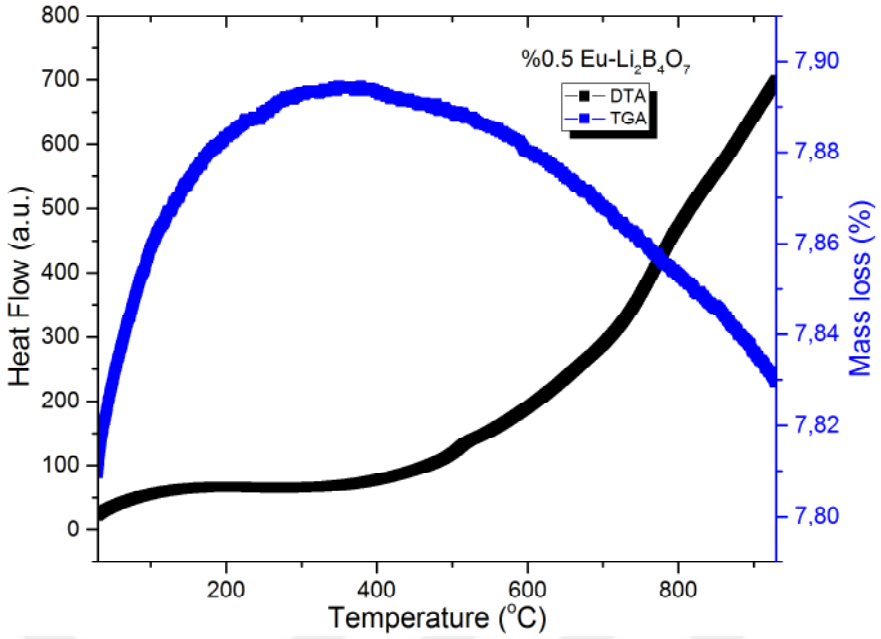

Figure 5.96: DTA/TGA curves of 0.5 % Eu-doped $Li_2B_4O_7$ samples.

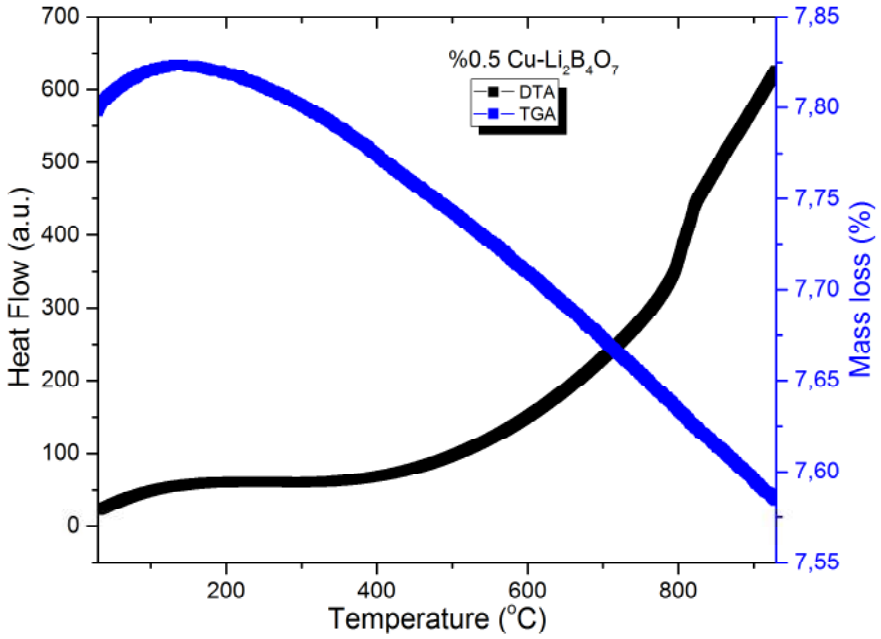

Figure 5.97: DTA/TGA curves of 0.5 % Cu-doped $Li_2B_4O_7$ samples.

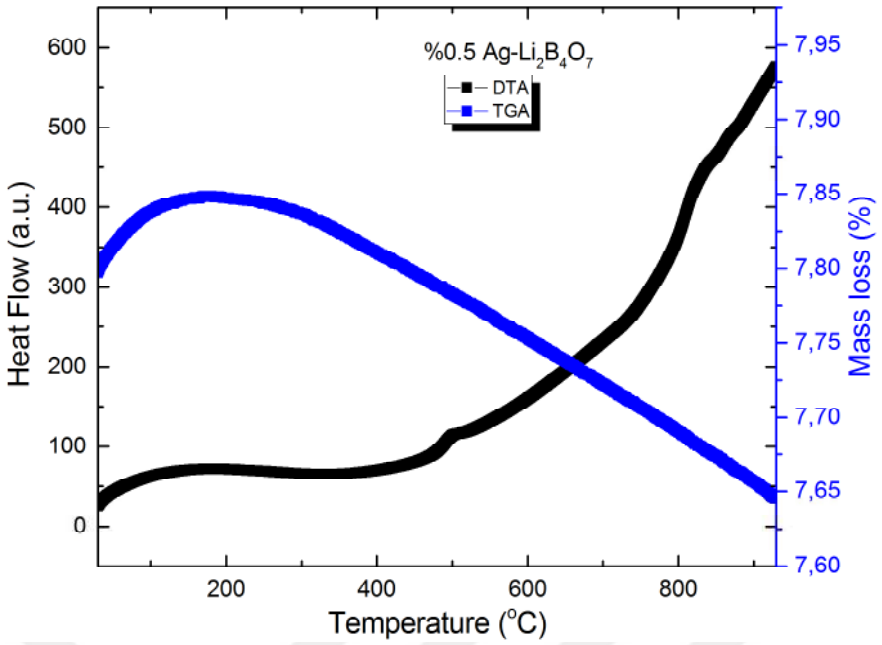

Figure 5.98: DTA/TGA curves of 0.5 % Ag-doped $Li_2B_4O_7$ samples.

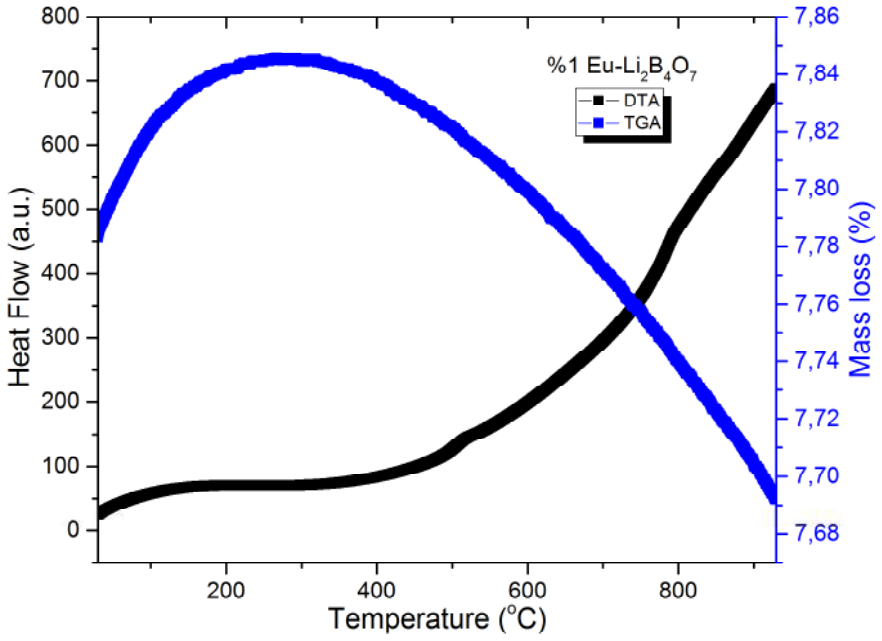

Figure 5.99: DTA/TGA curves of 1 % Eu-doped $Li_2B_4O_7$ samples.

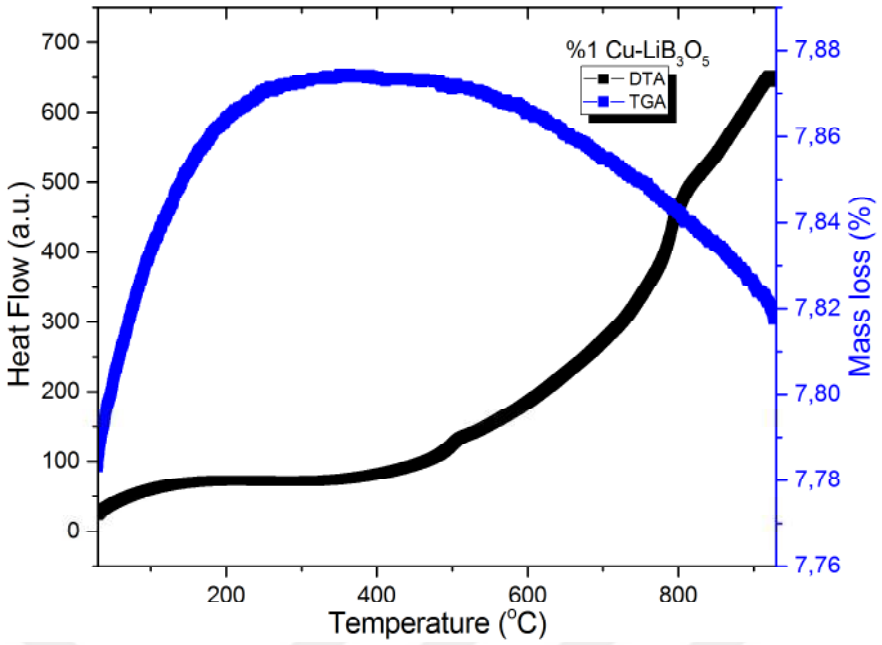

Figure 5.100: DTA/TGA curves of 1 % Cu-doped LiB_3O_5 samples.

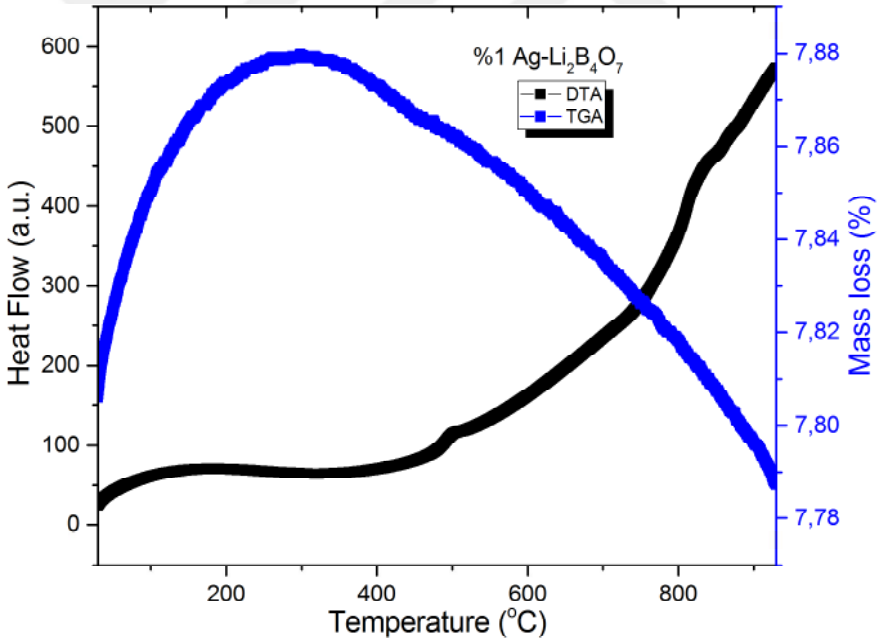

Figure 5.101: DTA/TGA curves of 1 % Ag-doped $Li_2B_4O_7$ samples.

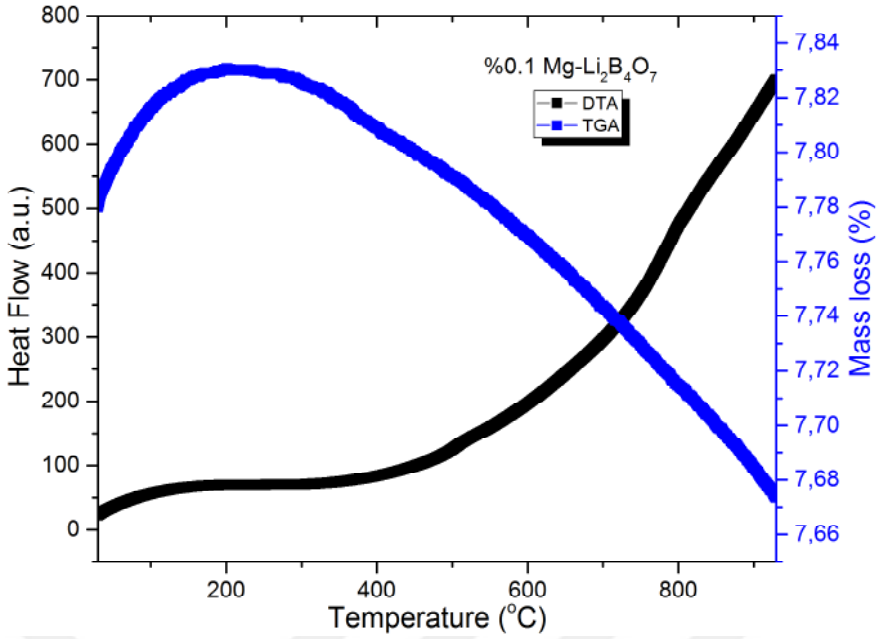

Figure 5.102: DTA/TGA curves of 0.1 % Mg-doped $Li_2B_4O_7$ samples.

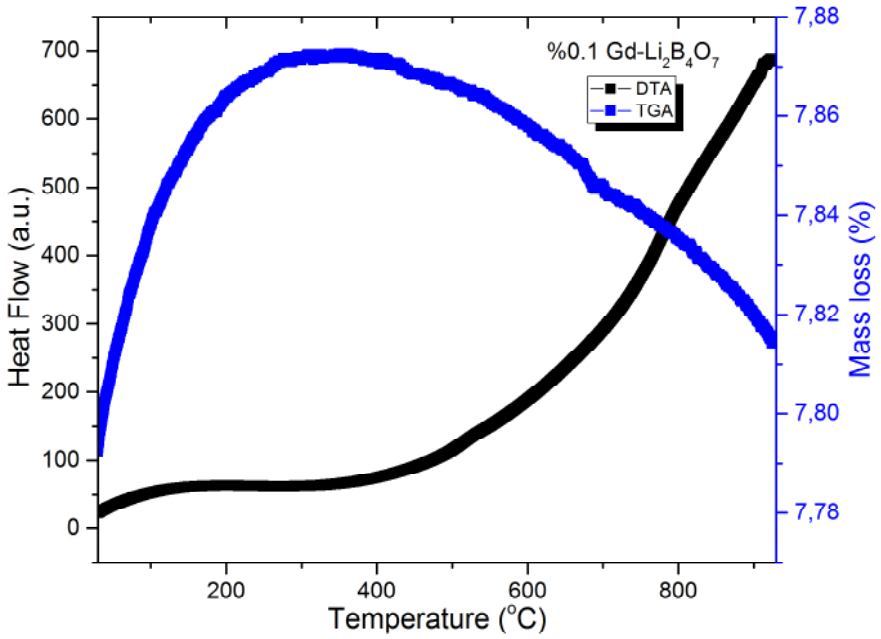

Figure 5.103: DTA/TGA curves of 0.1 % Gd-doped $Li_2B_4O_7$ samples.

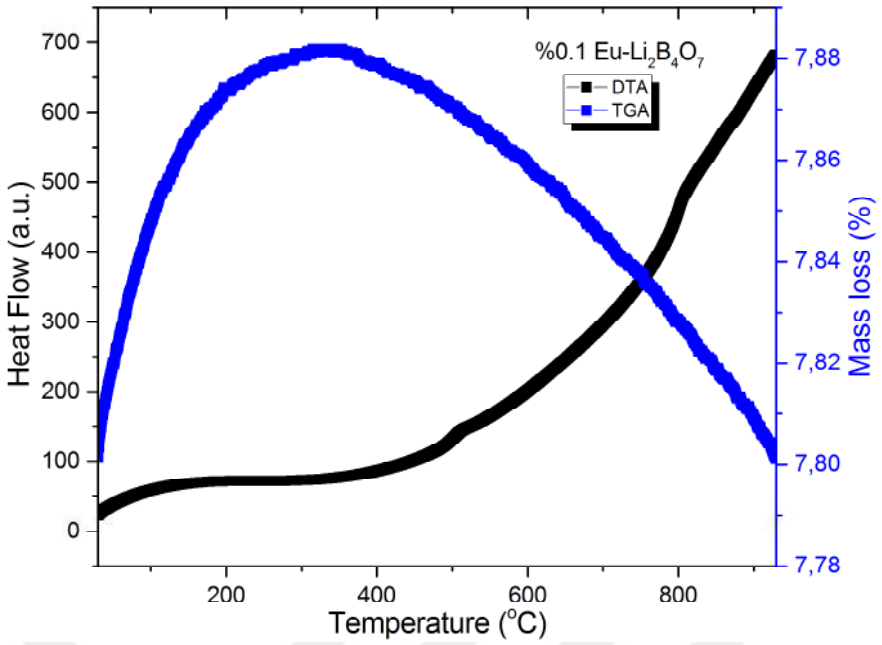

Figure 5.104: DTA/TGA curves of 0.1 % Eu-doped $Li_2B_4O_7$ samples.

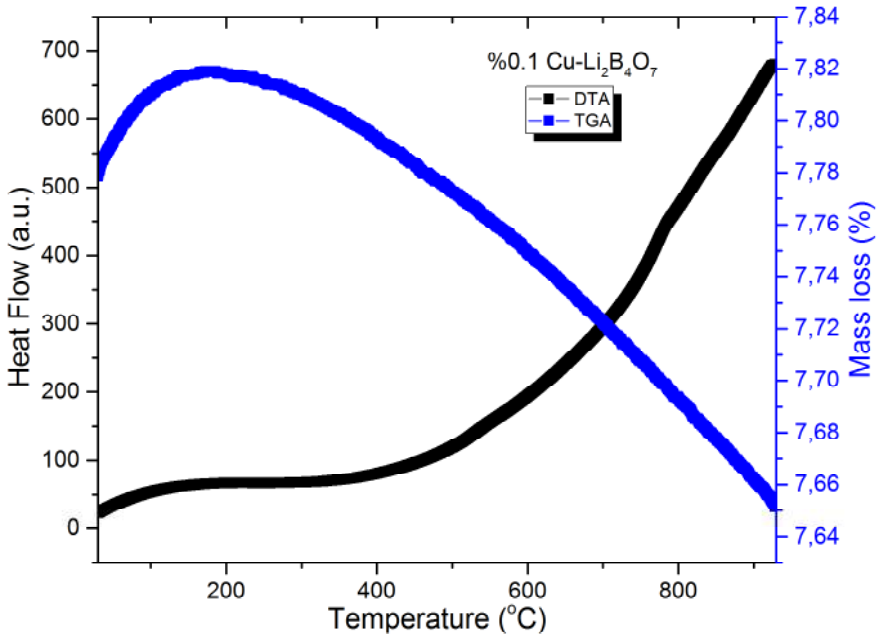

Figure 5.105: DTA/TGA curves of 0.1 % Cu-doped $Li_2B_4O_7$ samples.

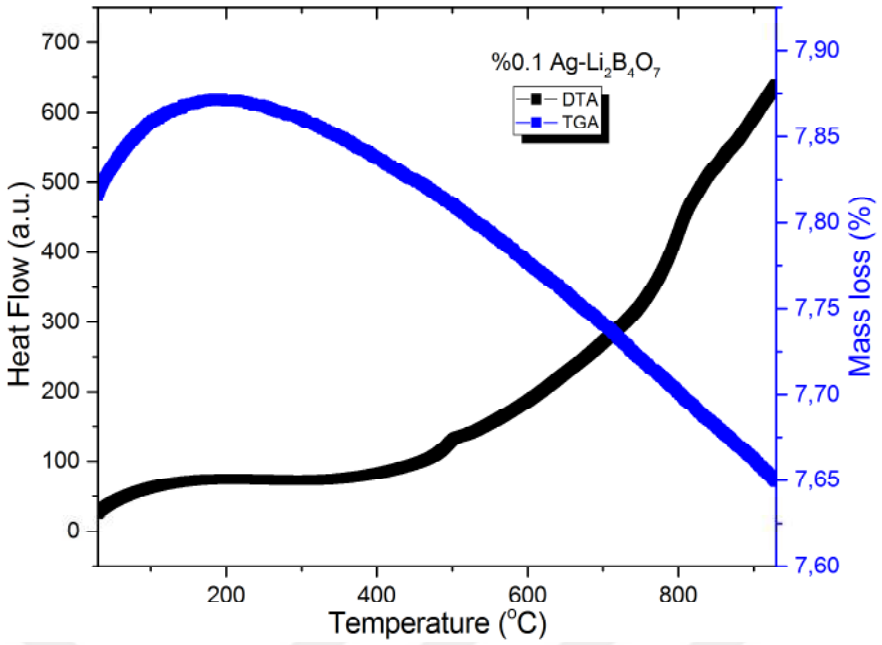

Figure 5.106: DTA/TGA curves of 0.5 % Eu-doped $Li_2B_4O_7$ samples.

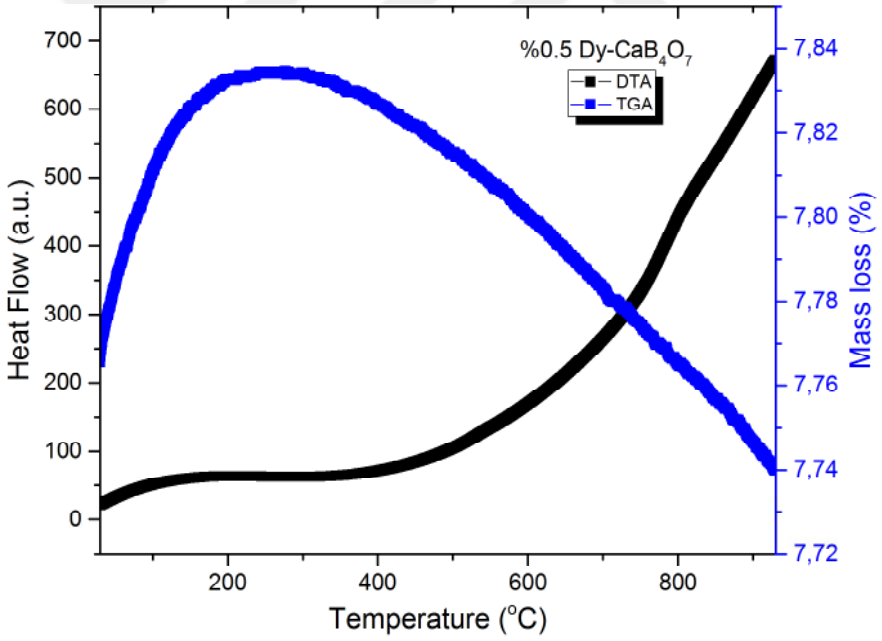

Figure 5.107: DTA/TGA curves of 0.5 % Dy-doped CaB_4O_7 samples.

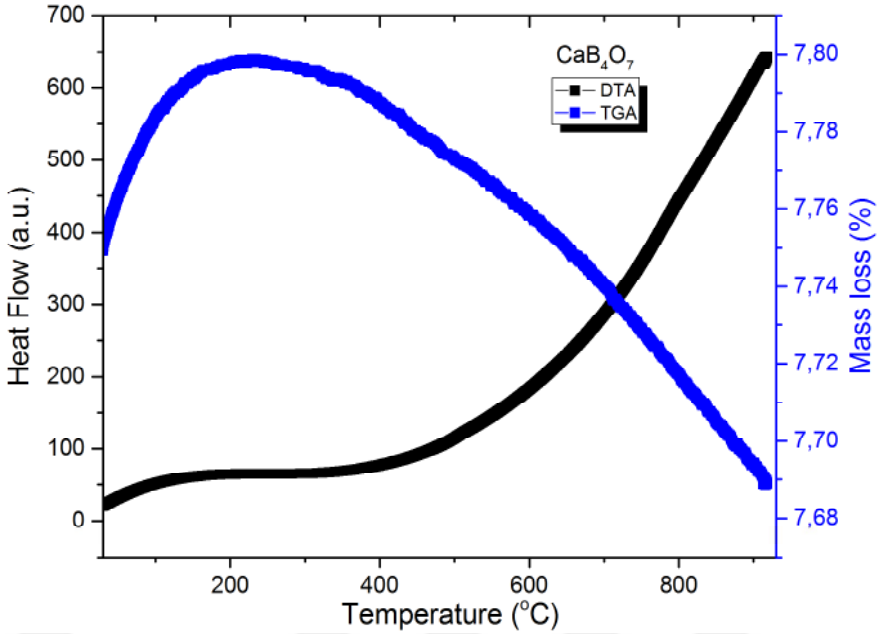

Figure 5.108: DTA/TGA curves of CaB_4O_7 samples.

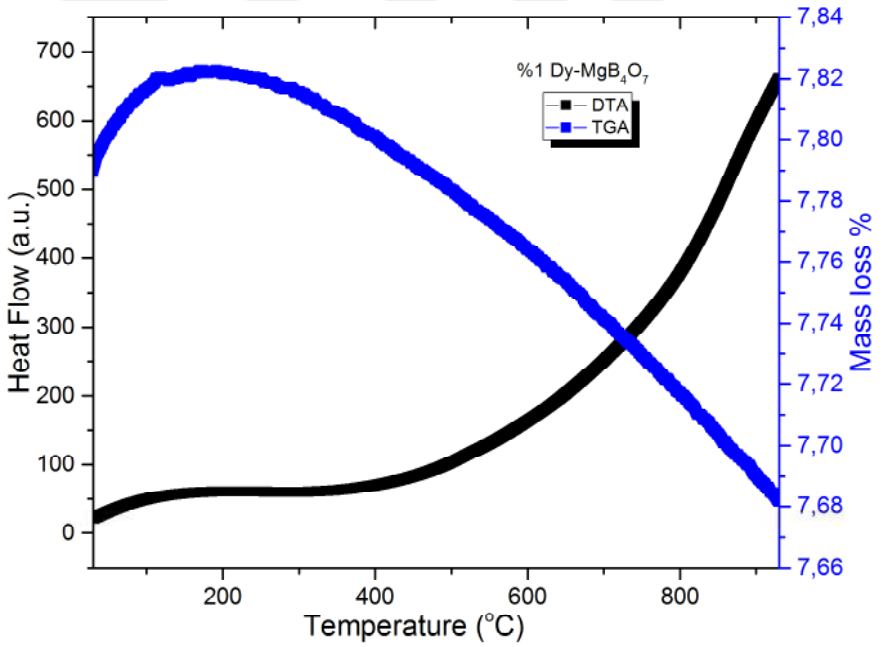

Figure 5.109: DTA/TGA curves of 1 % Dy-doped MgB_4O_7 samples.

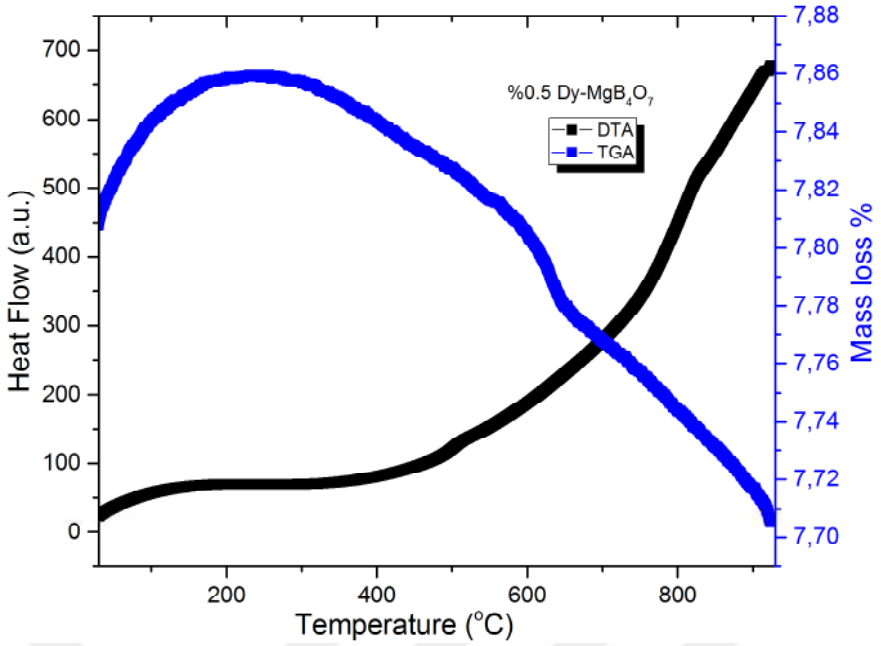

Figure 5.110: DTA/TGA curves of 0.5 % Dy-doped MgB_4O_7 samples.

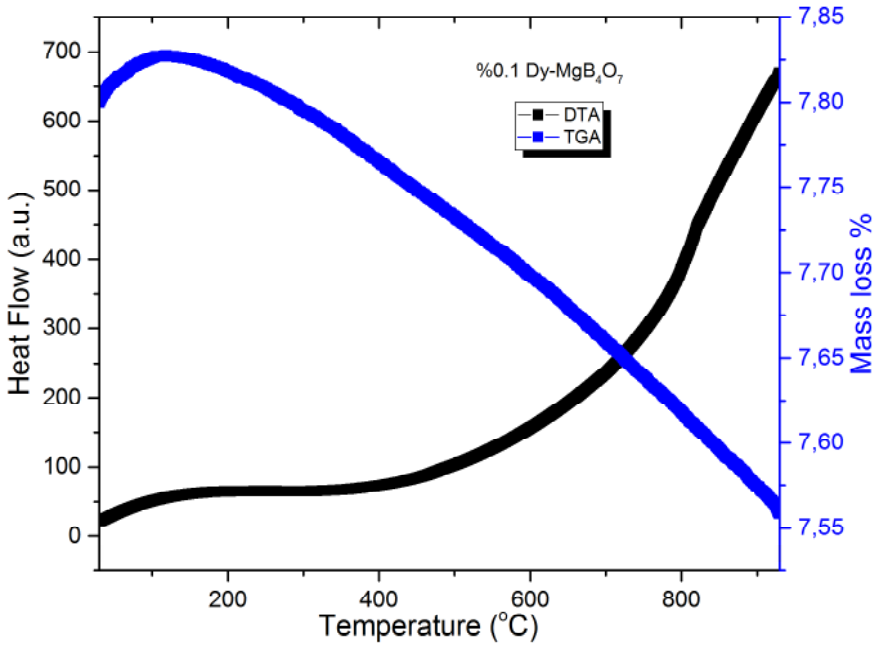

Figure 5.111: DTA/TGA curves of 0.1 % Dy-doped MgB_4O_7 samples.

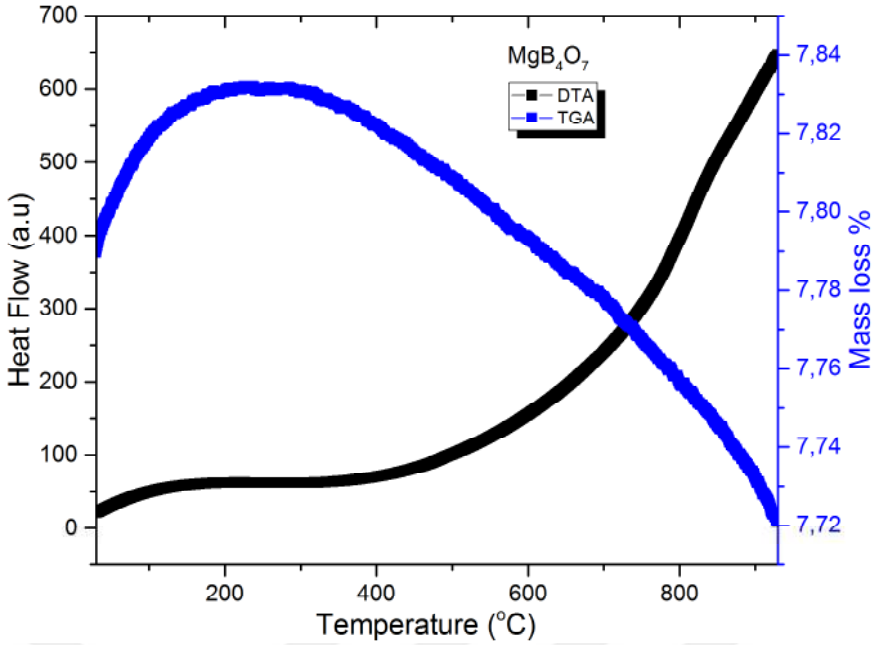

Figure 5.112: DTA/TGA curves of MgB_4O_7 samples.

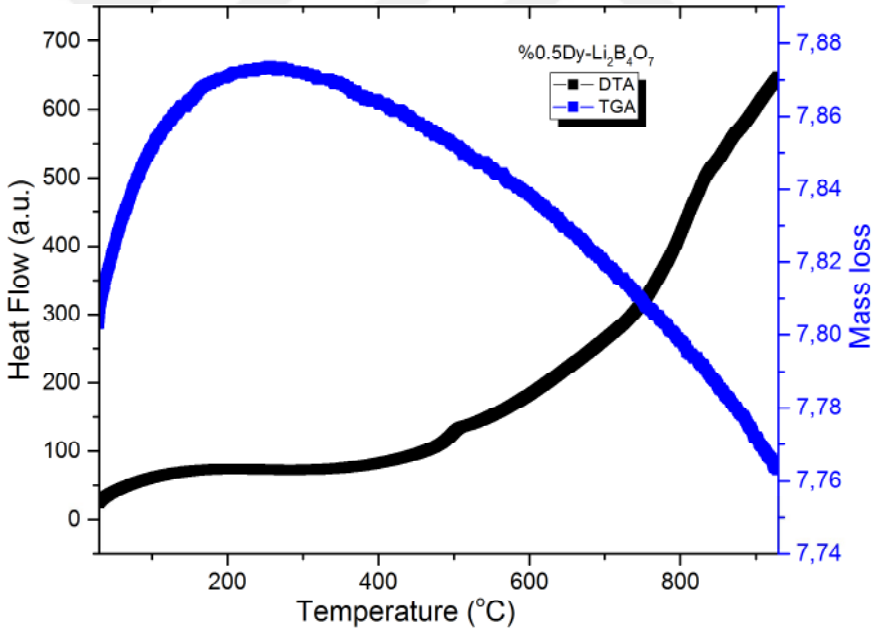

Figure 5.113: DTA/TGA curves of 0.5 % Dy-doped $Li_2B_4O_7$ samples.

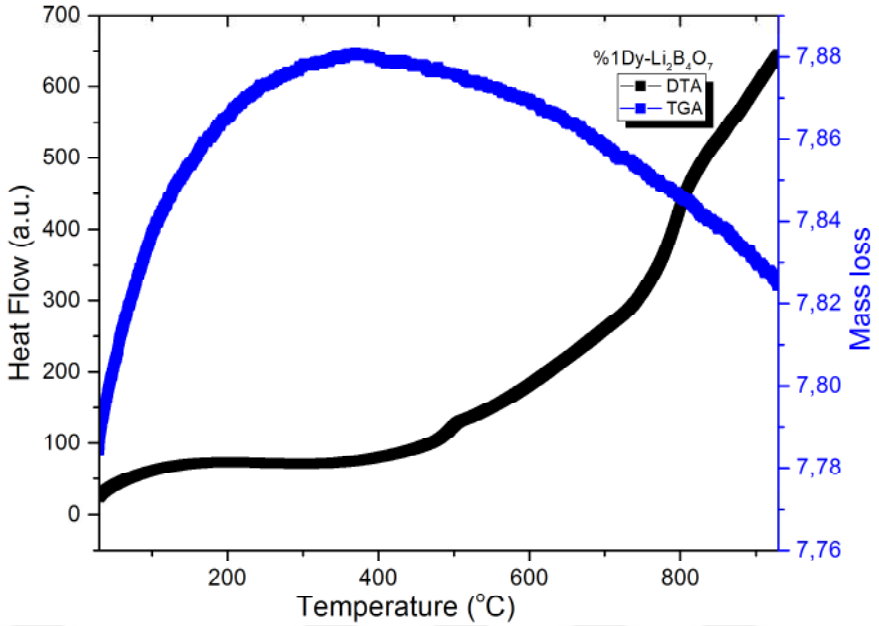

Figure 5.114: DTA/TGA curves of 1 % Dy-doped $Li_2B_4O_7$ samples.

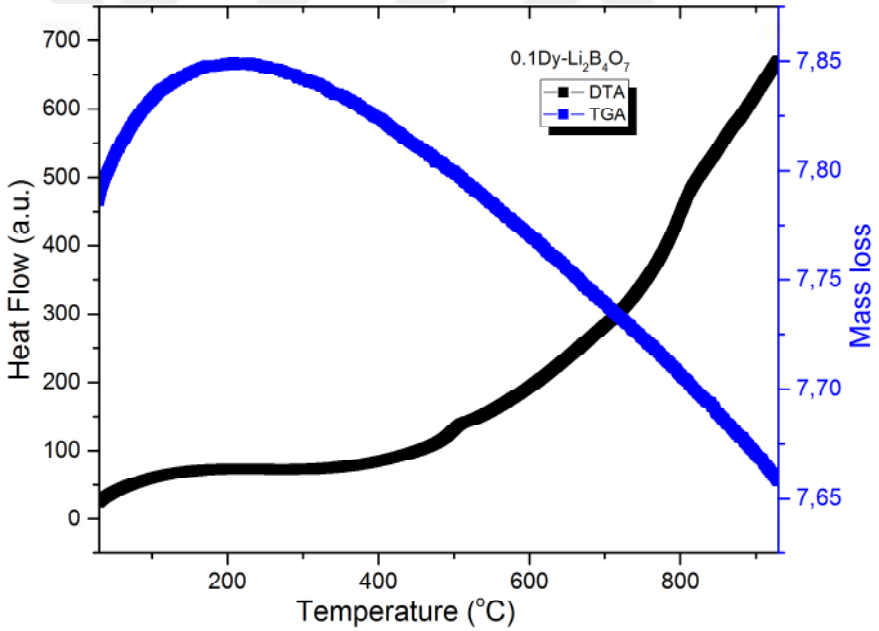

Figure 5.115: DTA/TGA curves of 0.5 % Eu-doped $Li_2B_4O_7$ samples.

5.1.4 Scanning Electron Microscopy (SEM) Results

The scanning electron microscopy (SEM) images revealed the morphological characteristics of un-doped and doped borate compounds produced by using solid state method. In the given study, the SEM images of developed samples are shown in Figures 5.116 and 5.135. As seen, it could be said that the particles size are in the range of ∼5 - 100 μm, and there is homogeneous distribution among particles. These SEM images show that the compounds are not exactly crystalline. The compounds are thought to be molten. It can be said that the particles are "agglomerate"because they appear to be attached.

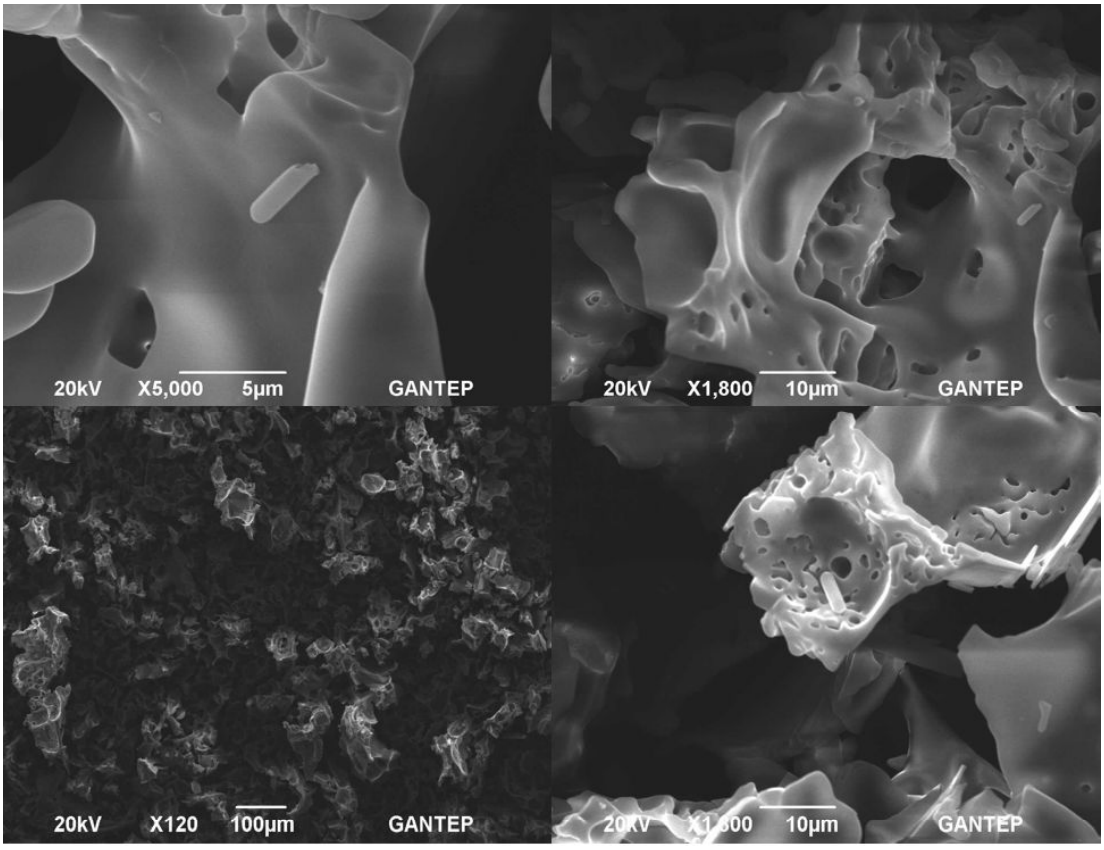

Figure 5.116: SEM images of 1 % Cu doped LiB_3O_5 sample.

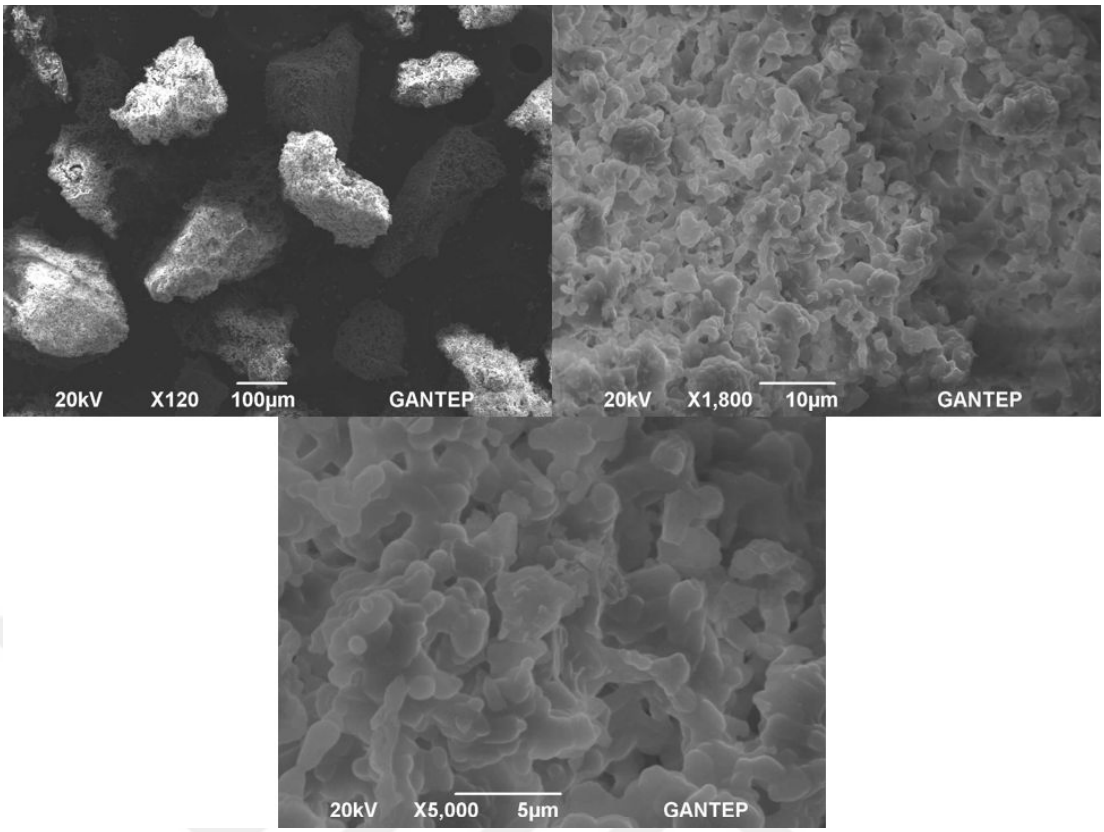

Figure 5.117: SEM images of 0.5 % Dy doped CaB_4O_7 sample.

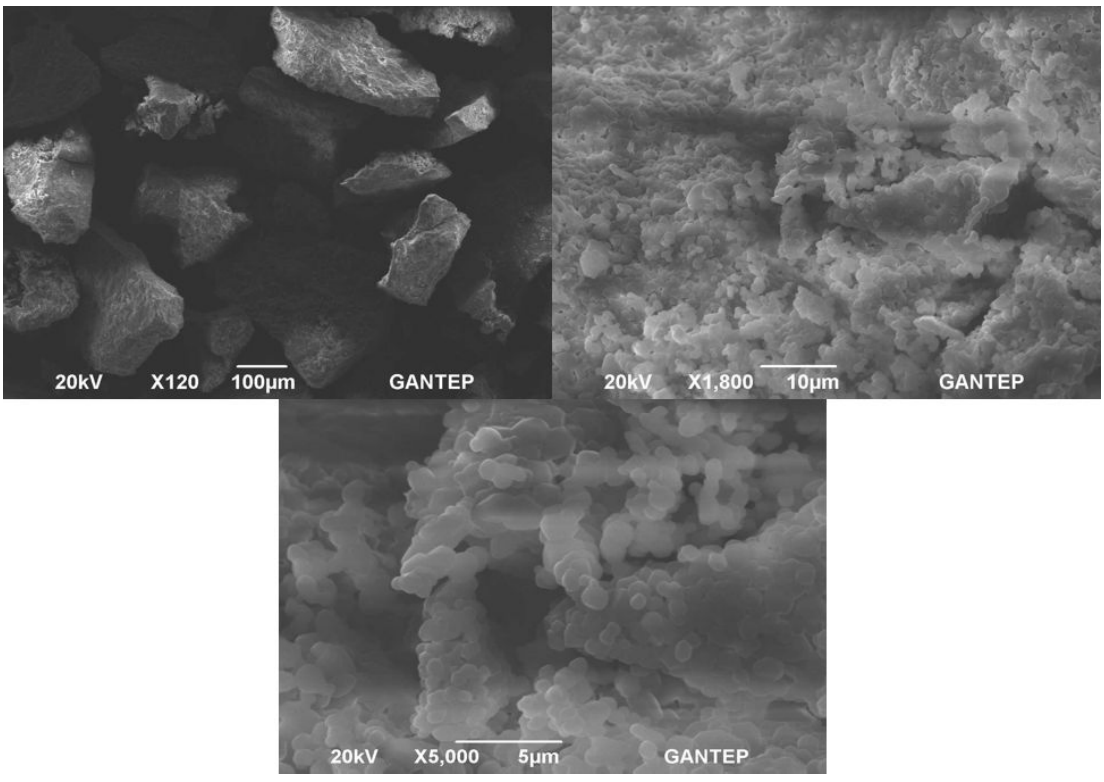

Figure 5.118: SEM images of 1 % Ag doped $Li_2B_4O_7$ sample.

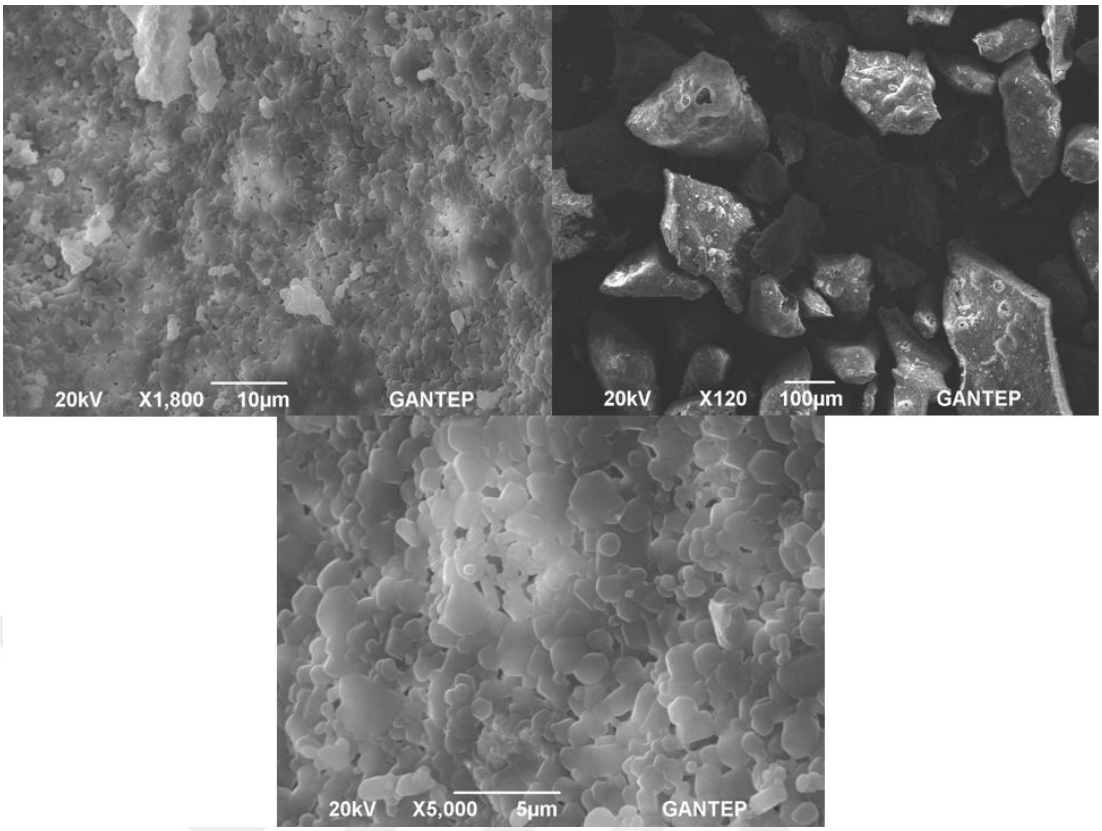

Figure 5.119: SEM images of 1 % Dy doped $Li_2B_4O_7$ sample.

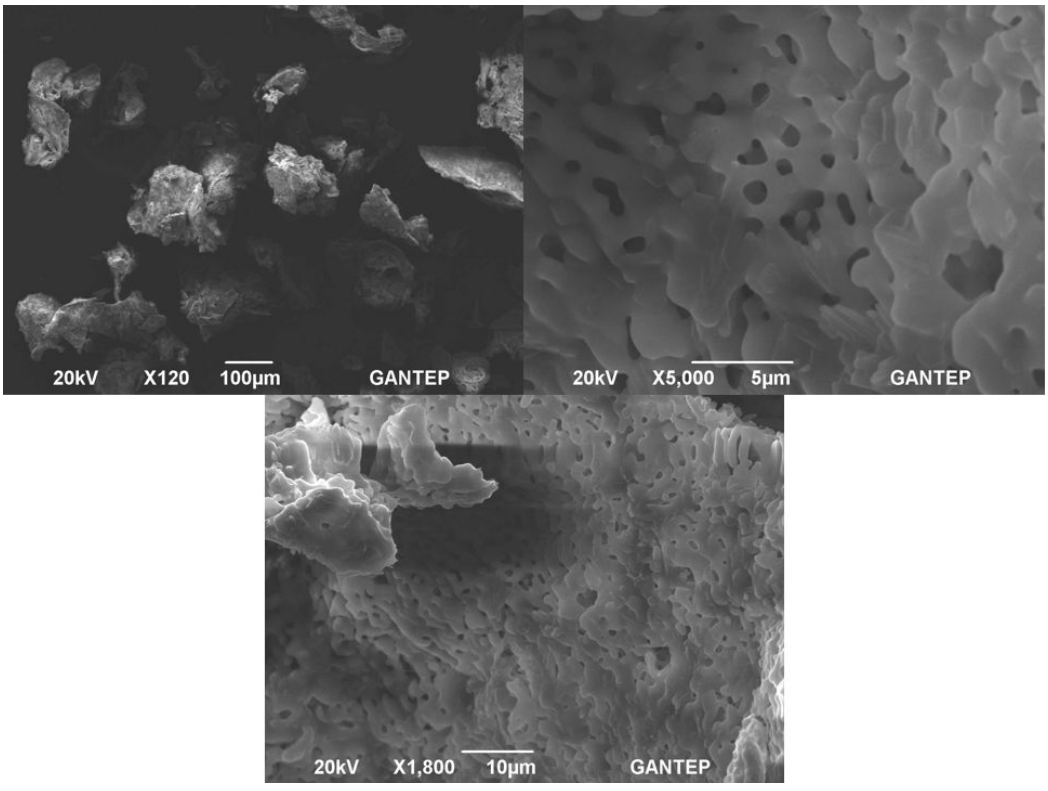

Figure 5.120: SEM images of 1 % Dy doped MgB_4O_7 sample.

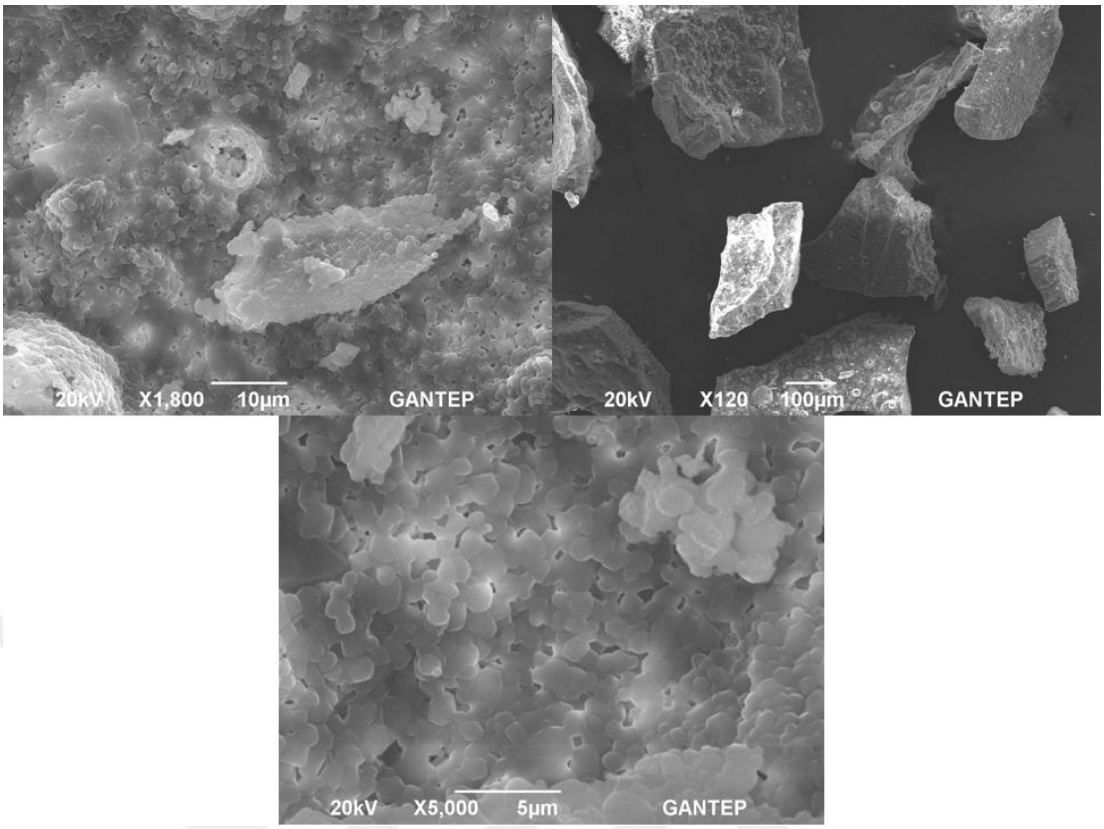

Figure 5.121: SEM images of 1 % Eu doped $Li_2B_4O_7$ sample.

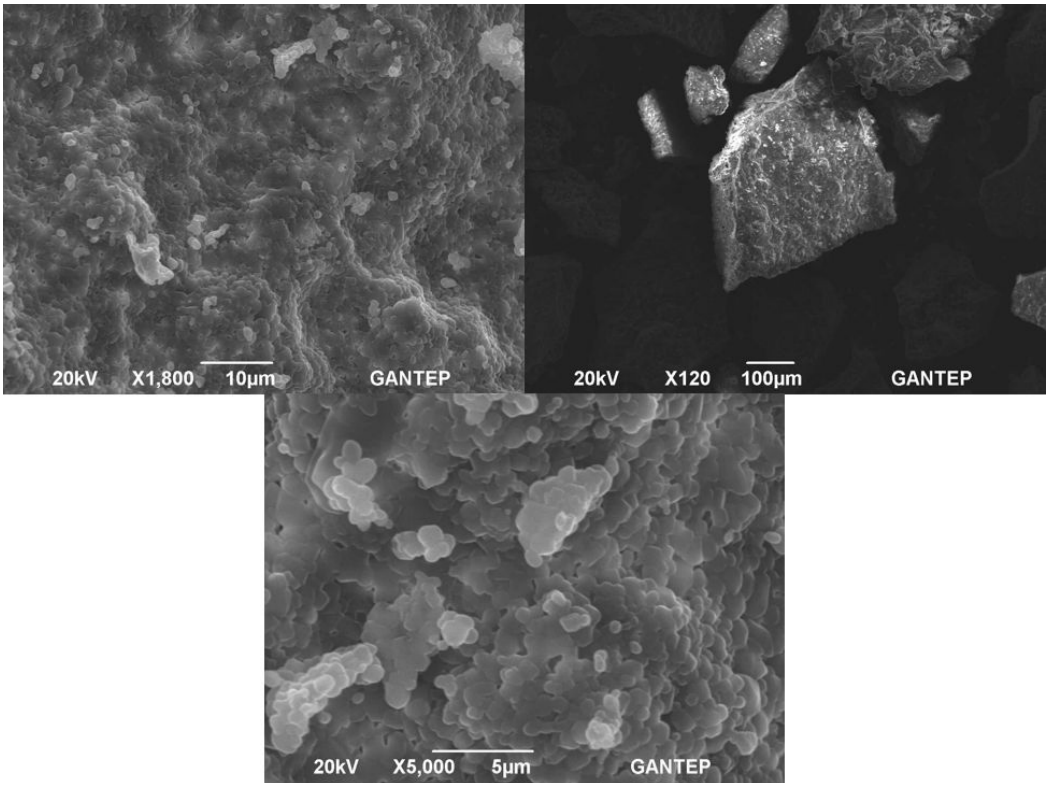

Figure 5.122: SEM images of 0.1 % Ag doped $Li_2B_4O_7$ sample.

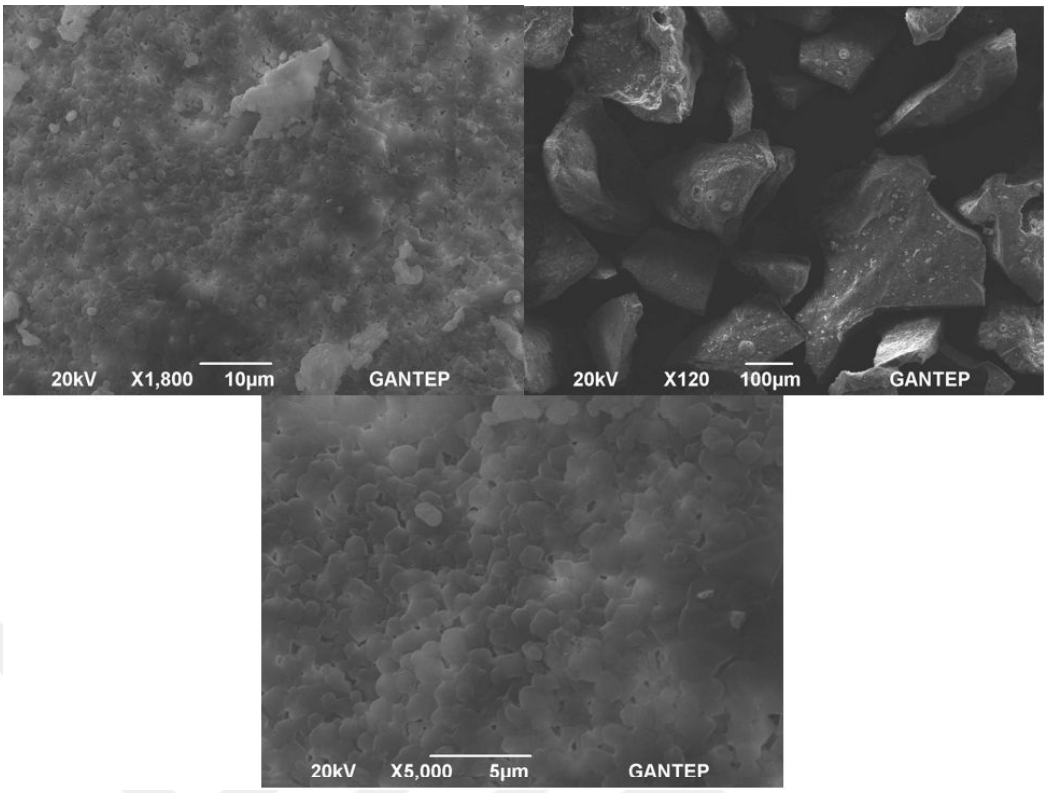

Figure 5.123: SEM images of 0.1 % Cu doped $Li_2B_4O_7$ sample.

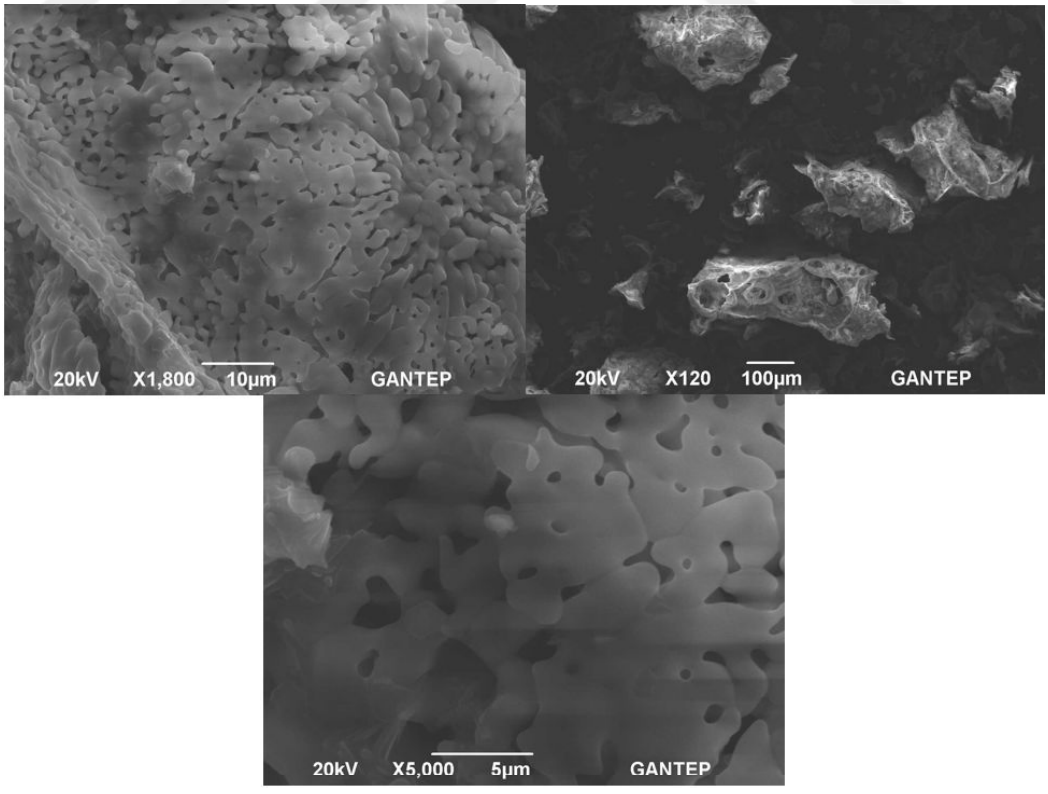

Figure 5.124: SEM images of 0.1 % Dy doped MgB_4O_7 sample.

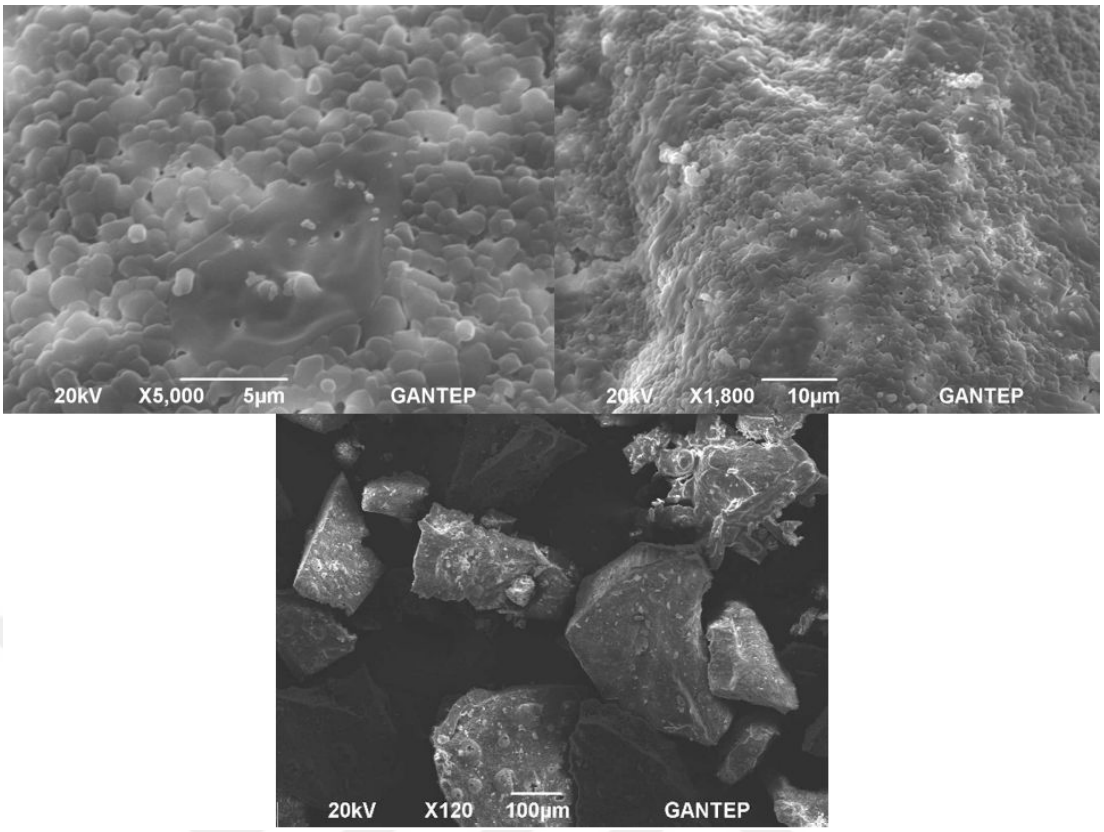

Figure 5.125: SEM images of 0.1 % Dy doped $Li_2B_4O_7$ sample.

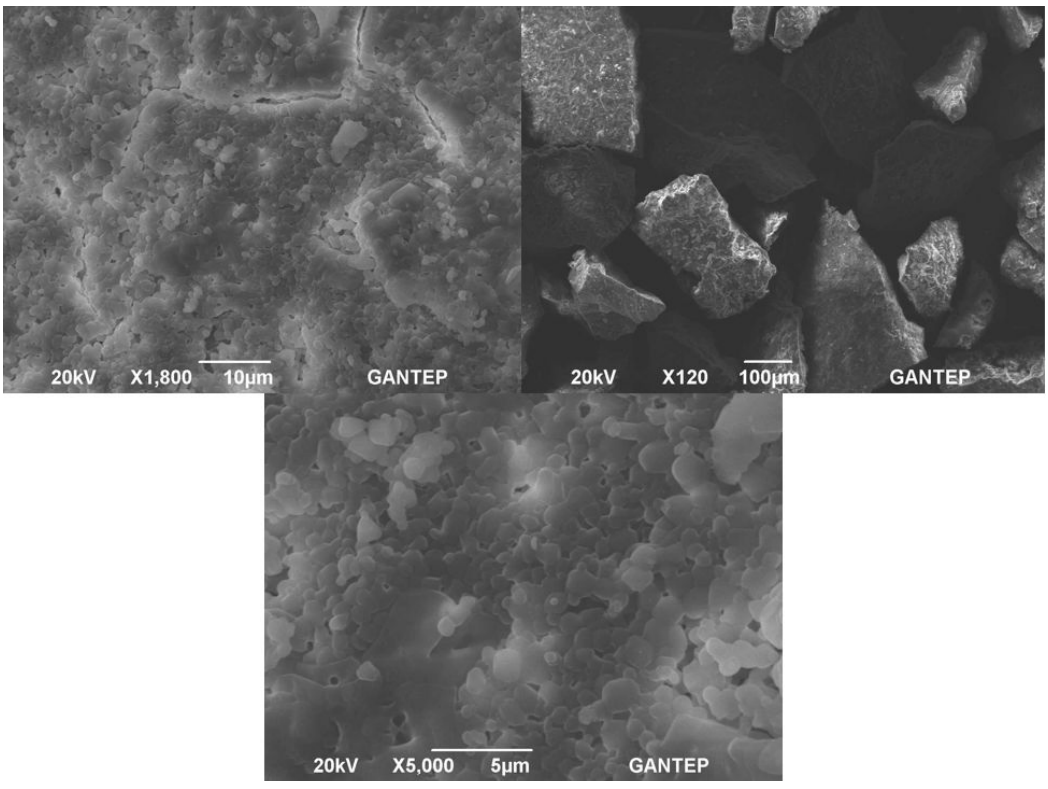

Figure 5.126: SEM images of 0.1 % Eu doped $Li_2B_4O_7$ sample.

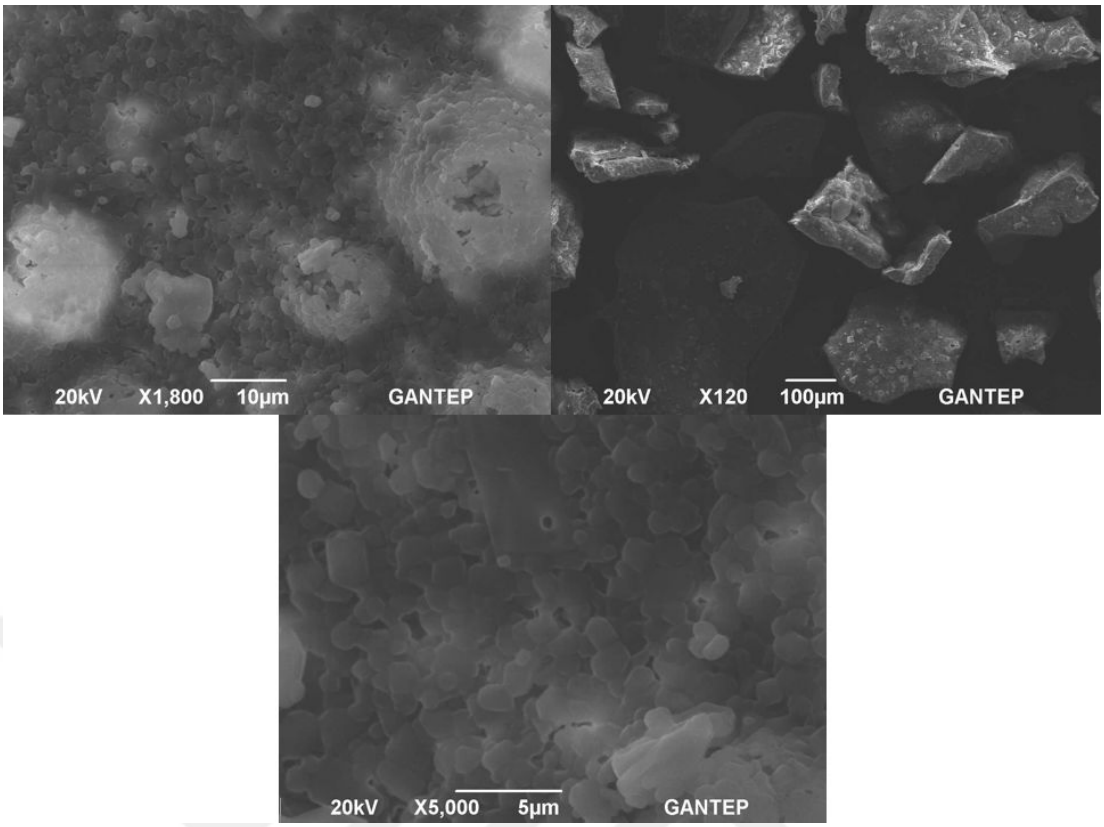

Figure 5.127: SEM images of 0.1 % Gd doped $Li_2B_4O_7$ sample.

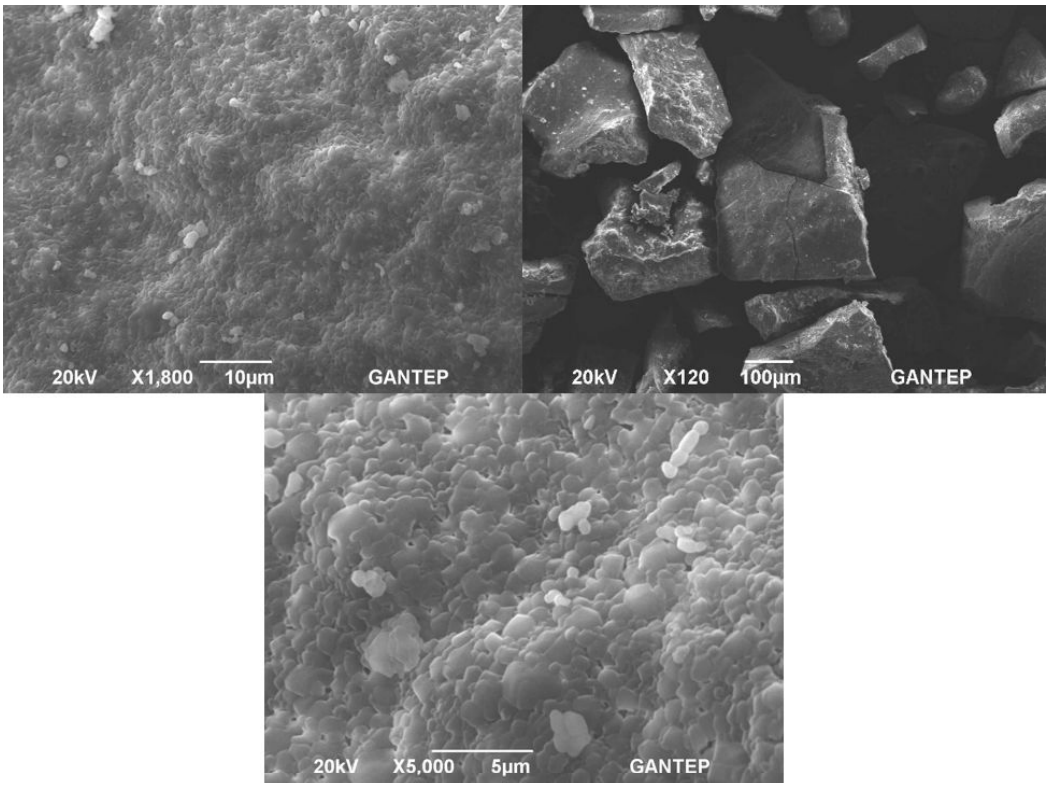

Figure 5.128: SEM images of 0.1 % Mg doped $Li_2B_4O_7$ sample.

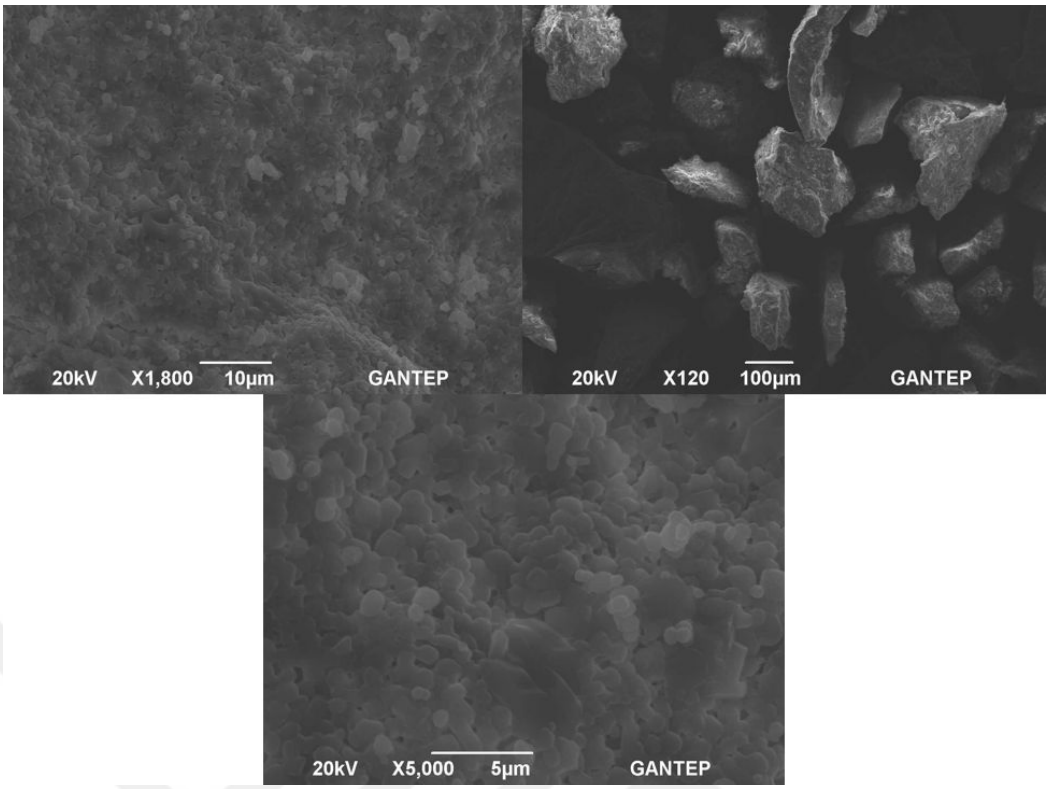

Figure 5.129: SEM images of 0.5 % Ag doped $Li_2B_4O_7$ sample.

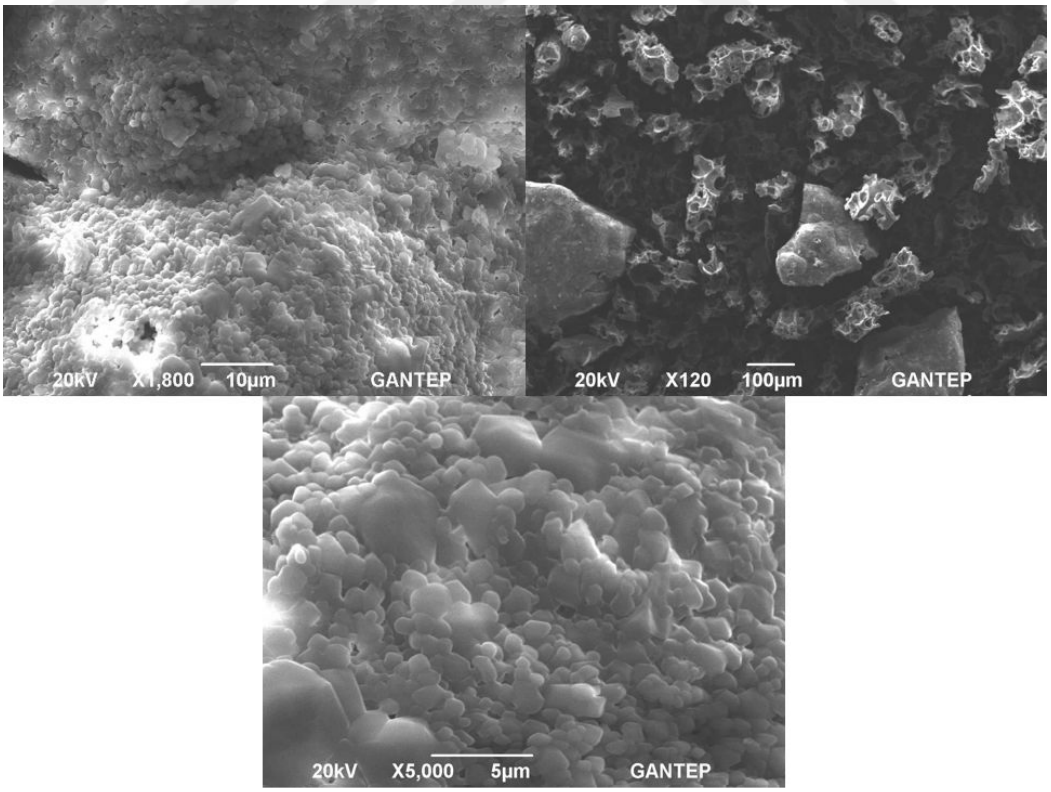

Figure 5.130: SEM images of 0.5 % Cu doped $Li_2B_4O_7$ sample.

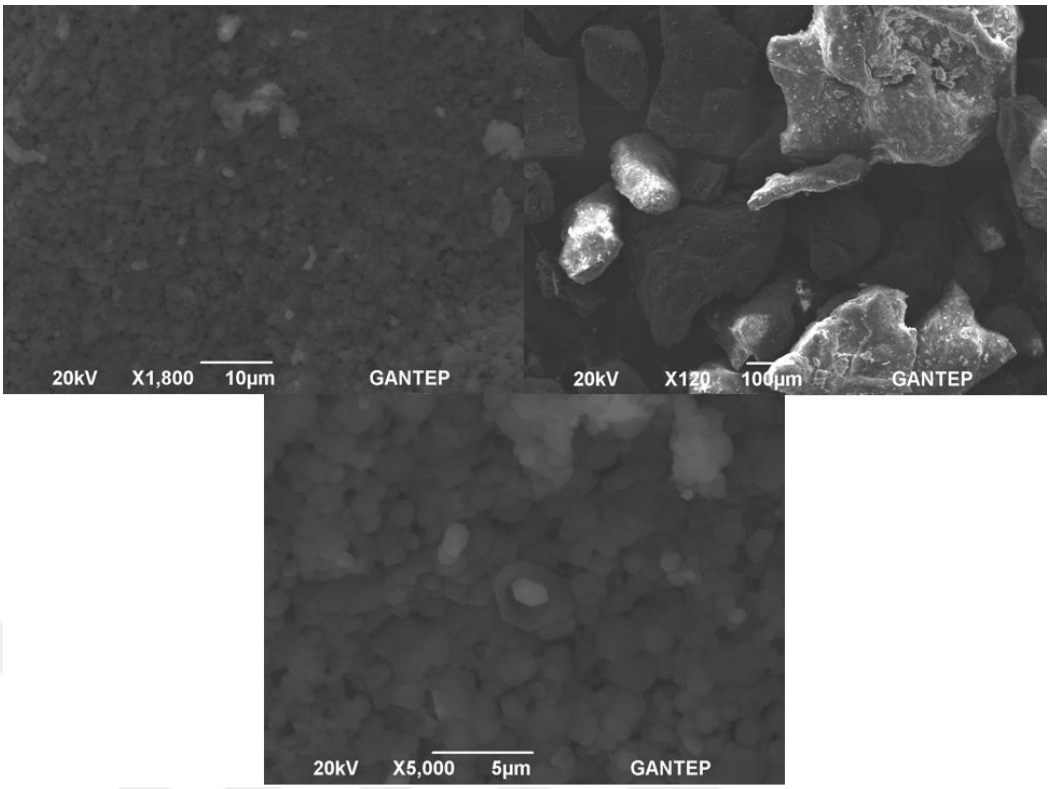

Figure 5.131: SEM images of 0.5 % Dy doped $Li_2B_4O_7$ sample.

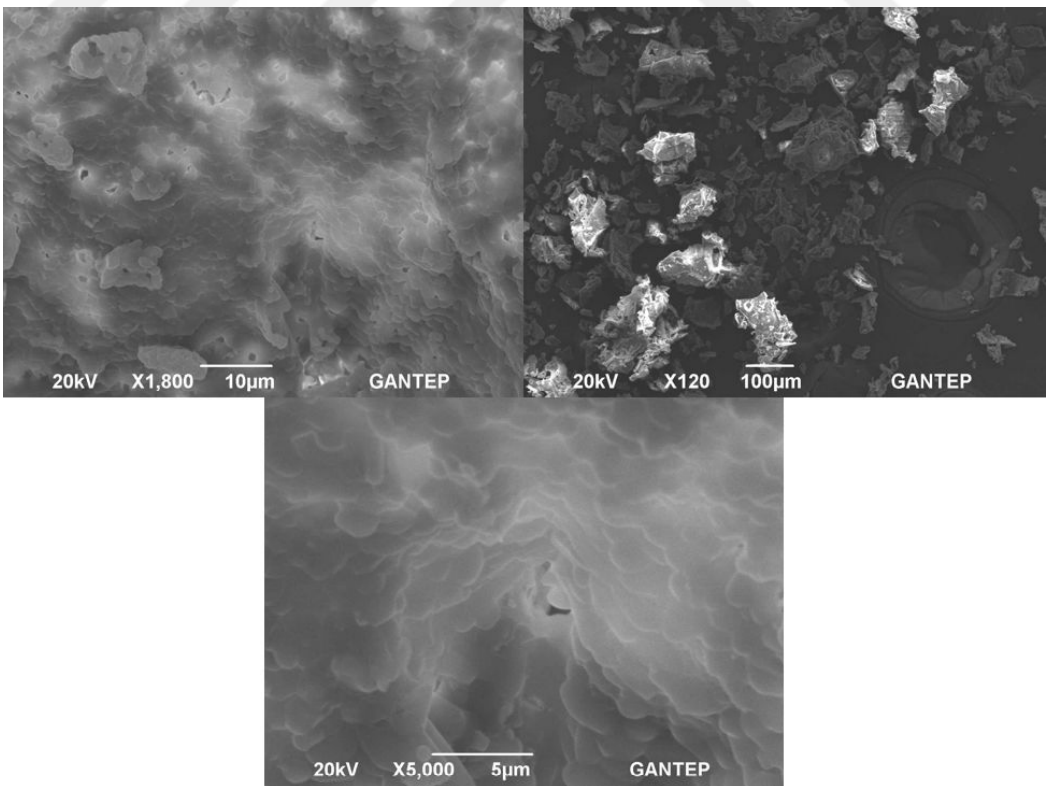

Figure 5.132: SEM images of 0.5 % Dy doped MgB_4O_7 sample.

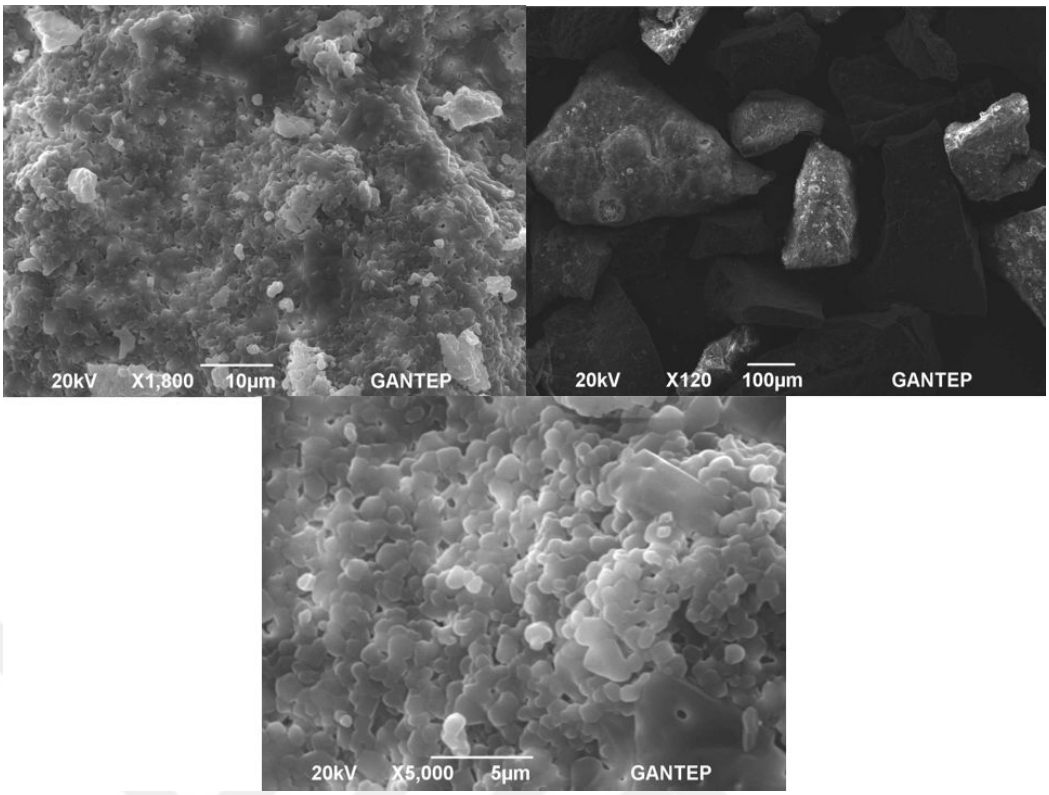

Figure 5.133: SEM images of 0.5 % Eu doped $Li_2B_4O_7$ sample.

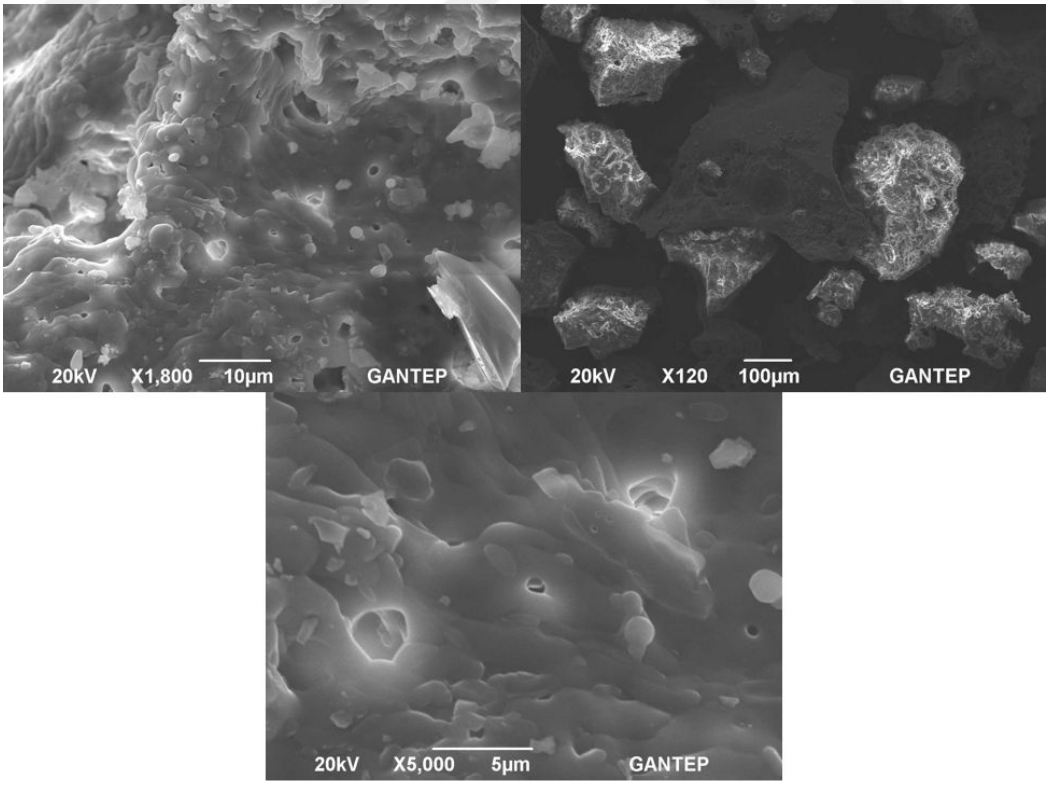

Figure 5.134: SEM images of CaB_4O_7 sample.

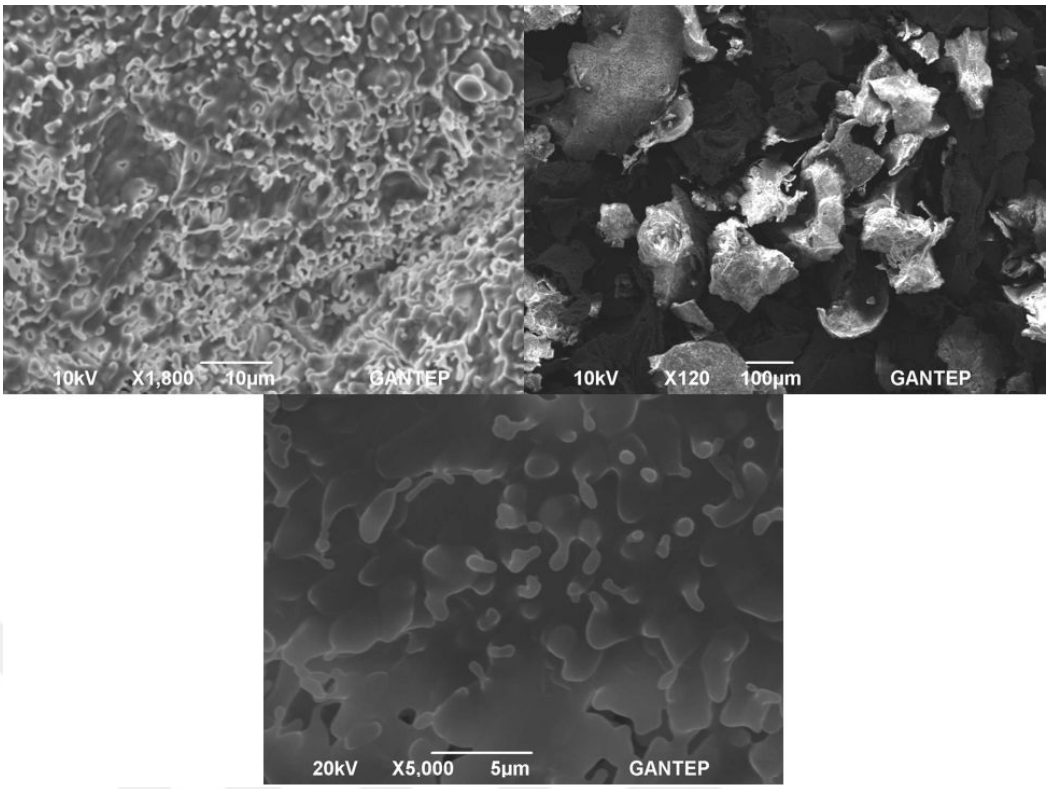

Figure 5.135: SEM images of MgB_4O_7 sample.

CHAPTER 6

CONCLUSION

Firstly, the borate compounds were synthesized by solid state method in this study. In METU, this method was previously used in the synthesis of lithium triborate and lithium tetraborate compunds. However, this method has been used as first time for the synthesis of magnesium tetraborate, barium tetraborate and calcium tetraborate compounds in this work.

The doping of metal ions was carried out after the synthesis of the compounds. The lithium tetraborate was doped by the solution method. A solid-solid homogeneous mixture was obtained by adding metal ion after synthesis to the lithium triborate compound, and the resulting mixture was then fired and doped. Additionally, magnesium, calcium and barium tetraborate compounds were synthesized simultaneously as mentioned previously for lithium tetraborate. The XRD and FT-IR spectra measurements were investigated after synthesis and doping processes. According to XRD results, they are coincided with JCPDS cards.

The thermal analyses (DTA-TGA) were carried out after finding the neutron sensitivity of borate based compounds that show neutron dosimetric properties. The thermal analysis was carried out up to a temperature of 930 °C from the temperature of 30 °C. According to the measurement results, the borate-based compounds display to maintain their thermal stability according to temperature change.

Then; the TL glow curves of boron-based compounds were measured to investigate its radiation dosimetric properties. The neutron sensitivity of developed samples was found in the thermoluminescence measurements after irradiation by a ^{252}Cf neutron source in this study. The TL glow curve measurements were repeated two times for each sample before and after neutron irradiation. It was seen that the thermoluminescence measurements did not exhibit appropriate results after neutron irraditions. On the other hand, it was observed that the annealing

process have probable effects on the TL glow curves of these compounds and they start to exhibit glow curves after annealing processes. Therefore, all compounds were annealed at 600 °C for 1 hour before TL glow curve measurements and then they were exposed to neutron radiation to measure their glow curves. These results are the borate-based neutron dosimeter compounds that were aimed to be developed in this thesis.

TL neutron sensitivity of the samples was also compared with TLD-600 and TLD700 by calculating the glow curve area per unit of mass of dosimeter and per unit of dose of neutrons. Among the samples CaB_4O_7:Dy (0,5%) and MgB_4O_7:Dy (1%) have the highest sensitivity. CaB_4O_7:Dy (0,5%) approximately 4,35 and 3,36 times higher than that of TLD-600 and TLD-700 respectively. TL intensity of MgB_4O_7:Dy (1%) approximately 1,9 and 1,47 times higher than that of TLD-600 and TLD-700 respectively. The TL neutron sensitivity of the other samples are below both TLD-600 and TLD-700. The compounds with positive results are considered to be in accordance with the conditions necessary for their acceptance as an ideal neutron dosimetry. As shown in Figure 5.75; 0.5% Dy-doped calcium tetraborate (CaB_4O_7) compound gives the highest thermoluminescence intensity among the all developed samples. According to obtained results in this study, the intensity of thermoluminescence glow curve increases when the amount of dysprosium increases in magnesium tetraborate (MgB_4O_7) composition. Additionally, the lithium tetraborate ($Li_2B_4O_7$) compounds when doped with Ag, Dy, Eu, Mg, Gd and Cu gave good TL results after neutron radiation. The maximum peak temperature values of all of the neutron-sensitive compounds developed in this study are in agreement with the value required for the dosimetric material.

Within the scope of this thesis, the aims have been achieved. 75% of the source the compounds from the borates in our country were synthesized and compounds sensitive to neutron were obtained. Increasing nuclear power plants today are of great importance for nuclear energy and for people working in these fields. This thesis is considered as a great importance because of the difficulties in detection of neutrons and the fact that there are few studies and researches have been carried out on this subject worldwide. With the support of this work, neutron sensitive borate compounds were obtained from the developed materials. Borate compounds doped with metal ions were synthesized and characterization analyzes were performed and borate compounds sensitive to neutron radiation were obtained.

The neutron detector and materials prepared at Gaziantep University and material prepared at Middle East Technical University and the neutron source for this study have been reinforced with the infrastructure of the central thermoluminescence laboratory, and a great step has been taken to develop neutron measurements and to make new studies. Some of the important experimental instruments in the TL & OSL laboratory, which are still used for limited applicant, could be used more widely with this thesis achievement and provides personal dose measurements for individuals exposed to radiation due to working conditions in Gaziantep and surrounding areas. It is considered that the obtained results from this study could have probable contribute to the future scientific studies.

REFERENCES

[1] Pownsner RA, Pownsner ER. 2006. Essential Nuclear Medicine Physics. Second Edition Published by Blackwell Publishing Ltd.

[2] Leo W.R. 1994. Techniques for Nuclear and Particle Physics Experiments. Second Revised Edition Springer-Verlag.

[3] Knoll GF. 2010. Radiation Detection and Measurement. Fourth Edition. John Wiley Sons Inc.

[4] Roth E, Poty B. 1989. Nuclear Methods of Dating. 5 vol. Kluwer Academic Publishers.

[5] Chen R, Kirsh Y. 1981. Analysis of Thermally Stimulated Processes. Pergamon Press, Oxford.

[6] Arnold W, Sherwood HK. 1957. Are chloroplasts semiconductors? Proc Natl Acad Sci USA 43: 105114.

[7] Das A, Ferbel T. 2003. Introduction to Nuclear and Particle Physics. Second Edition. World Scientific Publishing Co. Pte. Ltd.

[8] LAnnunziata MF. 2003. Handbook of Radioactiviy Analysis. Second Edition. Acedemic Press.

[9] Schulman JH, Kirk RD, West EJ. 1967. Proceedings of the International Conference on Luminescence Dosimetry. Stanford University. CONF-650637, p.113.

[10] Leonyuk, N. I. (1997). Structural aspects in crystal growth of anhydrous borates. *J. Cryst. Growth.* **174**, 301-307.

[11] Voda, M., Balda, R., Al-Saleh, M., de Ocariz, I. S., Cano, M., Lobera, G., Fernandez, J. (2001). Optical properties of Pr-doped lithium tetraborate glasses. *J. Alloys Compd.* **323-324**, 250-254.

[12] Kaczmarek, S. M. (2002). Li2B4O7 glasses doped with Cr, Co, Eu and Dy. *Opt. Mater. (Amst).* **19**, 189-194.

[13] Pradhan, A. S. (1985). Thermoluminescence Dosimetry and Its Applications. *Radiat. Prot. Dosimetry.* **1**, 153-167.

[14] Bos, A.J.J. (2001).High sensitivity thermoluminescence dosimetry. *Nuc.Inst. And Meth. in Phy. Res. B* **184** 3-28.

[15] Wiedemann, E., Schmidt, G.C. (1895).Ueber Luminescenz von festen Körpern und festen Lösungen. *Ann, Phys.Chem.*, **54**, 604.

[16] Przibram, K. *et al.*(1923).Verfärbung und Lumineszenz durch Becquerelstrahlen. *Akad. Wiss. Wien [Ila].* **132**, 262- 285

[17] Randall, J.T., Wilkins, M.H.F. (1945). Phosphorescence and Electron Traps. I. The Study of Trap Distributions. *Proc.* R. Soc., London Ser. A 184.

[18] Garlick, G.F.J., Gibson, A.F. (1948). The electron trap mechanism of luminescence in sulphide and silicate phosphors.*Proc. Phys. Soc.* **60**, 574.

[19] Johnson, N.M. (1960). Thermoluminescence in biogenic calcium carbonate.*Journal Of Sedimentary Research* **30**, 305-313.

[20] Kwon JH., Ahn JJ., Shahbaz HM. 2014. Food Engineering Fundamentals, Pages 427-490.

[21] Daniels, F., Boyd, C.A, Saunders, D.F. (1953).Thermoluminescence As A Research Tool. *Science* **117**, 343.

[22] McKeever SWS. 1985.Thermoluminescence of Solids. Cambridge University Press. Cambridge.

[23] MosisekM. 1966.Therm. of Some Irradiated Polymers, Proc. 2nd Tihany Symp.Radiat.Chem. DoboJ. And Hedvig P. Eds, Budapest.

[24] Mosisek, M. (1968). Thermoluminescence of Some Irradiated Polymers. *Jaderna Energ.* **14**, 198.

[25] Fleming, S.J. (1969).Thermoluminescence from Irradiated Polymers. *Proc. R. Aust. Chem. Inst.* **36**, 199.

[26] Partridge, R.H. (1972).Thermoluminescence. in polymers, *in Radiation Chemistry of Polymers.***1**, 194.

[27] Tomita, A. (1970).Thermoluminescence of γ-Irradiated Polytetrafluoroethylene. *J. Phys. Soc. Jap.***28**, 731.

[28] Mozisek, M. (1970). Radiothermoluminescence of polyethylene and polypropylene. *J.Appl. Radiat. Isotopes.***21**, 11.

[29] Lyman, T. (1935).The Transparency of the Air Between 1100 and 1300A.*Phys. Rev.* **48**, 149.

[30] Tousey, R. (1951).Measurements of Solar Extreme Ultraviolet and X-Rays from Rockets by Means of a $CoSO_4$: Mn Phosphor. *Phys. Rev.* **83**, 792.

[31] Watanabe, K. (1951).Properties of $CaSO_4$: Mn Phosphor under Vacuum Ultraviolet Excitation. *Phys. Rev.* **83**, 785.

[32] Kossel, W., Mayer, V., Wolf, H.C. (1954). Simultaneous dosimetry of radiation fields in living objects. *Sim. Von. Str. Am leb ObNaturwissenschaften,* **41**,209.

[33] Wick, F.G. and Slattery, M.K. (1928).Thermoluminescence Excited By X-Rays. *J.Opt. Soc. Am.***16**, 398.

[34] Ginther , R.J. (1954). Sensitized Luminescence of CaF_2:(Ce+Mn). *Electrochem. Soc.* **101**, 248.

[35] Ginther, R.J., Kirk, R.D. (1957). The Thermoluminescence of CaF_2: Mn. *J. Electrochem. Soc.***104**,365.

[36] Gorbics, S.G. *et al.* (1968). LiF and CaF_2: Mn thermoluminescent dosimeters in tandem. *Int. J.Appl, Radiat. Isotopes.***19**, 81.

[37] Morehead, F.F., Daniels, F. (1952). Storage of radiation energy in crystalline lithium fluoride and metamict minerals. *J.Phys.Chem.**56***, 546.

[38] Schulman JH. et al. 1963. Thermoluminescent Methods in PersonnelDosimetry, Proc.Symp.Pers. Dos. Techn., Madrid, OECD/ENEA, Paris, 319.

[39] Mandeville , C.E., Albrecht, H.O. (1954). Luminescence of beryllium oxide. *Phys. Rev.* **94**, 44.

[40] Becker, K., Cheka, J.S., Oberhofer, M. (1970).Thermally stimulated exoelectron emission, thermoluminescence, and impurities in LiF and BeO. *Health Phys.***19**,391.

[41] Scarpa, G. (1970). The dosimetric use of beryllium oxide as a thermoluminescent material: a preliminary study. *Phys. Med. Biol.* **15**, 667.

[42] Yamashita, T., Nada, N. Onishi, H. Kitamura, S. (1971). Calcium sulfate activated by thulium or dysprosium for thermoluminescence dosimetry. *Health Phys.***1**, 295.

[43] Spurny, Z. 1972. IAEA/SM-160/52 Proc.Symp. Dosimetry Techniques Applied to Agriculture, Industry, Biology, andMedicine, IAEA, Vienna, 1.

[44] Luchner, K. (1957).On the thermoluminescence of natural fluorspar. *Ann. Phys.* **149**,435.

[45] Schayes R. et al.(1963).La Dosimetrie par Thermoluminescence.*Rev. MBLE, Brussels. Belgium.***6**, 33.

[46] Botshvar, I.A., *et al.* (1963).Energy storage and the balance of producers and decomposers in ecological systems. *At. Energ.* **15**,48.

[47] Ginther, R.J. (1965).Therbium-Activated Thermoluminescent Glass for-Dosimetry. *in Luminescence Dosimetry.* CONF-650637,118.

[48] Furetta C.1937. Handbook of Thermoluminescence. London: World Scientific.

[49] Mckeewer SWS., Chen R. 1997. Theory of Thermoluminescence and Related Phenomena. World Scientific. Singapore.

[50] Industrial Minerals, IMA Europe, www.ima-europe.eu.

[51] Bates RL, Jackson JA., eds. 1987. Glossary of Geology, 3rd ed., American Geological Institute, Alexandria, VA, 778 pp.

[52] Lyday, P.A. (1991). "Boron-1990," Mineral Commodify Summaries, US Bureau of Mines, 9 pp.

[53] Travis NS, Cocks ES. 1984. The Tincal Trail, Chapter. I, Harrap, London. 311 pp.

[54] Keszler, D.A. (1999). Synthesis, crystal chemistry, and optical properties of metal borates.*Current Opinion in Solid State and Materials Science* **4**, 155-162.

[55] Zachariasen, W. H. (1964). The crystal structure of lithium metaborate. *Acta Cryst.,* **17**, 749.

[56] Krogh-Moe, J. (1962). The crystal structure of lithium diborate, $Li_2O.2B_2O_3$.*Acta Cryst.*, **15**, 190.

[57] Chen, C., (1989).New nonlinear-optical crystal: LiB_3O_5. *Laser Focus World.*

[58] Gorelik, V.S., Vdovin, A.V., and Moiseenko, V.N. (2003).Raman and hyper-Rayleigh scattering in lithium tetraborate crystals. *Journal of Russian Laser Research*, Volume **24**.

[59] Mainman, T.H. (1960). Stimulated optical radiation in ruby. *Nature* **187**, 493.

[60] Furukawa, Y., Sato, M. (1995). Lithium triborate and optical device using it. *Jpn. KokaiTokkyoKoho, 3 p, Patent written in Japanese, Application JP* 94-103966 19940518.

[61] Takatomo, S., Yusuke, M., Masashi, Y. (2001). Development of new NLO borate crystals.*Journal of Nonlinear Optical Phyics and Materials* **10**, 2, 249.

[62] Mori, Y., Yap, Y.K., Kamimura, T., Yoshimura, M., Sasaki, T. (2002). Recent development of nonlinear optical borate crystals for UV generation.*Optical Materials* **19**, 1.

[63] Ogorodnikov, I.N., Isaenko, L.I., Kruzhalov, A.V., Porotnikov, A.V. (2001). Thermally stimulated luminescence and lattice defects in crystals of alkali metal borate LiB_3O_5 (LBO).*Radiation Measurement.***33**, 577–581.

[64] Iwai, M., Kobayashi, T.,Furuya, H., Japaneese. (1997).Crystal Growth and Optical Characterization of Rare-Earth (Re) Calcium Oxyborate $ReCa_4O(BO_3)_3$ (Re= Y or Gd) as New Nonlinear Optical Material. *Journal of Appied. Phyicss***36**, L276.

[65] Yang, Z., Lin, J.H., Su, M.Z. (2000). Photon cascade luminescence of Gd^{3+} in $GdBaB_9O_{16}$.*Journal of Alloys Compounds*, **308**, 94.

[66] He, M., Chen, X.L., Hu, B.Q., Zhou, T., Xu, Y.P., Xu, T. (2002).The Ternary System Li_2O–Al_2O_3–B_2O_3: Compounds and Phase Relations. *Journal of Solid State Chemistry*, **165**, 187-192.

[67] Dewey C.F., Cook Jr. W.R., Hodgson Jr. R.T., Wynne J.J. (1975). Frequency Doubling in $KB_5O_8 \cdot 4H_2O$ and $NH_4B_5O_8 \cdot 4H_2O$ to 217.3 nm.*Applied Physiscs Letter*, **26**, 714.

[68] Liebertz, J., Stahr, S. (1983). Zurtieftemperaturphase von BaB_2O_4.*Z. Kristallographi***165**, 91.

[69] Wu, Y.C., Sasaki, T., Nakai, S. (1993). CsB3O5: A new nonlinear optical crystal. *Applied Physics Letter,* **62**, 2614-2615.

[70] Mei, L.F., Wang, Y.B., Chen, C.T. (1993).Nonlinear optical materials based on MBe_2 BO_3F_2 (M= Na, K). *Journal of Applied Physics,* **74**, 7014-7015.

[71] Mori Y., Kuroda I., Nakajima I.S. (1995). New nonlinear optical crystal: cesium lithium borate.*Applied Physics Letter*, **67**, 1818 – 1820.

[72] Chen, C., Wang, Y., Wu, B., Wu, K., Zeng, W., Yu, L., (1995). Design and synthesis of an ultraviolet-transparent nonlinear optical crystal $Sr_2Be_2B_2O_7$. *Nature*, **373**, 322 – 324.

[73] Aka, G., Harari, K., Vivien, D., Benietz, J.M., Salin, F., Godard, J.J.(1996).*Solid State Inorganic Chemistry.***33**, 727.

[74] Hu, Z.G.,Higazhiyama, T., Yoshimara, M.(1998).A new nonlinear optical crystal $K_2Al_2B_2O_7$. *Jpn.Journal of Applied Physics.***37**, L1093-L1094.

[75] Helwing, H., Liebertz, J., Bohatu L. (1999). Exceptional large nonlinear optical coefficients in the monoclinic bismuth borate BiB_3O_6 (BIBO). *Solid State Commun.* **109**, 249.

[76] Boric Acid. From Wikipedia, the free encyclopedia. https://en.wikipedia.org/wiki/Boric_acid

[77] Triolo A., Brai M., Gennaro G., Bartolotta A. (2007). Alanine blends for ESR measurements of thermal neutron fluence in a mixed radiation field.*Radiat Prot. Dosimetry*, **126**(1-4):333-6.

[78] Yukihara E. G., Mittani J. C., Vanhavere F., Akselrod M. S.(2008). Development of new optically stimulated luminescence (OSL) neutron dosimeters.Radiation Measurements.43, (2–6), 309-314.

[79] Horowitzt Y. S., Shachart B. B.(1988). Dosimetric characterisation of the high temperature peaks of LiF: Mg, Ti and CaF_2: Tm using computerised glow curve deconvolution.*Radiation Protection Dosimetry.* **23**, 401-404.

[80] Mittani, A.A.R. da Silva, Vanhavere F., Akselrod M.S., Yukihara E.G.(2007). Investigation of neutron converters for production of optically stimulated luminescence (OSL) neutron dosimeters using Al_2O_3: C.*Nuclear Instruments and Methods in Physics Research B.***260,** 663-671.

[81] Dhanuskodi, S., Mohandoss, R., Vinitha G. (2014).Preparation and optical properties of cobalt doped lithium tetraborate nanoparticles. *Optical Materials.***36**, 1598-1603.

[82] Kimberlee, J., Kearfott, William Geoffrey West, Muhammad Rafique. (2015).The optically stimulated luminescence (OSL) properties of LiF: Mg, TI, $Li_2B_4O_7$: CU, $CaSO_4$: Tm, and CaF_2: Mnthermoluminescent (TL) materials. *Applied Radiation and Isotopes.***99**, 155–161.

[83] Tou Ying Lim, Wagiran, H., Hussin, R., HashimS. (2015). Thermoluminescence response of dysprosium doped strontium tetraborate glasses subjected to electron irradiations. *Applied Radiation and Isotopes.***102**, 10–14.

[84] Annalakshmi, O.,Jose, M., Madhusoodanan,T., U., Sridevi, J.,Venkatraman, B., Amarendra G., and Mandal A., B. (2014). Radiation-induced defects in manganese-doped lithium tetraborate phosphor. *Radiation Protection Dosimetry*, 1–8.

[85] Furetta, C., Sanipoli C., Scacco, A., Somaiah, K. (1996).Applicability in Dosimetry of Thermoluminescent Li2B407 Doped with Cu or Eu Impurities. *Radiation ProtectionDosimetry*, **339**-342.

[86] Zhengye, X. Qiang, T. Zhang, Z. (2007). Investigation of thermoluminescence in $Li_2B_4O_7$ phosphors doped with Cu, Ag and Mg. *Science in China Series G: Physics,Mechanics and Astronomy*, 311-320.

[87] Laksmanan, A.R., Chandra, B., and Rhatt, C.H. (1981). A Personnel Dosimeter TLD Badge Based on $CaSO_4$: Dy Teflon TLD Discs.*Rad .Proc. Dos.*191-198.

[88] Manam, J., Sharma, S.K. (2005).Evaluation of trapping parameters of thermally stimulated luminescence glow curves in Cu-doped $Li_2B_4O_7$ phosphor. *Radiation Physics and Chemistry,***72**, 423–427.

[89] Kelemen, A., Holovey, V., Ignatovych, M. (2008).Relative yields of radioluminescence and thermoluminescence in manganese-and silver-doped lithium tetraborate phosphors. *Radiation Measurements.***43,** 375-378.

[90] Driscoll, C. M. H.,Fisher,E. S.,Furetta,C.,Padovani,R.,Richards,D. J.,Wall, B. F. (1983). The thermoluminescence properties of lithium borate dosemeters. *Radiation Protection Dosimetry.***6**, 305-308.

[91] Huang, J., Shen, Y. R., Chen C. T. and Wu, B. C. (1991). Noncritically phase-matched second-harmonic generation and optical parametric amplification in a lithium triborate crystal.*Applied Physics Letter.* **58,** 1579-1581.

[92] Ukachi, T., Lane, R.J., Bosenberg, W.R., Tang, C.L. (1992).Measurements of noncritically phase-matched second-harmonic generation in a LiB_3O_5 crystal.*Appl. Phys. Lett.* **57**, 980.

[93] Ardiçoğlu, B., Özbayoğlu, G., Özdemir, Z., and Yılmaz, A. (2006). Production and identification of rare-earth doped lithium triborate.*Journal of Alloys and Compounds.***418**, 77-79.

[94] Özdemir, Z., Özbayoğlu, G., Yılmaz, A. (2007). Production and identification of rare-earth doped lithium triborate.*J. Material Science.***42**, 8501-8508.

[95] Ogorodnikova, I.N., Isaenkob, L.I., Kruzhalova, A.V., Porotnikova, A.V. (2001).*Radiation Measurements.***33**, 577–581.

[96] Senguttuvana, N. *et al.* (2002). Crystal growth and luminescence properties of $Li_2B_4O_7$ single crystals doped with Ce, In, Ni, Cu and Ti ions. *Nuc. Ins.and Meth.in Phys.Res.A.***486**, 264-267.

[97] Chen, T. J., Tao, R., Rife, J. C., and Hunter, W. R. (1998). Optical constants and related electronic energy bands of lithium triborate crystal in the 6 12-eV region. *Journal of Opical Society of American B.***15**, 47, 1998.

[98] Wu, B., Chen, N., Chen, C. C., Deng, D., Xu, Z. (1989). Highly efficient ultraviolet generation at 355 nm in LiB_3O_5.*Opt. Lett.* **14**, 1080.

[99] Kato, K. (1990). Parametric oscillation in LiB_3O_5pumped at 0.532 μm. *IEEE.J. Quant. Electron.* **26**, 2043.

[100] Robertson, G., Padgett, M.J., Dunn, N.H. (1994). Continuous-wave singly resonant pump-enhanced type II LiB_3O_5 optical parametric oscillator.*Opt. Lett.***19**, 1735.

[101] Davis, G.M., Zhang, L., Chandler, P.J., Townsend, P.D. (1996).Planar and channel waveguide fabrication in LiB3O5 using MeV He+ ion implantation. *Journal of Applied Physics.* **79**, 2863.

[102] Krogh-Moe, J. (1968). Refinement of the crystal structure of lithium diborate $Li_2O.\ 2B_2O_3$. *Acta CrystallographiB.* **24**, 179.

[103] Van Eijk, C W E. (1997).*Proc. Int. Conf. on Inorganic Scintillators and Their Applications (Shanghai, China, 22–25 September 1997),* 3–12.

[104] Mazzetti, C., Carli, F.D. (1926). Borati anidri di litio, cadmio, piombo, manganese.*Gazetta Chimica Italiana,* **56**, 23.

[105] Rollet, A.P., Bouaziz, R. (1955). The binary system lithium oxide-boric anhydride.*Comptes Rendus.***240**, 2417.

[106] Mathews, M.D., Tyagi, A.K., Moorthy, P.N. (1998). High-temperature behaviour of lithium borates: Part I: Characterization and thermal stability.*Thermochimicia Acta.* **320**,89.

[107] Wei, L., Guiqing, D., Qingzhen, H., Z. An, L. Jingkui.(1990). Anisotropic thermal expansion of LiB_3O_5. *J. Phys.D: Appl. Phys.* **23**, 1073.

[108] König, H., Hoppe, R. (1978).Borates of Alkaline-Metals. 2. Knowledge of LiB_3O_5. *Zeitschrift Fur Anorganische Und Allgemeine Chemie.* **439**, 71.

[109] Shepelev, Y. F., Bubnova, R.S., Filatov, S.K., Sennova, N.A., Pilnev, N.A. (2005). LiB_3O_5 crystal structure at 20, 227 and 377 °C. *J. Solid State Chemistry* **178**, 2987.

[110] Surovtsev, N.V., Malinousky, V.K., Solntsev, V.P., Davydov, A.V., Tsvetkov, E.G., (2008). Peculiarities of LiB_3O_5crystallization from melts studied by Raman spectroscopy.*Journal of Crystal Growth.***310**, 3540-3544.

[111] Eugene, G. T., Pylneva, N.A., Davydov, A.V. (2006).Some aspects of lithium–boron melts structuring. *Journal of Crystal Growth.***292**, 358-363.

[112] Leonyuk, N.I. (1997). Structural aspects in crystal growth of anhydrous borates.*Journal of Crystal Growth.***174**, 301-307.

[113] Furetta, C., Prokic, M.,Salamon, R., Kitis, G. (2000).Dosimetric characterisation of a new production of MgB_4O_7: Dy, Na thermoluminescent material. *Appl. Radiat. Isot.***52**, 243-50.

[114] Campos, L.L., Fernandes, F. (1990). ThermoluminescentCharacterisation of MgB_4O_7: Dy Sintered Pellets.*Radiation Protection Dosimetry*, 111-113.

[115] Kawashima, Y.S., Gugliotti, C.F., Yee, M., Tatumi, S.H., Mittani, J.C.R. (2014). Thermoluminescence features of MgB_4O_7: Tb phosphor. Radiation Physics and Chemistry, **95**, 91–93.

[116] Driscoll, C.M.H., Mundy, S.J., and Eliot, J. M. (1981). Sensitivity and fading characteristics of thermoluminescent magnesium borate.*Radiation Protection Dosimetry*, 135-137.

[117] Sahare, P.D., Singh, M., Kumar, P. (2015). Synthesis and TL characteristics of MgB_4O_7: Mn, Tb phosphor.*Journal ofLuminescence.***160**, 158–164.

[118] Furetta, C.*et al.* (1999). Thermoluminescence characteristics of MgB_4O_7: Dy, Na. *Nucl. Inst. Meth. In Phys. Res. A* **420**, 441-445.

[119] Souza, J.H, Ferrari, V.A., And Freitas de L.C. (1993). TL peak structure of MgB_4O_7: Dy. *Radiation Protection Dosimetry.*239-242.

[120] Annalakshmi, O., Jose, M.T., Madhusoodanan, U., Venkatraman, B., Amarendra, G., (2013).Synthesis and thermoluminescence characterization of MgB_4O_7: Gd, Li. *Radiation Measurements.* **59**, 15-22.

[121] Adrovic, F, Prokic M, Ninkovi, M.M, Glisi, R. (2004).Measurements of environmental background radiation at location of coal-fired power plants.*Rad. Prot. Dosimetry,* **112**,439-42.

[122] Pradhan, A.S. (1981).Thermoluminescence dosimetry and its applications. *Radiation Protection Dosimetry.* **1**, 153.

[123] Karali, T., Rowlands A.P, Prokic M, Townsend P.D, Halmagean E. (2002). Thermoluminescent spectra of rare earth doped MgB_4O_7dosemeters. *RadiatProt Dosimetry.* **100**(1-4):333-6.

[124] Fukuda, Y., Okuno, T., and Takeuchi N. (1983).Thermoluminescence of borate glass containing copper. *Radiation Protection Dosimetry,* 309-312.

[125] Haghiri, M. E., Saion,E., Soltani, N., Abdullah W. S., Navasery M., Saraee., K. R. E., Deyhimi, N. (2014). Thermoluminescent dosimetry properties of double doped calcium tetraborate (CaB_4O_7: Cu–Mn) nanophosphor exposed to gamma radiation. *Journal of Alloys and Compounds.***582**, 392–397.

[126] Prokic, M. (2000).Effect of lithium co-dopant on the thermoluminescence response of some phosphors. *Applied Radiation and Isotopes* **52**, 97-103.

[127] Padlyak, B., Drzewiecki, A. (2013). Spectroscopy of the CaB_4O_7 and $LiCaBO_3$glasses, doped with terbium and dysprosium.*Journal of Non-Crystalline Solids.***367**, 58–69.

[128] Fukuda, Y., Okuno, T., and Takeuchi, N. (1986).*Radiation Protection Dosimetry.***17**, 97-401.

[129] Rojas, S.S, Yukimitu, K., A.S.S. de Camargo, Nunes, L.A.O. and Hernandes, A.C. (2006). Undoped and calcium doped borate glass system for thermoluminescent dosimeter.*Journal of Non-Crystalline Solids.* **352,**32-35, 3608-3612.

[130] Manam, J., Sharma, S. K. (2004). Thermally stimulated luminescence studies of BaB_4O_7 compound. *J. Mat.Science.***39**, 6203 – 6208.

[131] Juan, L. *et al.* (2004). *Nuclear Instr. and Meth. in Phy. Res. B.*

[132] Mishra, G.C., Upadhyay, A.K., Dwiwedi, S.K., Dhoble, S.J., Kher, R.S., (2012). Correlation between thermoluminescence and mechanoluminescenceof γ-ray-irradiated Dy-doped BaB_4O_7 phosphors. *Journal of Materials Science*, **47**, 2752-2756.

[133] Sangeeta, S.C. Sabharwal. (2004). Kinetics of thermally stimulated luminescence from alkaline earth borates.*Journal of Luminescence.***109**, 69-74.

[134] Candu Fundaamentals. `https://canteach.candu.org/Content\%20Library/20040700.pdf`

[135] BurnhamJU. 1992. Radiation Protection. Rev. 3. Point Lepreau Generating Station. NB: New Brunswick Power Corporation.

[136] LeroyC., RancoitaPG. 2009. Principles of Radiation Interaction in Matter and Detection. 2nd Edition.Word Scientific Connecting Great Minds.

[137] Martin JE. 2013. Physics for Radiation Protection. 3rd Edition. ISBN: 978-3-527-66708-6. Wiley-VCH.

[138] KnollGF. 2010. Radiation Detection and Measurement.4th Edition. John Wiley & Sons, Inc. Printed in the United States of America.

[139] Yaramiş, B. 1985. Nükleer Fizik. İ.T.Ü. Fen Edebiyat Fakültesi. Yayin No:7 İstanbul, Türkiye.

[140] Zeren MA. Atomlar Moleküller. Birsen Yayinevi. Fen Edebiyat Kitaplari. İstanbul.

[141] Protons and Neutrons.Hyper Physics. http://hyperphysics.phy-astr.gsu.edu/hbase/particle/proton

[142] Doğan, M. (2008). Development of New Sensitive Thermoluminescent Materials for Radiation Dosimetry. January. Gaziantep Üniversitesi.

[143] Depci, T., Ozbayoglu, G., Yılmaz, A., Yazici,A. N. (2008). The thermoluminescent Properties of Lithium Triborate, LiB_3O_5 activated by aluminium.*Nuclear Instruments and Methods in Physical Research B.* **266**, 755-762.

[144] Pekpak,E.,Yılmaz,A.,Ozbayoglu,G.(2011).The effect of synthesis and doping procedures on thermoluminescent response of lithium tetraborate. *Journal of Alloys and Compounds.* **509**, 2466-2472.

[145] Pekpak, E., Yılmaz,A., Ozbayoglu, G. (2010). An Overview on Preparation and TL Characterization of Lithium Borates for Dosimetry Use. *Open Miner.Process.J.***3**, 14-24.

[146] Kayhan, M., Yılmaz, A. (2011). Effects of Synthesis, Doping Methods and Metal Content on Thermoluminescence Glow Curves of Lithium Tetraborate.*Journal of Alloys and Compounds.***509**, 7819-7825.

[147] Touboul, M., Bétourné. 1997. Synthesis of lithium borates (B/Li≥3) as LiB_3O_5 by dehydration of hydrated precursors.*J. Alloys Compd.***255,** 91-97.

[148] Brant, A. T., Kananan, B. E., Murari, M. K., McClory, J. W., Petrosky, J. C., Adamiv, V.T., Burak, Y. V., Dowben, P. A., Halliburton, L. E. 2011. Electron and hole traps in Ag-doped lithium tetraborate ($Li_2B_4O_7$) crystals. *J. Appl. Phys.***110**, 9.

[149] Zhigadlo,E. K.,Zhang, M. 1976. An infrared spectroscopic study of sealants. *Scand. J. Dent. Res.***84**, 396–400.

[150] Rojas, S.S., Yukimitu, K., de Camargo, A.S.S., Nunes, L.A.O. 2006. Hernandes, A.C. Undoped and calcium doped borate glass system for thermoluminescent dosimeter. *J. Non-Cryst. Solids.* **352**, 3608–3612.

[151] Depci, T., Ozbayoglu, G., Yılmaz, A. 2010. Comparison of Different Synthesis Methods to Produce Lithium Triborate and Their Effects on Its Thermoluminescent Property. *Metall. Mater. Trans.* **41**, 2584–2594.

[152] Manam, J., Sharma, S.K. 2005. Evaluation of trappingparameters of thermally stimulated luminescence glow curves in Cu-doped Li2B4O7 phosphor. *J. Radiat. Phys. Chem.* **72,** 423–427.

[153] Ozdemir, Z., Ozbayoglu, G., Yılmaz, A. 2007. Investigation of thermoluminescence properties of metal oxide doped lithium triborate. *J. Mater. Sci.* **42**, 8501–8508.

[154] Xiong, Z. Y., Ding, P., Tang, Q., Chen, J.M., Shi, W. Q. 2010. Thermoluminescence Spectra of Lithium Tetraborate Single Crystal.*Adv. Mater. Res.* **160-162**, 252-255.

[155] Pekpak, E., Yılmaz, A., Ozbayoglu, G. 2011. The effect of synthesis and doping procedures onthermoluminescenct response of lithium tetraborate. *J. Alloy. Comp.* **509**, 2466–2472.

[156] Kumar, M., Chourasiya, G., Bhatt, B. C., Sunta, C. M. 2010. Dependence of peak height of glow curves on heating rate in thermoluminescence.*Journal of Luminescence***130**, 1216-1220.

[157] Yazici, A. N., Haciibrahimoğlu, M. Y., Bedir, M. 2000. The Effect of Various Experimental Parameters on Glow Peaks and Trapping Parameters of CaF_2:Dy (TLD-200) Crystals.*Turkish Journal Physics.***24,** 623-649.

[158] Rasheedy, M. S., Zahran, E. M. 2006.The effect of the heating rate on the characteristics of some experimental thermoluminescence glow curves.*Institute of Physics Publishing.***73,** 98-102.

[159] Kadari, A., Kadri, D. 2015.New numerical model for thermal quenching mechanism in quartz based on two-stage thermal stimulation of thermoluminescence model. *Arabian Journal of Chemistry.***8**, 798-802.

ÖZGEÇMİŞ

KİŞİSEL BİLGİLER

ADI SOYADI	SERA İFLAZOĞLU
DOĞUM TARİHİ	02.01.1986
TELEFON	0507 135 45 59
EMAIL	sera_iflazoglu@hotmail.com
ADRES	Ahmet Haşim Cad. 54/5 Öveçler Çankaya / ANKARA

EĞİTİM BİLGİLERİ

TARİH (BAŞ.-BİTİŞ)	ÖĞRENİM KURUMU	FAKÜLTE	BÖLÜM
2003-2007	Niğde Üniversitesi	Fen Edebiyat Fakültesi	Fizik Bölümü-Lisans
2007-2010	Niğde Üniversitesi	Fen Bilimleri Enstitüsü	Fizik Bölümü-Yüksek Lisans
2011-2017	Gaziantep Üniversitesi	Fen Bilimleri Enstitüsü	Fizik Mühendisliği-Doktora

Sınav	Puanı	Tarih
ÜDS	75	2010 - Sonbahar

LİSANS TEZİ:

Tezin Adı: Yıldız Kümeleri ve Diskler

Danışman: Doç. Dr. Orhan DÖNMEZ

Niğde - 2007

YÜKSEK LİSANS TEZİ:

Tezin Adı: Ametist'in Termolüminesans ve Optiksel Özelliklerinin Araştırılması

Danışman: Doç. Dr. Adil CANIMOĞLU

Niğde - 2010

DOKTORA TEZİ:

Tezin Adı: Development of New Thermoluminescent Dosimeters for Neutron Measurements

Danışman: Prof. Dr. A. Necmeddin YAZICI

Yardımcı Danışman: Doç. Dr. Vural Emir KAFADAR

Gaziantep - 2017

PROJELER:

1- Bilimsel Araştırma Projesi (BAP) - Gaziantep Üniversitesi

Proje Numarası: MF.14.16

Proje Adı: Nötron Ölçümleri için Yeni Termolüminesans Dozimetrelerinin Geliştirilmesi

Proje Yürütücüsü: A. Necmeddin YAZICI

Araştırmacılar: Doç. Dr. V. Emir KAFADAR-Sera İFLAZOĞLU

Proje Başlangıç ve Bitiş Tarihi: 11/2014 – 05/2016

2- TUBİTAK Hızlı Destek Araştırma Projesi

Proje Numarası: 115F268

Proje Adı: Nötron Ölçümleri için Yeni Termolüminesans Dozimetrelerinin Geliştirilmesi

Projec Yürütücüsü: Prof.Dr. A. Necmeddin YAZICI

Araştırmacılar: Prof. Dr. Ayşen YILMAZ - Doç. Dr. V. Emir KAFADAR

Bursiyer: Sera İFLAZOĞLU

Proje Başlangıç ve Bitiş Tarihi: 10/2015 – 10/2016

İŞ DENEYİMİ

Niğde Karatlı Kasabası Şehit Şahin Yılmaz İlköğretim Okulu	Ücretli Öğretmenlik
Niğde Hacıbeyli İlköğretim Okulu	Ücretli Öğretmenlik
Gaziantep Yöneylem Eğitim Ve Danışmanlık Hizmetleri	Ar-Ge Ve Proje Geliştirme Birimi
Siegen Universitesi– Doktora – Fizik Mühendisliği	Erasmus Programı

KATILDIĞI KURS / PROGRAMLAR

TARİH(BAŞ.-BİTİŞ)	KURUM	KONUSU	SERTİFİKA
18/09/2014-01/10/2014	Siegen Universitesi	Almanca Kursu	Sertifika
03/03/2012-03/03/2012	TMMOB Fizik Mühendisleri Odası	Çevresel Gürültünün Ölçümü, Değerlendirilmesi Ve Raporlanması	Katılım Sertifikası
03/03/2012-03/03/2012	TMMOB Fizik Mühendisleri Odası	Radyasyondan Korunma	Katılım Sertifikası
03/03/2012-03/03/2012	TMMOB Fizik Mühendisleri Odası	Medikal Fizik	Katılım Sertifikası
03/03/2012-03/03/2012	TMMOB Fizik Mühendisleri Odası	Deney Laboratuvarlarının Akreditasyonu İçin Ts En Iso 17025 Standard	Katılım Sertifikası
03/03/2012-03/03/2012	TMMOB Fizik Mühendisleri Odası	İş Sağlığı Ve Güvenliği	Katılım Sertifikası
28/09/2009-30/09/2009	Ege Üniversitesi Nükleer Bilimler Enstitüsü	3.Lüminesans Dozimetre Kongresi	Katılım Belgesi

MAKALELER:

S. İflazoğlu, V. E. Kafadar, B. Yazici, A. N. Yazici. 2017. Thermoluminescence Kinetic Parameters of TLD-600 and TLD-700 after ^{252}Cf Neutron+Gamma and ^{90}Sr- ^{90}Y Beta Radiations. *CHIN. PHYS. LETT. Vol. 34, No. 1, 017801.*

DOI: 10.1088/0256-307X/34/1/017801

ULUSAL VE ULUSLARARASI KONFERANSLARDA SUNULAN BİLDİRİLER:

Sera İFLAZOĞLU, Ahmet Necmeddin YAZICI, Emir Vural KAFADAR, TLD-600 (^{6}LiF:Mg, Ti) Termolüminesans Dosimetresinin Nötron ve Beta Doz Duyarlılığının İncelenmesi. *XI. Ulusal Nükleer Bilimler ve Teknolojileri Kongresi, 12-14 Ekim 2016, Kuşadası.*

S.İFLAZOĞLU, A.N. YAZICI, A.YILMAZ, V.E. KAFADAR, INVESTIGATION OF THERMOLUMINESCENCE PROPERTIES OF CaB_4O_7 AND Dy-DOPED CaB_4O_7 FOR NEUTRON SENSITIVITY. *Turkish Physical society 32nd International Physics Congress September 6-9, 2016 / Bodrum – Turkey.*

S.İFLAZOĞLU, A.N. YAZICI, V.E. KAFADAR, COMPERISON OF THE THERMOLUMINESCENCE PROPERTIES OF TLD-600 AND TLD-700 FOR NEUTRON AND BETA RADIATIONS. *Turkish Physical society 32nd International Physics Congress September 6-9, 2016 / Bodrum – Turkey.*

S. İflazoğlu, A.N. Yazıcı, A. Yılmaz, V.E. Kafadar, Synthesis and Investigation Thermoluminescence Properties of Undoped and Dy Doped MgB_4O_7 Samples for Neutron Dosimeters. *10th International Conference on Luminescence and ESR Dosimetry, 5-7 September 2016, Çukurova University, Adana, Turkey.*

S. İflazoğlu, A.N. Yazıcı, A. Yılmaz, V.E. Kafadar, Thermoluminescence Properties of $Li_2B_4O_7$:Ag, $Li_2B_4O_7$:Eu and $Li_2B_4O_7$:Dy Phosphor Samples for Neutron Measurements. *10th International Conference on Luminescence and ESR Dosimetry, 5-7 September 2016, Çukurova University, Adana, Turkey.*

S.İFLAZOĞLU, A.N.YAZICI, A.YILMAZ, V.E.KAFADAR, Investigation of Dosimetric and Thermoluminescence Characteristics of LiB_3O_5: Cu,Ag, *LUMİDOZ 6, 11-13 Eylül 2012, İzmir.*

S.İFLAZOĞLU, A.N.YAZICI, A.YILMAZ, V.E.KAFADAR, Investigation of the effect of heating rate on the dose dependence of TL glow curves of LiB_3O_5: Cu,Ag, *Türk Fizik Derneği 29.FIZIK KONGRESI 05-08 Eylül 2012, Bodrum.*

H.YÜREK, S. İFLAZOĞLU, A.CANIMOĞLU, Türkiye'den Çıkarılan Yeşil Opal ve Süt Opal Kristallerinin Termolüminesans ve Absorpsiyon Karakteristiklerinin Araştırılması*, Lümidoz VI, 6. Ulusal Lüminesans Dozimetri Kongresi, 11-13 Eylül 2012, İzmir.*

H.YÜREK, S. İFLAZOĞLU, A.CANIMOĞLU, Yeşil Opal ve Süt Opal Kristallerinin Termolüminesans Karakteristiklerinin Araştırılması, *Türk Fizik Derneği 29.FIZIK KONGRESI 05-08 Eylül 2012, Bodrum.*

S.İFLAZOĞLU, H.YÜREK, A. CANIMOĞLU, Yüksek Dozdaki X-ışını Radyasyon Sonrası Ametist'in Termolüminesans Özelliklerinin Araştırılması, *5. Ulusal Lüminesans Dozimetri Kongresi 08-09 Eylül 2011, Mersin.*

S. İFLAZOĞLU, A. CANIMOĞLU, Ametist'in Termolüminesans ve Optiksel Özelliklerinin Araştırılması, *Lümidoz IV, 4. Ulusal Lüminesans Dozimetri Kongresi 20-22 Eylül 2010, Gaziantep.*

S.İFLAZOĞLU, A.CANIMOĞLU, Searching Thermoluminescence and Optical Properties of Amethyst, *Türk Fizik Derneği 27. Fizik Kongresi 14-17 Eylül 2010, İstanbul.*

ÖDULLER:

1- Niğde Üniversitesi Fizik Bölümü İkincilikle Bitirme Ödülü

Niğde - 2007

2- MEB Sağlık İşleri Dairesi Başkanlığınca düzenlenen Verem Eğitimi ve Propaganda Haftası ile ilgili Kompozisyon yarışmasında kazanılmış Hatay il birinciliği

Hatay - 2000

BILGİSAYAR BİLGİSİ:

Yazılım	
Microsoft Windows OS	İyi Düzeyde
Origin Lab OriginPro	İyi Düzeyde
Microsoft Office	İyi Düzeyde
WinRems	İyi Düzeyde

HOBİLER:

Deney yapmak, Kitap Okumak, Müzik Dinlemek, Yemek Pişirme,